NTNU

Norwegian University of
Science and Technology

Synthesis of Thymidylate Kinase Inhibitor Precursors

Thomas Wean Haugen

Spring of 2019

Master thesis

Department of Chemistry

Norwegian University of Science and Technology

Supervisor 1: Professor Bård Helge Hoff, IKJ

Supervisor 2: Phd Candidate Fredrik Heen Blindheim, IKJ

Acknowledgements

All work regarding this master thesis has been done at the Department of Chemistry at NTNU, Trondheim, in the spring of 2019. The thesis has been written under the supervision of professor Bård Helge Hoff and Phd candidate Fredrik Heen Blindheim.

I would like to thank my supervisor, professor Bård Helge Hoff, for his guidance throughout this project. Thank you for taking me in as your master student, and for always being available to any questions when I needed it. I would also like to thank my co-supervisor Ph.D candidate Fredrik Heen Blindhem and Ph.D candidate Thomas Ihle Aarhus for good help and input to my practical laboratory work.

I want to thank Engineer Roger Aarvik for excellent service and fast delivery of my chemicals, and Head Engineer Susana Villa Gonzales for executing MS analysis.

Finally I would like to thank my family for all their patience and support through six years of study. A special thank you to my wife Magna Wean Haugen for sacrificing valuable time from her own study to take care of our two wonderful children, so that I could finish mine.

Trondheim, July 2019

Thomas Wean Haugen

Sammendrag

Multimedikamentresistente bakterier er en av de største helseutfordringene verden står ovenfor i dag, noe som gjør forskning og utvikling av ny antibiotika viktigere enn noen sinne. Hemming av et av nøkkelenzymene i DNA-syntesen, tymidylatkinase, har de siste årene vist lovende resultater. Dette har gjort at tymidylatkinase-hemmere har blitt et sentralt startpunkt for dette forskningsprosjektet.

Målet med denne masteroppgaven har vært å syntetisere 3-(fluorfenyl)propan-1-aminer med fluor i *para*-, *meta*- og *orto*-posisjon. Aminene skulle videre festes på et større molekyl i en amid-koblingsreaksjon, med et mål om å ende opp i en struktur som den eksisterende tymidylatkinase-hemmeren **6** (Scheme 1). Det er interessant å se om fluoratomets posisjon på fenylringen har en effekt på hemmerens aktivitet og reaktivitet. Ved videre forskning innen dette feltet, kan også effekten av å bytte ut fenylgruppen med andre aromater, testes. Heterosykliske ringsystemer kan være et eksempel på dette.

3-(4-Fluorfenyl)propan-1-amin (**1a**) ble syntetisert i en to-stegs syntese, ved en Horner-Wadsworth-Emmons-reaksjon fra 4-fluorbenzaldehyd, til 3-(4-fluorfenyl)akrylnitril **2a** i 48% utbytte. En reduksjon av både alken- og nitril-gruppen med litiumaluminiumhydrid, gav **1a** i 41% utbytte. *Meta*- og *orto*-analogene, **1b** og **1c** ble begge syntetisert ved hjelp av samme prosedyre, med henholdsvis 18- og 25% utbytte.

3-Brom-N-(3-fenylpropyl)benzamid (**5**) ble syntetisert ved å bruke den benzotriasol- og aminiumbaserte koblingsreagenten HATU sammen med Hünigs base i en amid-koblingsreaksjon med 3-brom-benzosyre. Dette gav **5** i 54% utbytte. Scheme 1 viser et skjematisk sammendrag av masteroppgaven.

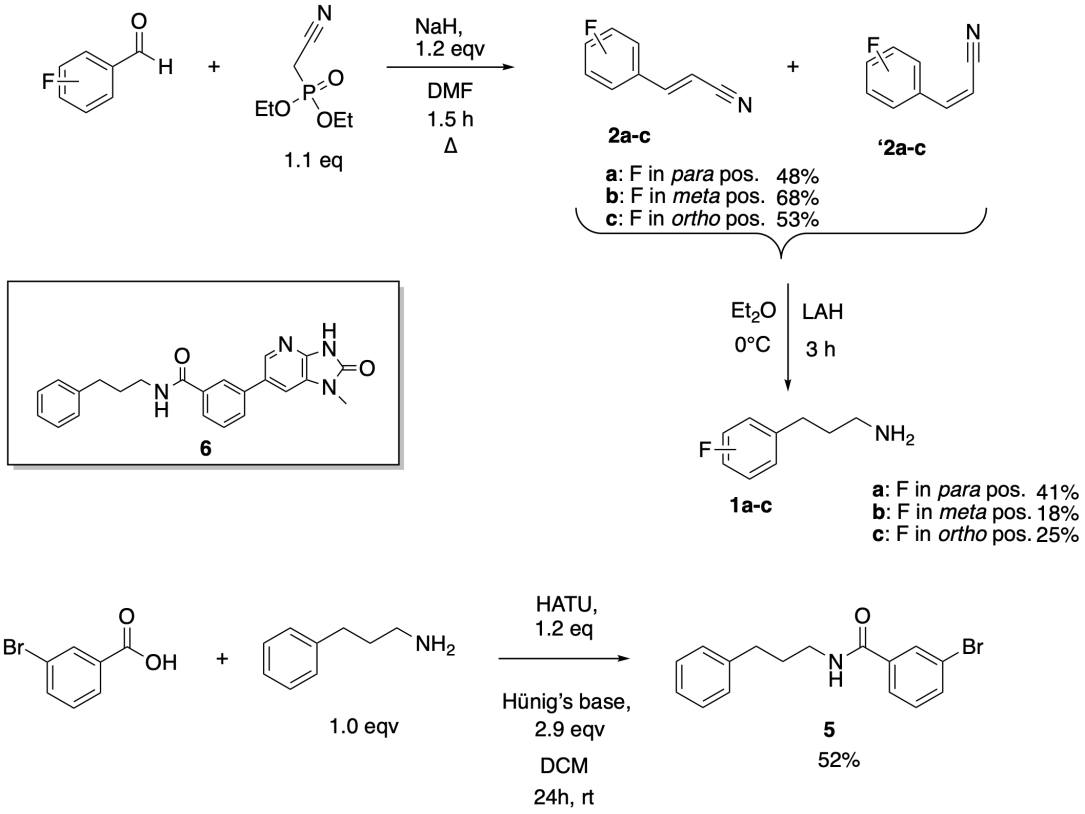

Scheme 1: Et sammendrag av syntesearbeidet gjort i dette prosjektet.

Abstract

Multidrug-resistant bacteria are one of the greatest threats to the human health, and the research on novel antibiotics has never been more important than it is now. The inhibition of one of the key enzymes in the DNA synthesis, thymidylate kinase, has the last couple of years shown some promising results, which has made it the corner stone of this project.

The purpose of this master's thesis was to synthesize 3-(fluorophenyl)propan-1-amines, with the fluorine in *para*, *meta* and *ortho* position. These amines should later on be attached to a bigger molecule in an amide coupling reaction, for eventually to end up in a structure like the existing thymidylate kinase inhibitor **6** (Scheme 2). It is interesting to see if the fluorine's position on the phenyl ring will have an effect on the activity and reactivity of the inhibitor. In future work, the effect of other substituents, like heterogeneous aromatic ring systems, could also be an interesting study.

3-(4-Fluorophenyl)propan-1-amine (**1a**) was synthesized in a two-step synthesis, starting with a Horner-Wadsworth-Emmons reaction of 4-fluorobenzaldehyde, yielding 3-(4-fluorophenyl)acrylonitrile (**2a**) in 48% yield. A simultaneous reduction of the alkene- and nitrile group with Lithium aluminum hydride, gave **1a** in 41% yield. The same procedure was used to synthesize the *meta* and *ortho* analogues **1b** and **1c** in 18- and 25% yield, respectively.

3-Bromo-N-(3-phenylpropyl)benzamide (**5**) was synthesized using the benzotriazole- and aminium based coupling reagent HATU together with Hünig's base in an amide coupling reaction with 3-bromobenzoic acid, giving **5** in 54% yield. Scheme 2 illustrates a schematic summary of the work done in this master's thesis.

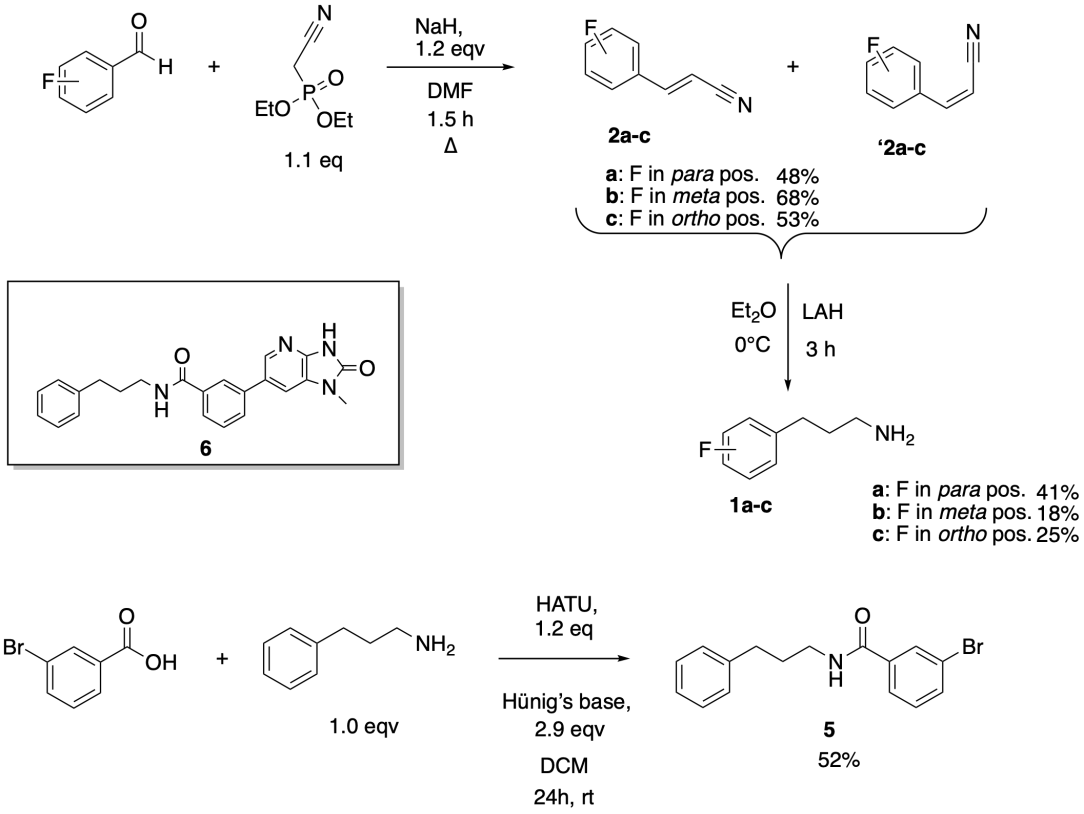

Scheme 2: A summary of the synthetic work done in this project.

Contents

Abbreviations and Symbols

br	Broad Signal
d	Duplet
DCM	Dichloromethane
DMF	Dimethyl Formamide
eqv	Equivalents
h	hour(s)
HWE	Horner-Wadsworth-Emmons
Hz	Hertz
J	Coupling Constant
LAH	Lithium Aluminium Hydride
LG	Leaving group
M	Molar concentration given in moles/litres
m	Multiplet
MDR	Multidrug-resistant
ppm	Parts Per Million
q	Quartet
rt	Room Temperature
s	Singlet

t Triplet

THF Tetrahydrofurane

TLC Thin Layer Chromatography

TMK Thymidylate Kinase

UV Ultraviolet

List of Tables

List of Schemes

List of Figures

1. Introduction and Objective

Multidrug-resistant (MDR) bacteria are one of the greatest threats to the human health. Even bacteria which have been isolated from the surface of the earth for 4 million years, have on their own developed a resistance to synthetic antibiotics made in the 20th century. This means that the nature has most likely already developed an antibiotic resistance to drugs we have not invented yet. Even though this may seem like a battle we can not win, it is crucial that the research on novel antibiotics continues [1]. Finding new ways to efficiently disarm harmful bacteria is more important now than ever, and one promising way to go, seems to be the inhibition of thymidylate kinase, a key enzyme for the bacteria's DNA synthesis [2].

1.1 Thymidylate Kinase

Thymidylate Kinase (TMK) is an essential enzyme in the synthesis of thymidine triphosphate, one of the building blocks of the DNA molecule [3]. Kaustubh Sinha and Gordon S. Rule have compared the human TMK's functionality and structure with TMKs from several prokaryotic organisms, including *Candida albicans* (yeast) and *Plasmodium falciparum* (the cause of 95% of the mortality rate from malaria [4]), and found that the differences are significant, so that TMK absolutely could be a target for novel antibiotics [5].

1.2 Objective of the Project

During the last 10 years there have been done some research on this topic, and Choi *et. al.* found that compound **6** was a good choice for TMK inhibition of the *Pseudomonas aeruginosa* bacteria (Scheme 1.1) [6]. This thymidylate kinase inhibitor was then chosen as the

foundation of this project, and the plan was to modify the terminal phenyl group by attaching a fluorine atom in *para-* *meta-* or *ortho* position.

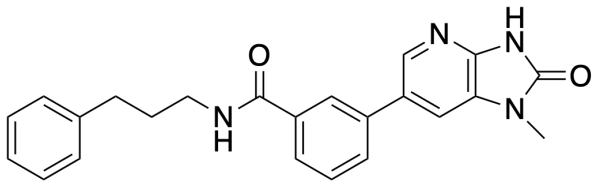

6

Scheme 1.1: *P. aeruginosa* TMK inhibitor.

The objective of this project was to synthesize 3-phenylpropan-1-amines with fluorine in *para-* *meta-* or *ortho* position , in order to see if the activity of the potential inhibitor would be affected by the fluorine's position. The target amines are shown in Scheme 1.2.

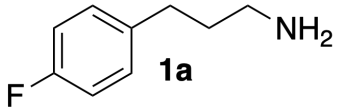

1a

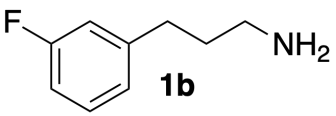

1b

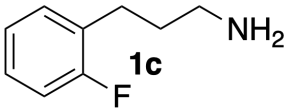

1c

Scheme 1.2: Target molecules of this project.

A secondary objective of this thesis, was to perform an amide coupling reaction, using the target amines as reactants to yield new precursors for the potential thymidylate kinase inhibitors **3a-c** and **4a-c** (Scheme 1.3).

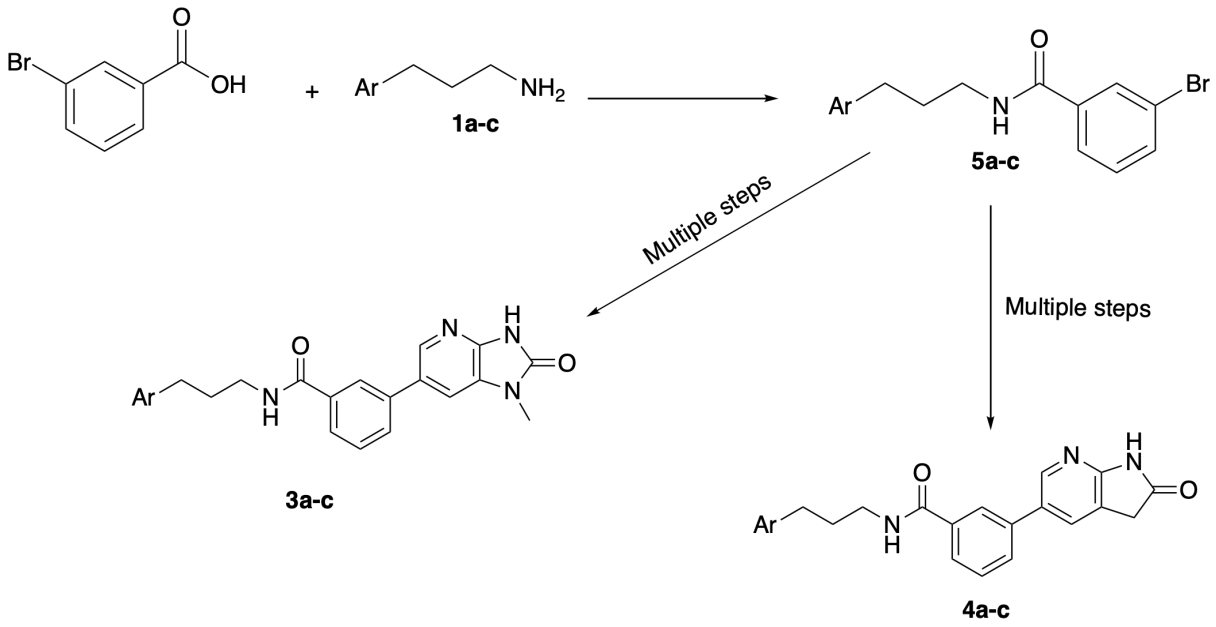

Scheme 1.3: Amide coupling reaction in order to yield **5a-c**, a new precursor for the potential thymidylate kinase inhibitors **3a-c** and **4a-c**.

1.2.1 Previous Work

The synthetic plan was initially to do a cyanomethylation from a 4-fluorobenzyl bromide, followed by a reduction of the nitrile using $LiAlH_4$, in order to yield **1a** as the primary amine (Scheme 1.4) [7, 8].

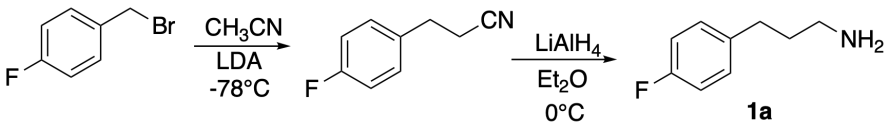

Scheme 1.4: Initial plan: Cyanomethylation of 4-fluorobenzyl bromine, followed by a reduction of 3-(4-fluorophenyl)propanenitrile, to yield **1a**

This was tried several times in a preliminary study, but the cyanomethylation gave some impurities which were difficult to separate from the desired product. Hence the yields became poor. An alternative approach was tried in the end of the project, where the first step was replaced by a Wittig-like reaction, the Horner-Wadworth-Emmons reaction [9]. This gave quite good yields (50-60%), and made a good starting point for this project. All relevant reactions theories will be presented in chapter 2.

2. Theory

2.1 The Chemistry to 3-Arylpropaneamines

3-Arylpropaneamines can be synthesized in multiple ways, including Knoevenagel condensations [10, 11], cyanomethylations [7] and different forms of Wittig reactions [9, 12]. This section will cover three common approaches to the 3-arylpropaneamines, all illustrated in Scheme 2.1.

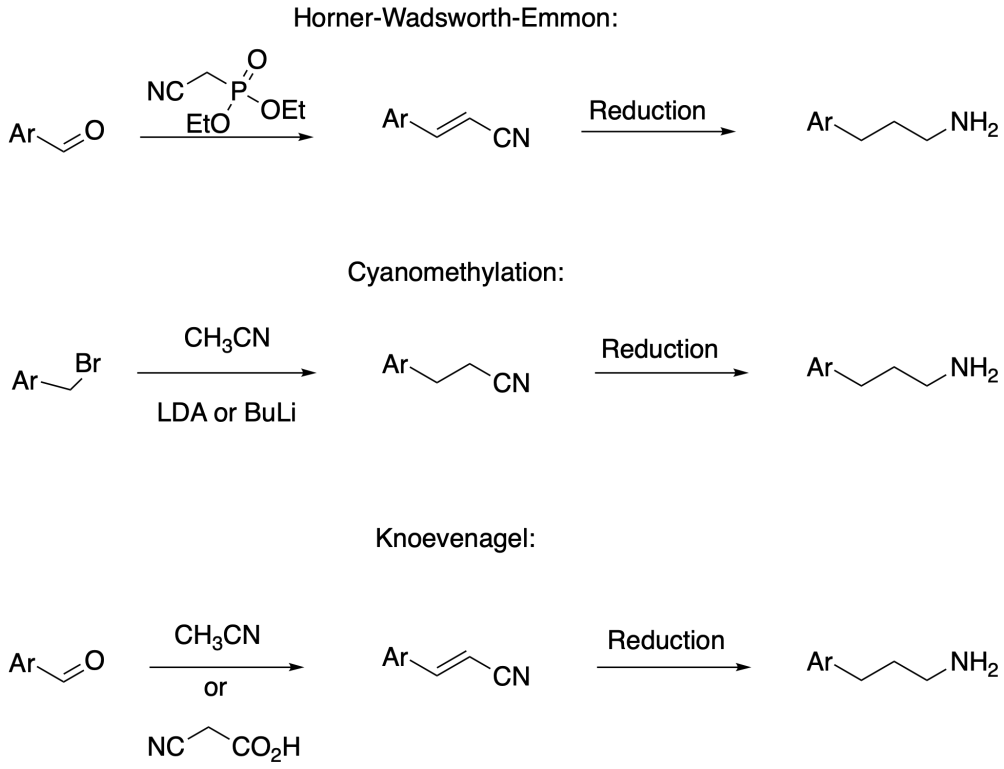

Scheme 2.1: Different routes to 3-arylpropaneamines.

All of the strategies above involve two steps: First creating a nitrile, which later on is to be reduced. The following sections will first focus on the different ways to synthesize the nitriles, and then move the scope towards the reduction step, and look at different options there.

2.1.1 The Horner-Wadsworth-Emmons reaction

The Horner-Wadsworth-Emmons (HWE) reaction is a modification of the Wittig reaction, where the triphenyl phosphorious ylides used in the traditional Wittig reaction, are replaced with phosphonate carbanions [13]. There have been discovered several advantages for the HWE reaction, compared to the Wittig reaction, including:[13]

1. Easier and cheaper preparation of the phosphonate carbanions compared to the phosphorous ylides.

2. The phosphonate carbanions are more nucleophilic than the ylides, which gives higher reactivity of the reactants, and the ability to reactions with practically all aldehydes and ketones under mild conditions.

3. Easier separation after the reaction, due to the water-soluble by-products of the HWE reaction.

The mechanism of the HWE olefination is illustrated in Scheme 2.2[13–17].

The HWE reaction gives a high (E)-selectivity of disubstituted alkenes, which can be maximized with increased size of the alkylgrups R and R' [13]. As both the nitrile- and alkene group is to be reduced later, the optimization of the *(E)/(Z)* ratio is not an important issue in this project.

2.1.2 Cyanomethylation

Cyanomethylation is the second route towards 3-arylpropaneamines, illustrated in Scheme 2.1. When acetonitrile is treated with a strong base in excess (LDA or BuLi), it is completely converted into the cyanomethyl anion, decreasing the chance of self-condensation [18]. The cyanomethyl anion acts as a nucleophile, and reacts with the benzyl bromide in a nucleophilic substition reaction, with bromide as the leaving group (LG)[19]. The proposed mechanism of the reaction is presented in Scheme 2.3 [18, 19]. An advantage of this approach, is that the resulting nitrile is saturated, and therefore requires a single reduction to yield the target amine in the last synthetic step.

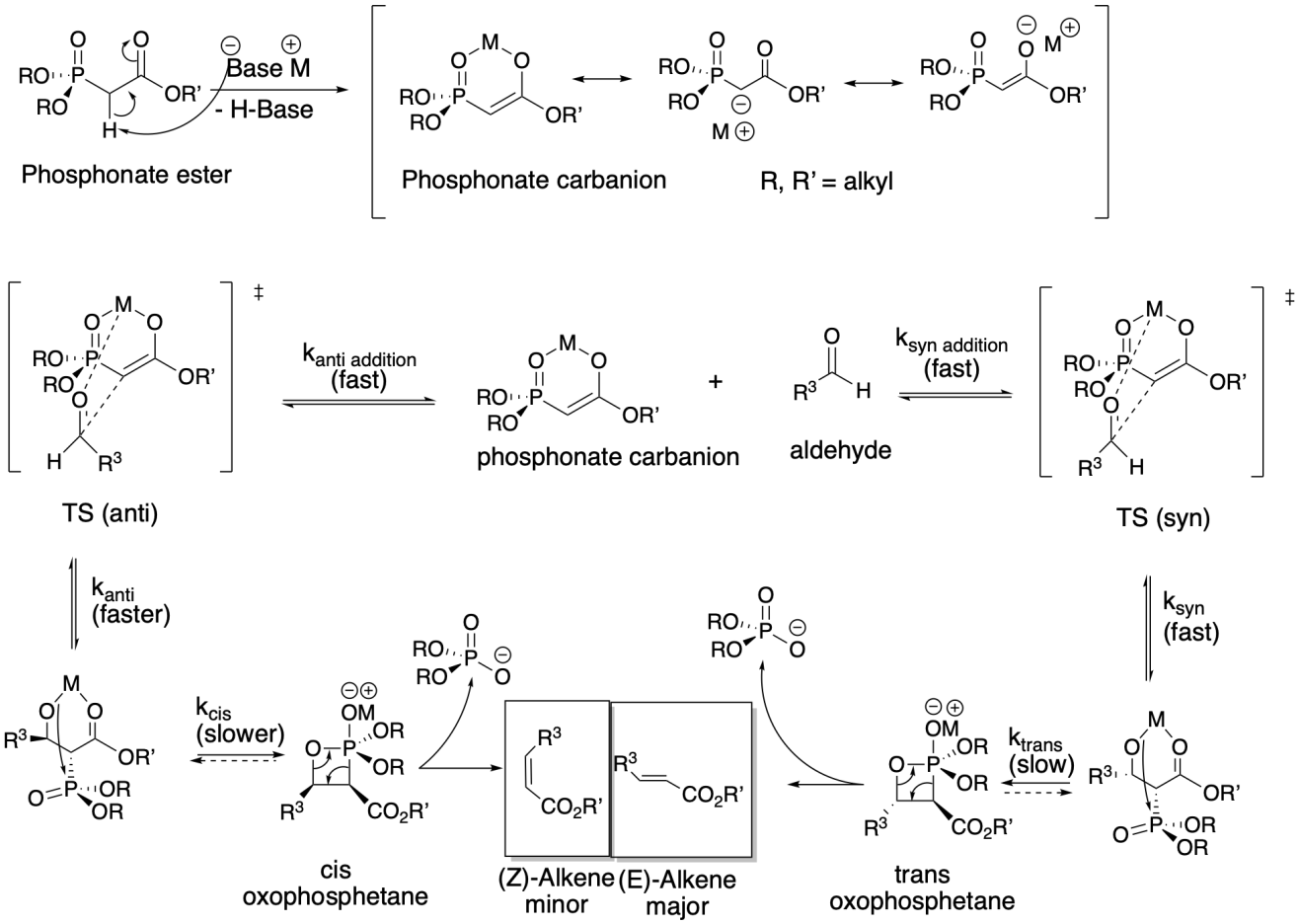

Scheme 2.2: The proposed mechanism of the Horner-Wadsworth-Emmons reaction [13–17].

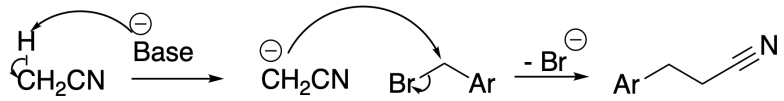

Scheme 2.3: The proposed mechanism of the cyanomethylation of benzyl bromide [18, 19].

2.1.3 The Knoevenagel reaction

The Knoevenagel reaction follows an aldol-like reaction mechanism, catalyzed by a weak base [13]. The typical features of the reaction, is that an active methylene compund is treated with a weak base (amines are often used), and so attacks the carbonyl carbon of an aldehyde or ketone, to yield a α, β-unsaturated product [13].

The mechanism of the reaction depends on the catalyst/base used in the reaction. The mechanism of the reaction with use of tertiary amines as the catalyst, was found in 1904 by A. C. O. Hann and A- Lapworth [20]. In this case, the beta-hydroxydialkyl intermediate is expected, but when primary- and secondary amines are used, an iminium salt is made from the aldehyde and amine (see Scheme 2.4). The final step of the mechanism is a 1,2 elimi-

nation, where water is released, giving the α,β-unsaturated product in the end. The water is removed by azeotropic distillation or addition of molecular sieves, or other drying agents. The best choice of solvent for this reaction is aprotic solvents, as the protic solvents will inhibit the last 1,2-elimination step [13]. The mechanism of the Knoevenagel condensation is illustrated in Scheme 2.4 [13, 20–35].

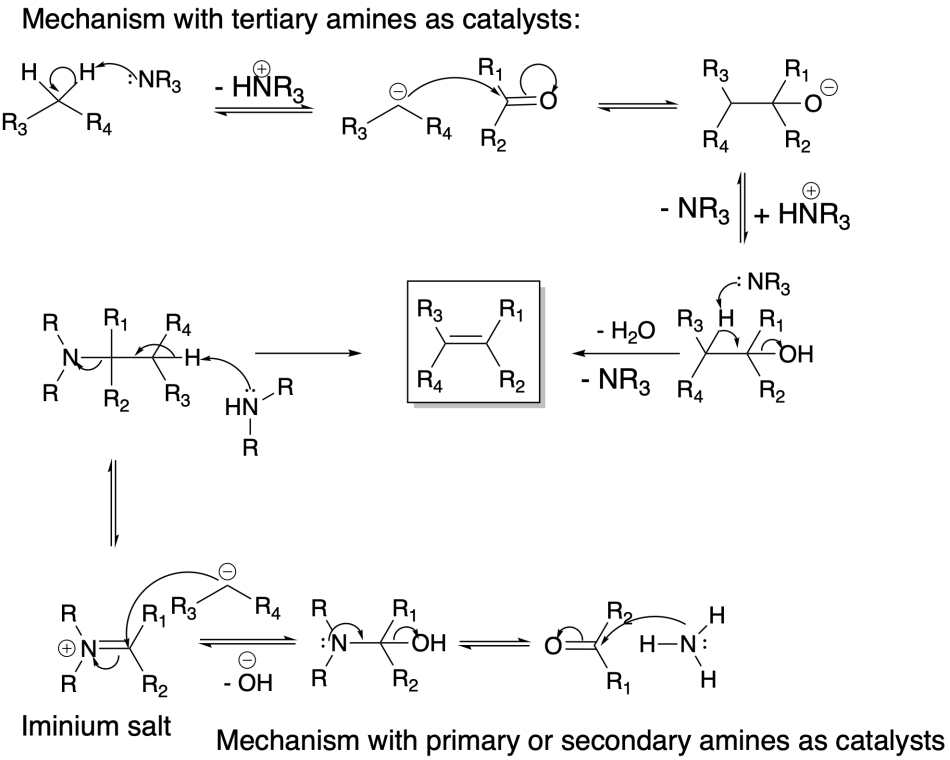

Scheme 2.4: The proposed mechanism of the Knoevenagel condensation with tertiary, secondary or primary amines as catalyst. [13, 20–35]

The Knoevenagel reaction, as the HWE reaction, gives a mixture of *(E)*- and *(Z)*- products. The *(E)*/*(Z)* ratio is mostly determined by steric effects, and the thermodynamic most stable product, will be the major product.

2.1.4 Reducing agents

There are multiple ways of yielding the target amines by reducing the nitriles made in the first step of the synthetic routes (Scheme 2.1), and this section will cover some alternatives. For the Knoevenagel- and HWE route, where the cyanoacrelate is to be reduced, there have been reported simultaneous reduction of the double bond and the nitrile with the use of Raney-Ni [36], SmI_2 [37], or $NaBH_4 \cdot CoCl_2$ [38] as the reducing agent. The reducing agents used in

this study are two different borane approaches [9, 39], and two different $LiAlH_4$ methods [8]. The theory behind- and the mechanisms of these methods will be discussed in the following sections.

Reduction with borane as the reducing agent

Hydrobration of an alkene is a starting point of several important synthetic procedures, and led to the Nobel Price in 1979 to Herbert. C Brown, for the discovery of the hydroboration reaction [40]. The hydroboration follows an *anti-Markovnikov* regiochemistry, meaning that the borane atom will attack the least substituted carbon. The mechanism of the hydroboration is illustrated in Scheme 2.5 [40].

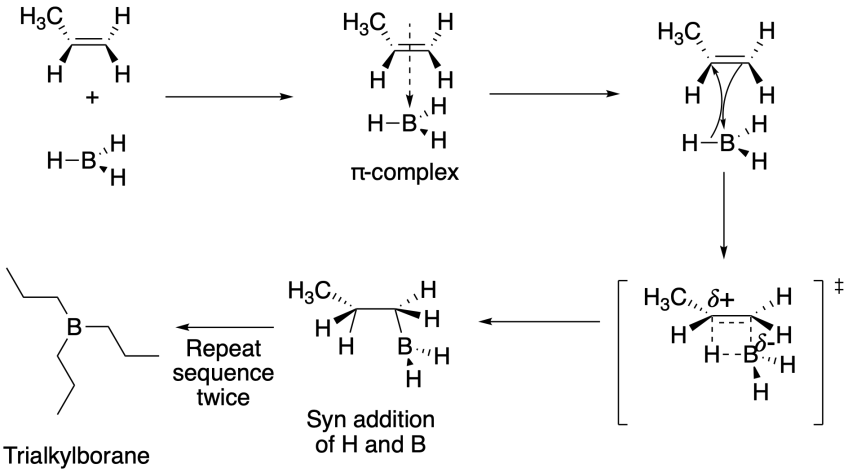

Scheme 2.5: The proposed mechanism of the hydroboration of an alkene [40].

The alkylborane is normally not the final product in the synthesis, and are usually oxidized and hydrolyzed to yield alcohols as the final product. Another approach is to treat the trialkylborane with acetic acid and heat, to cause cleavage of the C-B bond and replace it with a hydrogen atom [40]. This will give an alkane as the final product (Scheme 2.6). Hydroboration is also used to reduce nitriles to primary amines [13, 39], following the same mechanisms as Scheme 2.5 and 2.6 illustrates.

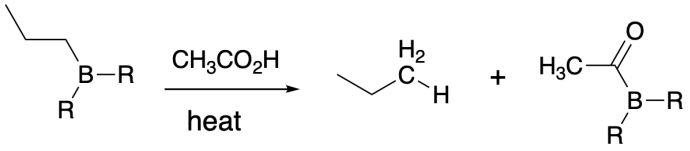

Scheme 2.6: Protonolysis of alkylborane [40].

Reduction with $LiAlH_4$ as the reducing agent

Lithium aluminum hydride (LAH) is a strong hydride donor, which reduces carboxylic acids and esters to primary alcohols [40, 41]. As LAH reacts violently with proton donors or other weakly acidic solvents as water and alcohols, great care must be taken [40]. Drying of solvents and equipment are therefore important prior to the experiment.

The mechanism of the nitrile reduction with LAH as the reducing agent, is presented in Scheme 2.7 [40, 41]. LAH donates two hydrides to the nitrile carbon, giving an intermediate with the negative charge located between the nitrogen and alumnium atom. An aqueous workup yields the primary amine.

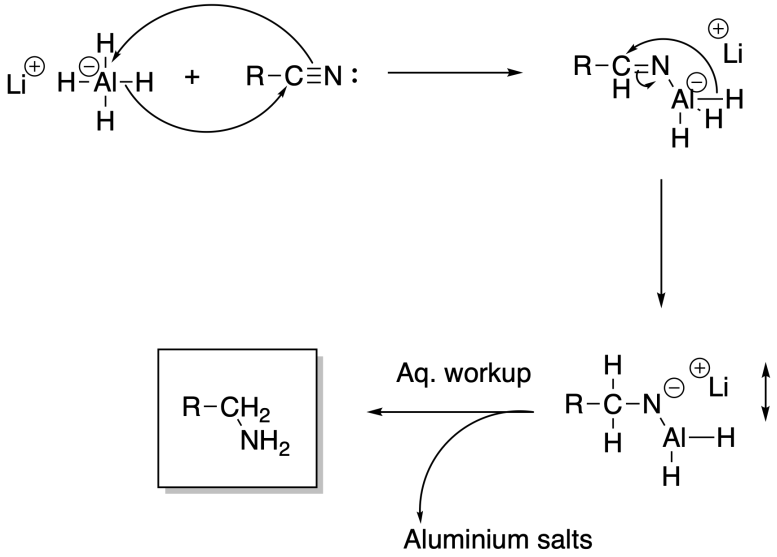

Scheme 2.7: Nitrile reduction, with $LiAlH_4$ as the reducing agent [40, 41].

The workup after a LAH reduction could be messy, giving difficult emulsions. A way around that problem is to use the Fieser's workup [42, 43], which goes like this: To work up a reaction where x g LAH is used,

1. Dilute with ether and cool to 0 °C.
2. Add x mL water.
3. Add x mL 15% aqueous sodium hydroxide.
4. Add 3x mL water
5. Warm up to rt (room temperature), and stir for 15 min.

6. Dry over sodium sulphate (or other drying agents).

7. Stir for 15 min and filter off the salts.

2.2 Amide coupling reactions

There are several popular starting compounds in these amide coupling reactions, including acyl chlorides, carboxylic acids, esters or acid anhydrides [40, 44]. All these methods involve nucleophilic addition-elimination reactions, by ammonia or amines, at an acyl carbon. Acid chloride is the most reactive option of the ones listed, and is one of the most popular approaches for amide synthesis (Scheme 2.8) [40].

The underlying strategy of most amide couplings, where carboxylic acid and amines are involved, is to activate the carboxylic acid by replacing the hydroxy group with a better leaving group [44]. The amine may then easily do the addition-elimination reaction on the resulting intermediate, and then yield the desired amide.

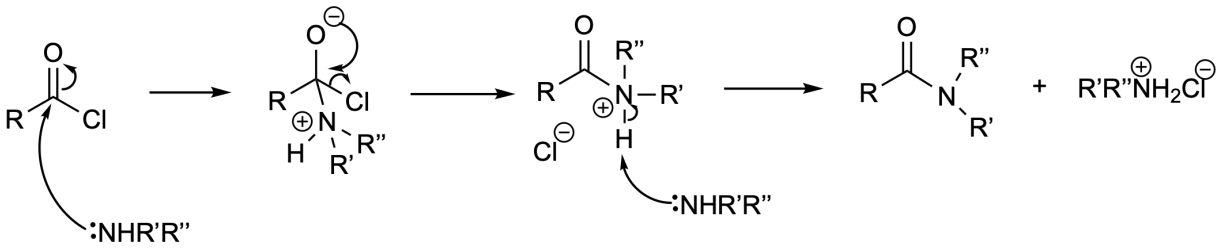

Scheme 2.8: Amide synthesis from acid chloride [40].

When amides are formed from esters, the ester undergoes an addition-elimination reaction of the acyl carbon when treated with ammonia (*ammonolysis*), or primary- and secondary amines (*aminolysis*) [40]. These reactions go slowly compared to that of the acid chlorides mentioned earlier, because the alkoxy group is not as good leaving group as the chloride ion. Even so, this method has been successful in organic syntehsis [40, 45]. The reaction mechanism of the aminolysis of an ester is presented in Scheme 2.9.

There are also alternative coupling reagents available, where one group is based on benzotriazoles and uronium/aminium salts (Scheme 2.10.

E. Valeur and M. Bradley have reviewed the use of these reagents [44, 46], and found that some of them perform very well compared to the more traditional methods. HATU

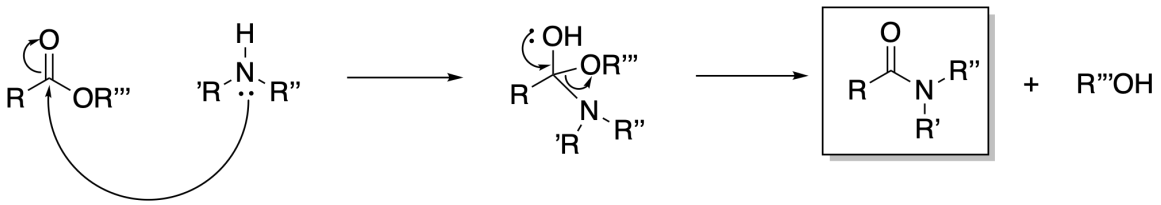

Scheme 2.9: Aminolysis of an ester [40].

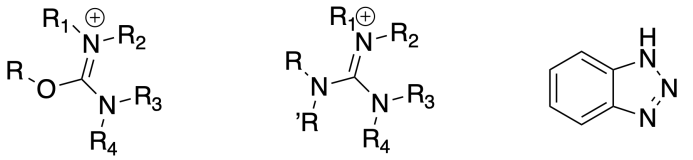

Scheme 2.10: Uronium- and aminium salts, and benzotriazole.

(1-[Bis(dimethylamino)methylene]-1H-1,2,3-triazolo[4,5-b]pyridinium 3-oxid hexafluorophosphate) was one of these coupling reagents that gave best results, giving fast kinetics and good yields [44, 46]. The HATU structure, and other similar coupling reagents, are illustrated in figure 2.1.

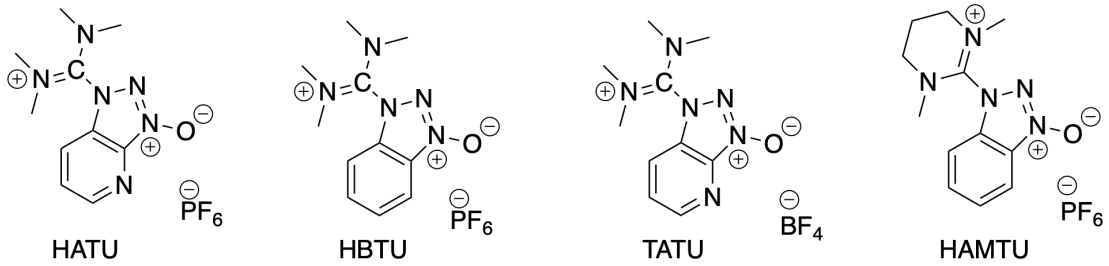

Figure 2.1: Some benzotriazole and uronium/aminium based coupling agents.

The starting material in these coupling reactions are also carboxylic acids, but they are not ammonolyzed/aminolyzed prior to the amide coupling. The carboxylic acid is deprotonated by a base, before the reaction subsequently follows the mechanism given in Scheme 2.11 [44].

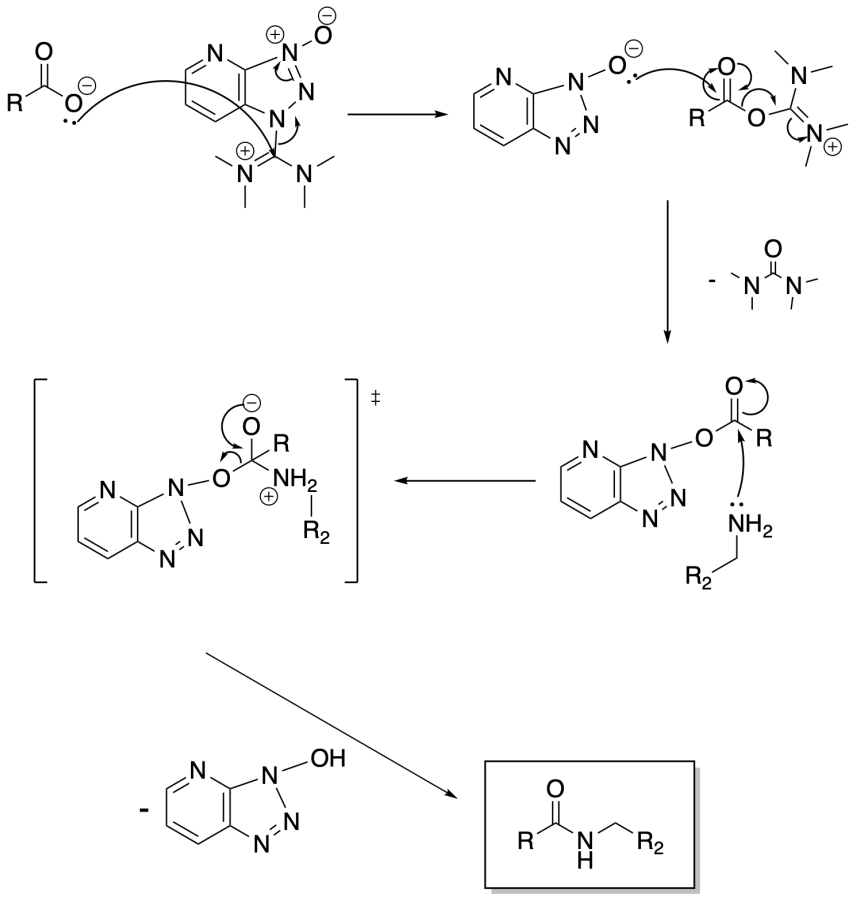

Scheme 2.11: HATU coupling mechanism.

3. Results and Discussion

In this chapter all synthesis towards the target amines **1a-c**, and the amide **5**, are presented. The synthetic work done in this project, follows the route presented in Scheme 3.1. Structural analysis of **1-ac**, **2a-c** and **5** may be found in the end of this chapter, and all spectroscopic data for the compounds are given in the appendices.

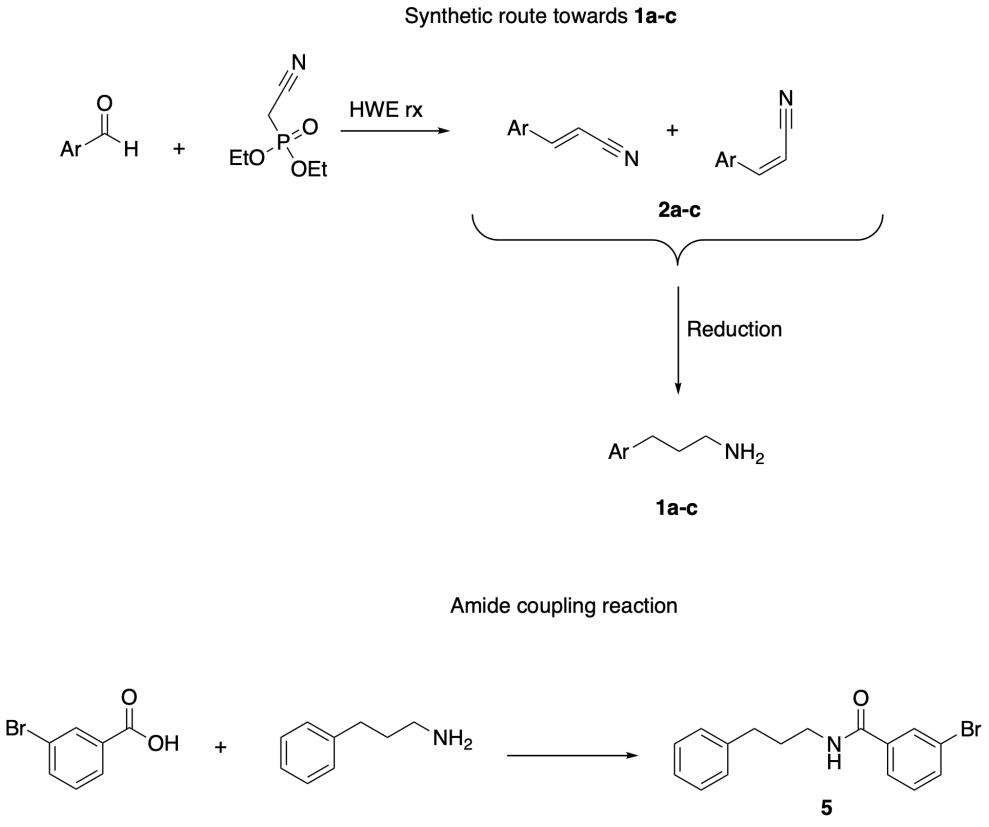

Scheme 3.1: The plan for the synthesis of **1a-c** and **5**.

3.1 The Synthesis of 3-(Fluorophenyl)acrylonitrile (2a-c)

As the synthetic route of the preliminary study did not give satisfying yields and purity, an alternative method for the first synthetic step was necessary. The Horner-Wadsworth-Emmons reaction had given 90% yield in a similar reaction in another study, and was therefore a promising reaction to proceed with [9]. The chosen strategy was to optimize the reaction and purification method, using 4-fluorobenzaldehyde as the starting material (Scheme 3.2). The reactivity of the other benzaldehydes with the fluorine in *meta-* and *ortho* position were estimated to be similar to that of the benzaldehyde with fluorine in *para* position.

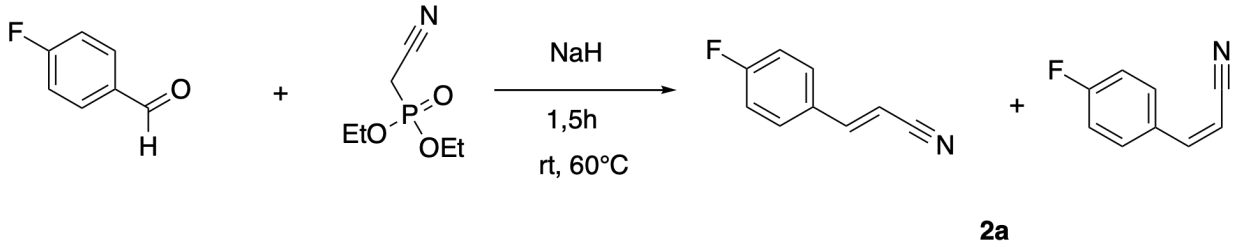

2a

Scheme 3.2: The HWE reaction of 4-fluorobenzaldehyde to yield **2a**.

3.1.1 Initial experiments

The first experiment with the HWE reaction was done in a 1 gram-scale, with 1.1 equivalents (eqv) of both sodium hydride and diethyl(cyanomethyl)phosphane, which gave 3-(4-fluoro)acrylonitrile (**2a**) as white crystals in 54% yield. The crude product was pure according to ^{1}H-NMR, and showed a E/Z ratio of 3/1.

After a successful first experiment, the same reaction was performed in a 2 gram-scale with the same conditions as the initial experiment. This time, the mixture suddenly turned dark red during the reaction, and so the crude product appeared as dark red crystals in 52% yield. The crystals looked as pure as the first experiment on ^{1}H-NMR, but a recrystallization of the crude product was attempted in order to remove the colour, using water as the solvent. This gave no crystallization at all after 24 h, and the product was extracted back to the organic layer with ethyl acetate.

The red colour of the mixture in the second reaction was thought to be a coincidence, and so the reaction was performed once more, this time in a 3 gram-scale. The reaction mixture

turned red once again, and gave dark red, almost purple crystals in 82% yield. The crude yield was better than previous experiments, but the ^{1}H-NMR spectrum also showed a lot of impurities on the base line. After flash column chromatography (ethyl acetate/n-pentane, 1:7), the pure E-product was isolated and used in the initial experiments of the reduction (section 3.2). The dark colour had high affinity to the silica gel, and was luckily therefore easy to remove. The rest of the product was still not pure though, as there had appeared an unknown spot on the Thin Layer Chromatography (TLC) plate during the column, most likely due to dirty equipment. The contaminated product was not further purified.

Even though the dark red colour still was an unsolved case, a 2 gram-scale synthesis of **2a** was done once more, giving the crude product in 73% yield. A different bottle of sodium hydride was used in these experiments, and the red colour did not appear. In fact, **2a** again appeared as white crystals. This could indicate that the sodium hydride bottle could have been contaminated, and therefore discoloured the products in the previous experiments. It could have been interesting to investigate this matter further, but unfortunately there was no time for that in this project. After purification with flash column chromatography (ethyl acetate/n-pentane, 1:7), **2a** was provided as white crystals in 48% yield. An overview of all initial experiments of the HWE reaction is given in table 3.1.

Table 3.1: Initial experiments of the HWE reaction.

Experiment no.	Eqv base	Eqv phosphonate ester	crude yield
1	1.1	1.1	54%
2	1.1	1.0	52%
3	1.3	1.1	52%
4	2.0	1.9	73%

From the table it can be seen that experiment 4 gave far higher crude product yield than the previous attempts. It is difficult to conclude a sure reason for this, because both the amount of base- and phosphane ester were doubled at the same time. The plan was to add 3 g of the arylaldehyde, but as there were just 2 g left in the bottle, the ratio was shifted for both the base and phosphonate ester. Also, the ^{1}H-NMR spectrum of the crude product of experiment 4, showed far more impurities than before, which definitely had an effect on the crude product yield (figure 3.1).

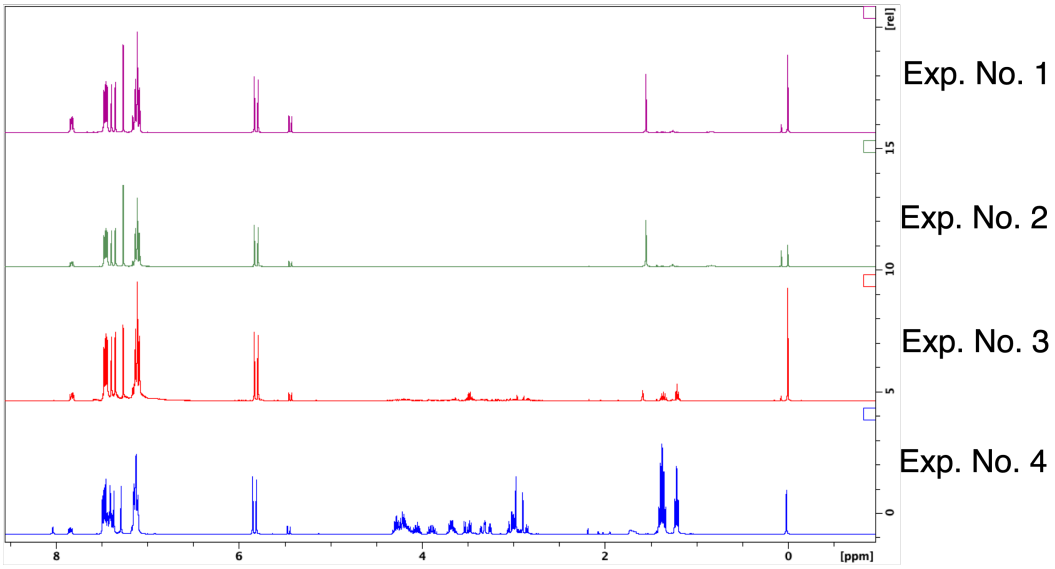

Figure 3.1: Comparison of the ^{1}H-NMR spectra of the crude products of **2a**.

3.1.2 Preparation of the *meta* and *ortho* analouges 2b and 2c

A 2 gram-scale synthesis of the 3-phenylacrylonitrile with fluorine in *meta*- and *ortho* position was done (**2b** and **2c**), giving crude products in 80%- and 68% yield, respectively. , **2b** appeared as partly crystalized, yellow oil, and **2c** as colorless oil.

The ^{1}H-NMR spectrum of the crude product of both **2b** and **2c** showed some noise at the base line, and purification was therefore necessary. For both **2b** and **2c**, the same eluent system was used in the flash column chromatography (ethyl acetate/n-pentane, 1:7), giving a pure product in 69%- and 53% yield, respectively. Because previous experiments had shown that the crystals of **2a** had been more soluble in ethyl acetate than diethyl ether, ethyl acetate was used in the work-up for **2b** as a test. That is a possible reason the yield was better for **2b** than of **2c**. The ^{1}H-NMR spectrum of **2b** and **2c** also showed an E/Z ratio of 71/29 and 70/30, respectively.

The overall effect of the fluorine's position at the phenyl ring is yet unknown, but the physical observation done so far indicates that the 3-phenylacrylonitrile crystalizes most easily when the fluorine is in the *para* position. At room temperature (rt), **2a** was purely crystalline, **2b** partly crystalline, and **2c** an oil.

Table 3.2: An overview of the HWE reaction results, yielding **1b**, **2b** and **3b**.

Compound	Crude yield	Yield after purification	Appearance
2a	73%	48%	White crystals
2b	85%	68%	Partly crystalized colorless oil
2c	68%	53%	Colorless oil

3.2 The Synthesis of 3-Fluorophenylpropan-1-amines (1a-c)

The last step of the two-step synthesis, was a double reduction of the acrylonitriles **2a-c**, to yield the primary amines **1a-c** (Scheme 3.3).

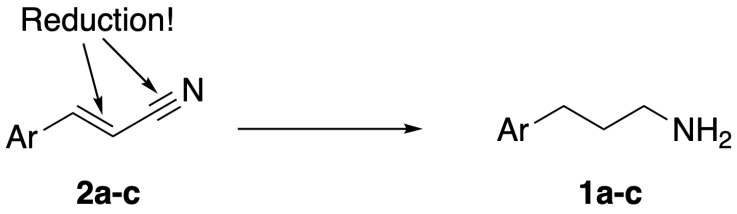

Scheme 3.3: Reduction reaction of **2a-c** to the target amines **1a-c**.

In the beginning of the project, this was considered to be the easy part of the synthesis, but it turned out to be more complicated than expected. The choice of the reducing agent for the reaction was not straight forward, and the different alternatives considered in this project is discussed in the following sections.

3.2.1 Lithium aluminium hydride (solution)

The first reduction attempt done in this project, was a reduction of **2a** with 2 M (moles/litres) lithium aluminium hydride (LAH) in tetrahydrofurane (THF), in order to yield **1a** (Scheme 3.4).

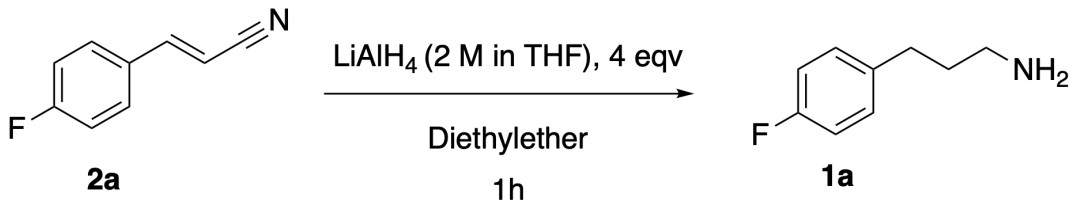

Scheme 3.4: Reduction of **2a** with 2M LAH in THF

The procedure was originally from Arutyunyan *et.al* [8], but because there were no solid LAH available in the lab at the time, 2M LAH in THF seemed like a good alternative. For some rea-

son, the reaction did not go as planned, even though the TLC indicated full conversion. From the ^{1}H-NMR spectrum, there seemed to be a solubility problem, and none of the expected amine peaks appeared [47]. As the reference spectra of **1a** are run in CDCl3, the amines are expected to be soluble in CDCl3, and so alternative reducing agents were considered.

3.2.2 Diborane

After a failed reduction with LAH in THF, diborane (B_2H_6) made in situ were tried with Van Wagener *et. al*'s procedure (Scheme 3.5) [9].

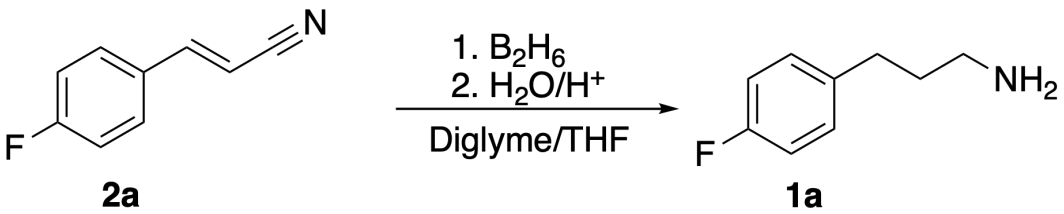

Scheme 3.5: Reduction of **2a** with diborane.

This reaction required a complicated setup, where an addition funnel were charged with $NaBH_4$ in bis(2-methoxyethyl) ether (diglyme), and added to Et_2OBF_3 in diglyme. The B_2H_6-gas produced were transferred to the reaction flask, containing **2a** in THF, using a low flow of N_2-gas. Figure 3.2 illustrates the setup used in the reaction [48].

$NaBH_4$ had quite low solubility in diglyme, which made some of the $NaBH_4$ stuck on the walls of the addition funnel. This most likely had a negative effect on the yield of the reaction.

According to Van Wagener *et. al.* this reduction should take 30 min [9]. The reaction was difficult to monitor, because of the closed system containing such a toxic gas as diborane. It was considered too hazardous to take out samples during the reaction, so after 1 h (hour), the reaction was quenched blindly. After an acid-base extraction, the crude product was collected as a yellow oil. From the ^{1}H-NMR spectrum, it could be seen evidence of some formation of the unsaturated version of **1a** (only the cyano group from **2a** was reduced), but due to the high risk, low yields and the difficulties of monitoring the reaction, this reaction was not pursued.

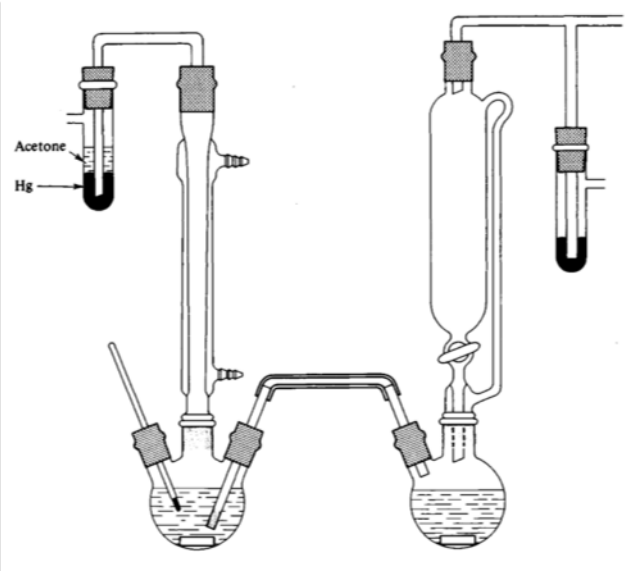

Figure 3.2: The setup of the diborane reduction [48]. The diborane was produced in the flask on the right hand side, which was transferred to the reaction flask on the left hand side.

3.2.3 BH_3-THF complex

An other reducing agent which essentially follows the same mechanism as diborane, is the BH_3-THF complex, which is commercially available. The advantage of this reagent, compared to the diborane reaction, was that no gas injection to the reaction was necessary. This was absolutely worth a try, and so a reduction of **2a** was done, using a procedure from Scott *et. al* (Scheme 3.6) [39].

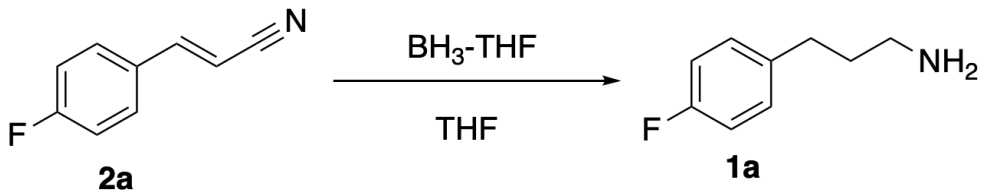

Scheme 3.6: Reduction of **2a** with BH_3-THF.

The procedure was quite simple: **2a** solved in THF was to be treated with dropwise addition of BH_3-THF, before the reaction mixture was to be stirred under reflux for 2.5 h. After 3 h though, no conversion could be seen on the TLC-plate. The ^{1}H-NMR spectrum confirmed that no reaction had occured, and the BH_3-THF strategy was set aside.

A reduction of **2a** to yield **1a**, using borane was a longshot after all. Earlier reports of reductions with BH_3-THF or B_2H_6, describe reductions of either alkenes [49], or nitriles [39, 50, 51], but not both in the same reaction. The relatively complicated mechanism (see section

2.1.4), may be one reason the reaction did not go as planned.

3.2.4 Lithium aluminium hydride (solid)

Since none of the previous attempts of reducing the cinnamonitrile had given satisfying results so far, it was time to sit down and review the matter one more time. It was incomprehensible that all these reactions should break down like this, so a new attempt using the first reducing agent, lithium aluminium hydride, was done. This time, a brand new bottle of solid LAH was opened, so no contamination of any kind could affect the results this time. The procedure was from Arutyunyan *et. al* [8], and the reaction was done in 150 mg scale.

The LAH powder was solved in diethyl ether. **2a**, which also was mixed with diethyl ether, was dropwise added to the LAH/ether mixture, as the temperature was kept at 0 °C. After stirring for 1 h, only one spot was seen at the baseline of the TLC-plate, and the reaction was quenched with water and worked up using Fieser's method (originally from Micovic et al. from 1953) [42]. This gave **1a** as a yellow oil in 70% yield. The ^{1}H-NMR spectrum of the crude product confirmed **1a**, but also the partly reduced 3-(4-fluorophenyl)prop-2-en-1-amine (figure 3.3).

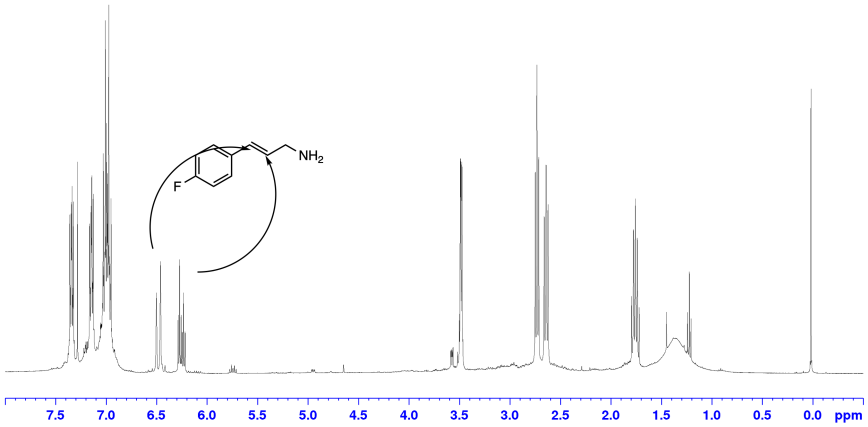

Figure 3.3: The crude ^{1}H-NMR spectrum of **1a**.

A purification of the crude product of **1a** was tried using flash column chromatography (10% MeOH in dichloromethane (DCM), 1% triethylamine), which gave unsatisfying results due to an insufficient eluent system.

Even though the purification did not give pure product in the first try, the reduction method

using solid LAH was concluded to be the best alternative for this reaction after all. For later studies on this reaction though, alternatives as Raney-Ni, SmI_2 or $NaBH_4 \cdot CoCl_2$ should be considered as reducing agents for these simultaneous reductions [36–38]. Further purification of the target amines will be covered in the next section.

3.2.5 Purification of the target amines

The purification of the target amines has been troubling. Flash column chromatography has been the primary method for purification of organic compounds in the project, but because of the high affinity to the silica, there has been difficult to find an appropriate eluent system for these amines. 10% MeOH in DCM with 1% triethylamine has been the only system that has moved the amine spot off the baseline on the TLC plate, but the separation was still not ideal. Scott *et. al* used 4% 7M NH_3/MeOH in DCM as their eluent system, with great yields (<70%) [39]. 7M NH_3/MeOH is commercially available, and was tried ordered for this project. The delivery time was too long, so that option was therefore not applicable this time, but should absolutely be considered as an option in later studies.

Distillation is often an option when it comes to purification of organic compounds, but it often requires a lot of material to make good yields. An alternative approach was ball tube distillation, which was at the end used to purify all target amines. The yields of **1a-c** after purification with ball tube distillation are presented in table 3.3.

Table 3.3: An overview of the results, yielding the final target amines **1a-c**.

Compound	Crude Yield	Yield after purification	Apperance
1a	70%	41%	colorless oil + white crystals
1b	67%	18%	colorless oil
1c	49%	25%	colorless oil

As table 3.3 shows, the crude product yields of **1a** and **1b** was fairly good

3.3 Synthesis of 3-bromo-*N*-(3-phenylpropyl)benzamide (5)

The target amines **1a-c** will be reagents in an amide coupling reaction, in another step towards the potential TMK inhibitor made by other students and researchers in the research

group. 3-Phenylpropan-1-amine was used instead of **1a-c**, in order to establish a good method before using the actual target amines. The initial strategy was to copy Bakka *et.al*'s procedure, and mix the 3-phenylpropan-1-amine and methyl 3-bromobenzoate in methanol, for so to stir under reflux for 2 days [45].

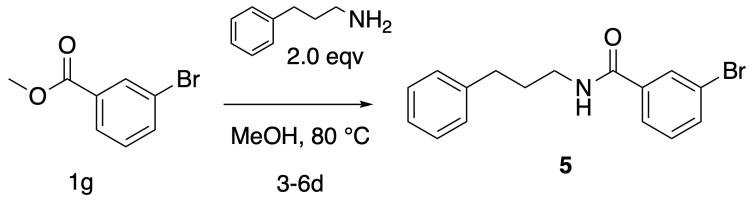

Scheme 3.7: Amide coupling reaction from methyl 3-bromobenzoate.

This reaction was slow, and after 6 days of reflux, the reaction was quenched before all starting material had reacted. Ultimately, it gave 3-bromo-*N*-(3-phenylpropyl)benzamide (**5**) in only 13% yield after purification, which was not acceptable. The purity of the product was not good enough either (from ^{1}H-NMR spectrum), so an alternative method had to be found.

In M. Baumann's doctoral thesis, the HATU reagent in combination with the Hünig's base (N,N-Diisopropylethylamine) (figure 3.4) was used in an amide coupling reaction, giving acceptable yields [52].

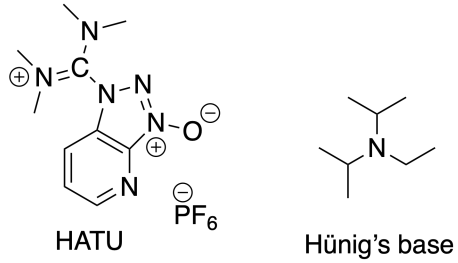

Figure 3.4: The HATU reagent and Hünig's base used in the amide coupling reaction.

The HATU coupling, explained in section 2.2, therefore seemed to be the best solution of this problem. The Hünig's base and the HATU reagent was first added to a stirring solution of 3-bromobenzoic acid in DCM, before 3-phenylpropan-1-amine was added 40 minutes later (Scheme 3.8).

The reaction was stirred for 48 h, and the reaction was stopped by removal of the solvent. The residue was dissolved in water and ethyl acetate, before the aquatic layer was extracted with ethyl acetate. The organic layer was then washed, and gave 3-bromo-*N*-(3-phenylpropyl)benzamide in 54% yield after purification with flash column chromatography (pentane/ethyl acetate,

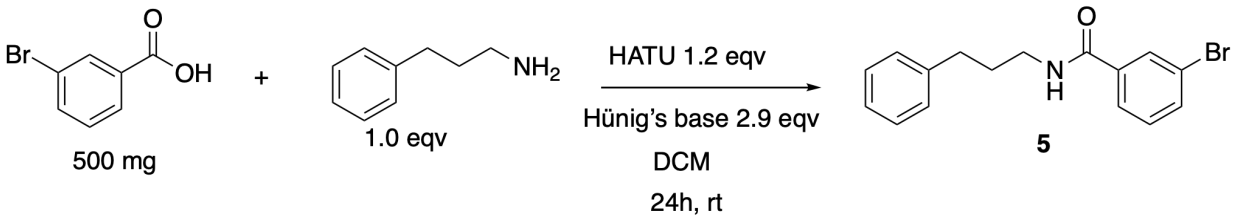

Scheme 3.8: Amide coupling reaction, using HATU and Hünig's base.

3:1). The results were consistent with Baumann's results (59% yield) [52], and this approach was therefore concluded to be the best alternative, regarding the amide coupling.

Further optimization of this reaction was not prioritized in this project, as the main objective was to synthesize the amines **1a**, **2a** and **3a**. The purpose of doing this amide coupling reaction, was to show the application of the target amines on the way towards the real target: A new potential thymidylate kinase inhibitor.

3.4 Structural Analysis of Compound 2a

The compound **2a** has been characterized by MS and NMR (spectra in appendix A). High resolution, accurate MS spectrometry shows *m/z* 148.0564 $[M+H]^+$ for compound **2a**, where the calculated is 148.0563. This confirms that the molecular formula C_9H_6FN is correct. The structure of compound **2a** is illustrated in figure 3.5, which is used for the NMR analysis.

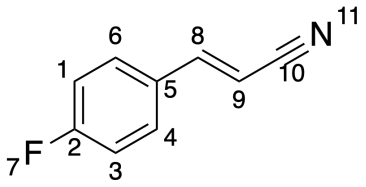

Figure 3.5: The numbering used for **2a**.

3.4.1 NMR

^{1}H-NMR spectra for both the *(Z)*- and *(E)*-product of **2a** have been found in the literature [53, 54]. The experimental ^{1}H-NMR data found for compound **2a** is consistent with this. The . A full characteristic of both the *(Z)*- and *(E)* product of **2a** was considered unnecessary, so the structural analysis of **2a** has, for the sake of order, only focused on the *(E)*-product of **2a**. This

is also done for the other nitrile analogues **2b** and **2c**. ^{1}H-NMR data , coupling constants and H,H-correlations (COSY) are given in table 3.4.

Table 3.4: ^{1}H-NMR data, coupling constants and COSY for compound **2a**.

Position	Multiplicity	Integral	^{1}H [ppm]	J [Hz]	COSY to [ppm]
1,3	t	2H	7.11	5.28	7,46
4,6	t	2H	7.46	8.62	7.11/7.37
8	d	1H	7.37	16.63	5.81/7.46
9	d	1H	5.81	16.64	7.37

^{13}C-NMR- and ^{19}F-NMR spectra for the *(E)*-product of **2a** have also been found [54], and are are also consistent with the experimental ^{13}C-NMR- and ^{19}F-NMR data found for **2a**. ^{13}C-NMR data, C,H-correlations (HSQC) and long distance C,H-correlations are given in table 3.5.

Table 3.5: ^{13}C-NMR data, HSQC and HMBC for compound **2a**.

Position	^{13}C [ppm]	J (C-F) [Hz]	HSQC to [ppm]	HMBC to position
1,3	116.4	22.4	7.11	1,3/2/4,6/5
2	164.4	253	-	1,3/4,6
4,6	129.4	8.74	7.46	1,3/4,6/8/9
5	129.9	8.78	-	/1,3/9
8	149.3	-	7.37	9/4,6
9	96.18	-	5.81	8
10	118.0	-	-	8/9

3.5 Structural Analysis of Compound 1a

The compound **1a** has been characterized by MS and NMR (spectra in appendix B). High resolution, accurate MS spectrometry shows *m/z* 154.1030 $[M+H]^{+}$ for compound **1a**, where the calculated is 154.1032. This confirms that the molecular formula $C_9H_{12}FN$ is correct. The structure of compound **1a** is illustrated in figure 3.6, which is used for the NMR analysis.

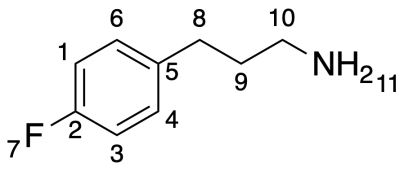

Figure 3.6: The numbering used for **1a**.

3.5.1 NMR

Two different ^{1}H-NMR spectra for **1a** has been found in the literature [47, 55], but the two are not consistent with each other. For instance, the signal for the amine protons seems to vary a lot. In one article the shift is reported at 2.25 ppm, but at 4.40 ppm in an other paper. A third paper, an article of Kurouchi *et.al*, reports ^{1}H-NMR-, ^{13}C-NMR- and ^{19}F-NMR data, which is consistent with the experimental NMR data found for compound **1a** [56]. ^{1}H-NMR data , coupling constants and H,H-correlations (COSY) are given in table **??**.

Table 3.6: ^{1}H-NMR data, coupling constants and COSY for compound **1a**.

Position	Multiplicity	Integral	^{1}H [ppm]	J [Hz]	COSY to [ppm]
1,3	m	2H	6.96	-	7.11/7.31
4	m	1H	7.11	-	6.96
6	m	1H	7.31	-	6.96
8	t	2H	2.61	7.95	1.72
9	m	2H	1.72	7.42	2.61/2.69
10	t	2H	2.69	7.15	1.72
11	s	2H	1.39	-	-

The experimental ^{13}C-NMR- and ^{19}F-NMR data are consistent with the literature [56]. ^{13}C-NMR data, C,H-correlations (HSQC) and long distance C,H-correlations are given in table 3.7.

Table 3.7: ^{13}C-NMR data, HSQC and HMBC for compound **1a**.

Position	^{13}C [ppm]	J (C-F) [Hz]	HSQC to [ppm]	HMBC to position
1	115.4	22.0	6.96	3/6
2	162.9	91.8	-	1/4/6
3	115.0	20.8	6.96	1/4
4	129.6	7.94	7.11	8/1/3
5	137.7	3.04	-	9/8/1/3
6	127.6	8.08	7.31	-
8	32.39	-	2.61	9/10/1/3
9	35.44	-	1.72	8/10/
10	41.61	-	2.69	9/8

3.6 Structural Analysis of Compound 2b

The compound **2b** has been characterized by MS and NMR (spectra in appendix C). High resolution, accurate MS spectrometry shows *m/z* 147.0481 $[M]^+$ for compound **2b**, where the calculated is 147.0484. This confirms that the molecular formula C_9H_6FN is correct. The structure of compound **2b** is illustrated in figure 3.7, which is used for the NMR analysis.

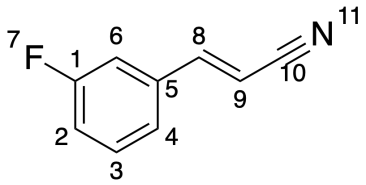

Figure 3.7: The numbering used for **2b**.

3.6.1 NMR

^{1}H-NMR spectra for **2b** have been found in the literature [57]. The experimental ^{1}H-NMR data found for compound **2b** is consistent with this. ^{1}H-NMR data, coupling constants and H,H-correlations (COSY) are given in table 3.4.

Table 3.8: ^{1}H-NMR data, coupling constants and COSY for compound **2b**.

Position	Multiplicity	Integral	^{1}H [ppm]	J [Hz]	COSY to [ppm]
2	m	1H	7.14	-	7.23/7.38
3	m	1H	7.38	5.78	7.14/7.23
4	d	1H	7.23	7.73	7.14/7.38
6	s	1H	7.13	-	-
8	d	1H	7.35	16.75	5.89
9	d	1H	5.89	16.64	7.35

^{13}C-NMR- and ^{19}F-NMR spectra for **2b** have also been found [57], and are are also consistent with the experimental ^{13}C-NMR- and ^{19}F-NMR data found for **2b**. ^{13}C-NMR data, C,H-correlations (HSQC) and long distance C,H-correlations are given in table 3.9.

Table 3.9: ^{13}C-NMR data, HSQC and HMBC for compound **2b**.

Position	^{13}C [ppm]	J (C-F) [Hz]	HSQC to [ppm]	HMBC to position
1	163.00	248	-	2/3/8
2	113.73	22.6	7.14	4/8/9
3	130.83	8.14	7.38	1/5
4	123.51	2.87	7.23	2/8/9
5	135.64	8.05	-	3/8/9
6	118.15	21.2	7.13	2/4//8/9
8	149.19	3.02	7.35	2/4/9/
9	97.97	-	5.89	8

3.7 Structural Analysis of Compound 1b

The compound **1b** has been characterized by MS and NMR (spectra in appendix D). High resolution, accurate MS spectrometry shows *m/z* 154.1031 $[M+H]^+$ for compound **1b**, where the calculated is 154.1032. This confirms that the molecular formula $C_9H_{12}FN$ is correct. The structure of compound **1b** is illustrated in figure 3.8, which is used for the NMR analysis.

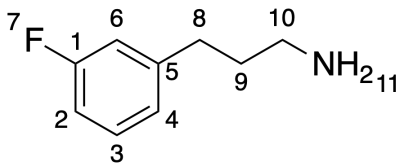

Figure 3.8: The numbering used for **1b**.

3.7.1 NMR

^{1}H-NMR-, ^{13}C-NMR- and ^{19}F-NMR spectra for **1b** has been found in the literature [58]. Experimental NMR data found for compound **1b** are consistent with this literature. ^{1}H-NMR data, coupling constants and H,H-correlations (COSY) are given in table 3.10.

^{13}C-NMR data, C,H-correlations (HSQC) and long distance C,H-correlations are given in table 3.11.

Table 3.10: ^{1}H-NMR data, coupling constants and COSY for compound **1b**.

Position	Multiplicity	Integral	^{1}H [ppm]	J [Hz]	COSY to [ppm]
2	m	1H	6.87	-	7.21
3	q	1H	7.21	-	6.87/6.95
4	d	1H	6.95	-	7.21
6	s	1H	6.86	-	-
8	t	2H	2.63	7.54	1.74
9	m	2H	1.74	7.28	2.63/2.70
10	t	2H	2.70	7.03	1.74
11	s	2H	1.45	-	-

Table 3.11: ^{13}C-NMR data, HSQC and HMBC for compound **1b**.

Position	^{13}C [ppm]	J (C-F) [Hz]	HSQC to [ppm]	HMBC to position
1	162.9	245	-	2,6/4
2	112.6	21.4	6.86	6/4/3
3	129.7	8.81	7.21	4
4	124.0	2.95	6.95	8/2/6/3
5	144.7	7.42	-	9/8/4/2
6	115.1	20.8	6.87	8/2/4/3
8	32.95	1.42	2.63	9/10/6/4
9	35.00	-	1.74	8/10
10	41.58	-	2.70	9/8

3.8 Structural Analysis of Compound 2c

The compound **2c** has been characterized by MS and NMR (spectra in appendix E). High resolution, accurate MS spectrometry shows *m/z* 148.0561 $[M+1]^{+}$ for compound **2c**, where the calculated is 148.0563. This confirms that the molecular formula C_9H_6FN is correct. The structure of compound **2c** is illustrated in figure 3.9, which is used for the NMR analysis.

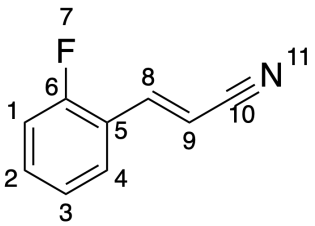

Figure 3.9: The numbering used for **2c**.

3.8.1 NMR

^{1}H-NMR spectra for **2c** have been found in the literature [59]. The experimental ^{1}H-NMR data found for compound **2c** is consistent with this. ^{1}H-NMR data , coupling constants and H,H-correlations (COSY) are given in table 3.12.

Table 3.12: ^{1}H-NMR data, coupling constants and COSY for compound **2c**.

Position	Multiplicity	Integral	^{1}H [ppm]	J [Hz]	COSY to [ppm]
1,4	m	2H	7.43	-	7.13/7.20
2	t	1H	7.13	9.28	7.20/7.43
3	t	1H	7.20	7.64	7.13/7.43
8	d	1H	7.48	16.84	6.04
9	d	1H	6.04	16.79	7.48

^{13}C-NMR- and ^{19}F-NMR spectra for **2c** were also found in the same article [59], and are are also consistent with the experimental ^{13}C-NMR- and ^{19}F-NMR data found for **2c**. ^{13}C-NMR data, C,H-correlations (HSQC) and long distance C,H-correlations are given in table 3.13.

Table 3.13: ^{13}C-NMR data, HSQC and HMBC for compound **2c**.

Position	^{13}C [ppm]	J (C-F) [Hz]	HSQC to [ppm]	HMBC to position
1	132.70	8.93	7.43	4
2	116.46	21.9	7.13	3
3	124.74	3.70	7.20	2
4	128.71	2.88	7.43	1/9
5	121.66	11.2	-	2/3/9
6	161.00	255	-	2/8
8	143.61	2.43	7.48	1/9
9	99.28	9.35	6.04	8
10	118.01	-	-	8/9

3.9 Structural Analysis of 1c

The compound **1c** has been characterized by MS and NMR (spectra in appendix F). High resolution, accurate MS spectrometry shows *m/z* 154.1022 $[M+1]^{+}$ for compound **1c**, where the calculated is 154.1032. This confirms that the molecular formula $C_9H_{12}FN$ is correct. The structure of compound **1c** is illustrated in figure 3.10, which is used for the NMR analysis.

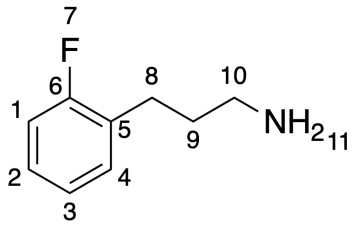

Figure 3.10: The numbering used for **1c**.

3.9.1 NMR

^{1}H-NMR spectra for **1c** has been found in the literature [60]. Experimental NMR data found for compound **1b** are consistent with this literature. ^{1}H-NMR data, coupling constants and H,H-correlations (COSY) are given in table 3.14. Reference data from ^{13}C-NMR and ^{19}F-NMR

Table 3.14: ^{1}H-NMR data, coupling constants and COSY for compound **1c**.

Position	Multiplicity	Integral	^{1}H [ppm]	J [Hz]	COSY to [ppm]
2	t	1H	6.99	9.03	7.04/7.16
3	t	1H	7.04	7.44	6.99/7.16
1,4	m	2H	7.16	-	6.99/7.04
8,10	m	4H	2.69	-	1.74
9	m	2H	1.74	7.17	2.69
11	s	2H	1.33	-	-

of **1c** have not been found. The articles presenting the ^{13}C-NMR- and ^{19}F-NMR spectra of the analogue amines **1a** and **1b** was therefore used as reference spectra for **1c**. The experimental NMR data were quite consistent, but were a little bit off i the aromatic area. The reference spectrum for **2c** was therefore used here. ^{13}C-NMR data, C,H-correlations (HSQC) and long distance C,H-correlations are given in table 3.15.

Table 3.15: ^{13}C-NMR data, HSQC and HMBC for compound **1c**.

Position	^{13}C [ppm]	J (C-F) [Hz]	HSQC to [ppm]	HMBC to position
1	127.5	8.14	7.16	4/6/8
2	115.1	22.0	6.99	3/5/6
3	123.9	3.47	7.04	2/5/6
4	130.6	5.25	7.16	1/8
5	128.9	16.1	-	9/8/10/2/3
6	161.1	244	-	8/2/3/1/4
9	35.00	-	1.74	5/8/10
8	26.27	3.01	2.69	1/4/5/6/9/10/
10	41.67	-	2.69	5/8/9

3.10 Structural Analysis of 5

The compound **5** has been characterized by MS and NMR (spectra in appendix G). High resolution, accurate MS spectrometry shows *m/z* 318.0497 $[M+1]^+$ for compound **5**, where the calculated mass is 318.0494. This confirms that the molecular formula $C_{16}H_{16}BrNO$ is correct. The structure of compound **5** is illustrated in figure 3.11, which is used for the NMR analysis.

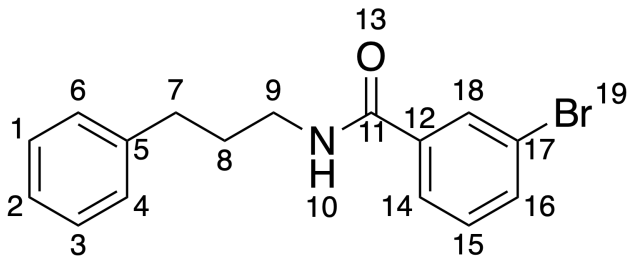

Figure 3.11: The numbering used for **5**.

3.10.1 NMR

No ^{1}H-NMR spectra for **5** has been found in the literature. Experimental NMR data found for compound **5** have been analyzed with traditional methods, using general cheats for NMR shifts, in addition to a predicted spectrum made by the chemical drawing software ChemDraw®. ^{1}H-NMR data, coupling constants and H,H-correlations (COSY) are given in table 3.16.

Table 3.16: ^{1}H-NMR data, coupling constants and COSY for compound **5**.

Position	Multiplicity	Integral	^{1}H [ppm]	J [Hz]	COSY to [ppm]
1,2,3	m	3H	7.23	-	7.30
4,6,15	m	3H	7.30	-	7.23/ 7.56/7.60/7.74
7	t	2H	2.74	7.31	1.98
8	m	2H	1.98	7.03	3.51/2.74
9	q	2H	3.51	5.90	1.98/5.97
10	s	1H	5.97	-	3.51
14	d	1H	7.56	8.11	7.30/7.60/7.74
16	d	1H	7.60	7.92	7.30/7.56/ 7.74
18	s	1H	7.74	-	7.30/7.56/7.60

^{13}C-NMR data, C,H-correlations (HSQC) and long distance C,H-correlations are given in table 3.17.

Table 3.17: ^{13}C-NMR data, HSQC and HMBC for compound **5**.

Position	^{13}C [ppm]	HSQC to [ppm]	HMBC to position	Note
1,3	128.4	7.23	7	CH
2	126.3	7.23	1/3/	CH
4,6	128.6	7.30	-	CH
5	141.4	-	7/8/4/6	
7	33.67	2.74	4/6/9	CH_2
8	30.99	1.98	8/9	CH_2
9	40.1	3.51	7/8	CH_2
11	165.9	-	9/14/18	CO
12	136.6	-	15	
14	125.5	7.56	18	CH
16	134.4	7.60	14/18	CH
17	122.7	-	15/18	CBr

4. Conclusion

The aim of this master's thesis was the preparation of amine precursors for potential new thymidylate kinase inhibitors, which later may be used in novel antibiotics. The target molecules for the project was 3-(fluorophenyl)propan-1-amines with fluorine in *para*, *meta* and *ortho* position. A reliable method for an amide coupling reaction was also to be prepared, where the target amines would be used in further reactions towards the potential thymidylate kinase inhibitors.

3-(4-Fluorophenyl)propan-1-amine (**1a**) was successfully synthesized in a two-step synthesis, starting with a HWE reaction of 4-fluorobenzaldehyde yielding 3-(4-fluorophenyl)acrylonitrile (**2a**) in 48% yield. A simultaneous reduction of the alkene- and nitrile group with LAH, ultimately gave **1a** in 41% yield. The same procedure was used to synthesize the *meta* and *ortho* analogues **1b** and **1c** in 18- and 25% yield, respectively.

Several reducing agents for the reduction of **2a-c** was considered both by paper- and experimental studies during this project, and it was found that solid LAH gave the most satisfying reaction yields. Though, other alternatives such as Raney-Ni and SmI_2, could be considered in future work.

3-Bromo-*N*-(3-phenylpropyl)benzamide (**5**) was synthesized using the benzotriazole- and aminium based coupling reagent HATU together with Hünig's base in an amide coupling reaction with 3-bromobenzoic acid, giving **5** in 54% yield after 48 h. Prior attempts of synthesizing **5** by aminolysis of methyl-3-bromobenzoate have also been tried, giving **5** in 13% yield after 6 days. Because of the better yield and efficiency, the HATU coupling reaction was concluded to be the preferable procedure for this reaction.

5. Further Work

This project is still in its initial phase, and there are therefore a lot of things to improve and optimize. So far only two different approaches towards the target amines are tried out, and there are most likely many good routes jet untried. As mentioned in chapter 2, the Knoevenagel route is probably a good choice as well. Other methods which not include a nitrile synthesis, followed by reduction, may also be an option. Organometallic options have jet not been considered, and could also be an alternative for further work.

The HWE route has proven to be a good start, and the reaction could be further optimized in future work. Varying factors like base, temperature, phosphonate equivalents, etc., could make this good reaction even better. The HATU coupling has only been done once in this thesis, and may be optimzed as well.

There have been some problems with the purification of the amines, due to bad eluent systems among other reasons. As mentioned in section 3.2.5, 4% 7M NH_3/meOH in DCM as the eluent system, has given respectable yields in the past, and could be worth trying.

6. Experimental Section

6.1 General

All the chemicals used in this project was estimated clean, and was used without further purification. There was used distilled water and 2 M NaCl solution (brine). All stirring during the experiments was done with teflon-coated magnets and a magnetic stirrer. The temperature baths used in the project are given in table 6.1:

Table 6.1: Temperature baths used in the project.

Temperature	**Compounds**
-10 °C	Acetone/ice
0 °C	Ice water
25 °C ++	Oil bath

6.1.1 Separational Techniques

All reactions in the project was followed by thin layer chromatography (TLC), and the following plates from Merck was used: Silica gel on aluminium plates, 60, F254. The visualization of the spots was done using ultraviolet radiation (254 nm)UV. Flash column chromatography with silica gel 60A from Fluka, with pore size 40-64 nm, was used as the primary purification method.

6.1.2 Spectroscopical Analysis

The ^{1}H-NMR spectra was recorded using either a Bruker 400 MHz Avance III HD, equipped with a 5-mm SmartProbe Z-gradiented probehead, or with a Bruker 600 MHz Avance III HD

equipped with a 5 mm cryogenic CP-TCI Z-gradiented probehead. All spectra were analyzed with Topspin. Chemical shifts are given in parts per million (ppm), and the integrals are given in number of protons. All chemical shifts relative to tetramethylsilane (TMS) (0.00). To describe the peaks, the following abbriviations has been used: s (singlet), d (duplet), t (triplet), q (quartet), m (multiplet) og br (broad signal). All coupling constants (J) are given in Hertz (Hz).

Accurate mass determination in positive and negative mode was performed on a "Synapt G2-S" Q-TOF instrument from Water TM. Samples were ionized by the use of ASAP probe (APCI) or ESI probe. No chromatographic separation was used previous to the mass analysis. Calculated exact mass and spectra processing was done by Waters TM Software Masslynx V4.1 SCN871.

6.2 Synthesis of *Z*- and *E*-3-(4-Fluorophenyl)acrylonitrile

The title compound **2a** was synthesized using a procedure from Van Wagenen *et.al* [9]. Sodium hydride (0.92 g, 38 mmol) in dry DMF (60 mL) and diethyl(cyanomethyl)phosphonate (6.6 g, 37 mmol) in dry DMF (40 mL) was mixed together and stirred under a nitrogen atmosphere for 1.5 h. 4-fluorobenzaldehyde (2.3 g, 19 mmol) was then added dropwise to the solution. After vigorously stirring for 90 minutes, the reaction flask was heated to 60 °C, and continued stirred for another 30 minutes. The reaction was then quenched with water (70 mL), before the reaction flask was cooled in an ice bath for 5 min. The organic layer was washed with water (4x70 ml) and brine (70 mL), and dried over sodium sulphate. The solvent was removed under reduced pressure, giving the crude product as white crystals in 73% yield. Purification with flash column chromatography (ethyl acetate/n-pentane, 1:7), gave white crystals in 48% yield. ^{1}H NMR (400 MHz, CDCl3) δ (ppm): 7.48 - 7.43 (m, 2H), 7.36 (d, J = 17 Hz, 1H) 7.14 - 7.08 (m, 2H), 5.81 (d, J = 17 Hz, 1H). ^{13}C NMR (100 MHz, CDCl3) δ (ppm): 166-163 (d, J = 253 Hz), 149, 129.9 (d, J = 8.78 Hz), 129.4 (d, J = 8.74), 118.0, 116.4 (d, J = 22.4 Hz), 96.18. ASAP+ HRMS: Calculated for C9H7FN+ ([M + H]+): 148.0653. Found: 148.0564.

6.3 Synthesis of 3-(4-Fluorophenyl)propan-1-amine

The title compound **1a** was synthesized using a procedure from Arutyunyan *et.al* [8]. **2** (1.02 g, 6.92 mmol) in dry diethyl ether (60 mL) was added dropwise to lithium aluminum hydride (1.51 g, 40.7 mmol) in dry diethyl ether (60 mL). The reaction was stirred under a N_2-atmosphere at 0 °C for 3 h. The reaction flask was then cooled down to -10 °C, before the reaction was quenched with water (1.6 mL). After an aquatic work-up with 15% NaOH (1.6 mL) and water (3.2 mL), the reaction flask was removed from the cooling bath and the mixture was stirred for 15 min. The water was then dried off with sodium sulphate, and all solids were filtered off. The solvent was removed under reduced pressure, giving **1a** as a bright yellow oil in 70% yield. The crude product were purified using ball tube distillation, giving **1a** as a colorless oil in 41% yield. ^{1}H NMR (400 MHz, CDCl3), δ (ppm): 7.48 - 7.42 (m, 2H), 7.14 - 7.08 (m, 2H), 2.70 (t, J = 7.2 Hz, 2H), 2.61 (t, J = 8.0 Hz, 2H), 1.77 - 1.68 (m, 2H), 1.39 (br, 2H). ^{13}C NMR (100 MHz, CDCl3) δ (ppm): 162.5 - 159.9 (d, J = 243 Hz), 129.6 (d, J = 8.00 Hz), 115.0 (d, J = 20.7 Hz), 41.6, 35.4, 32.4. ASAP+ HRMS: Calculated for C9H13FN+ ([M + H]+): 154.1032. Found: 154.1030.

6.4 Synthesis of *Z*- and *E*-3-(3-Fluorophenyl)acrylonitrile

The title compound **2b** was synthesized using a procedure from Van Wagenen *et.al* [9]. Sodium hydride (442 mg, 18.4 mmol) in dry DMF (40 mL) and diethyl(cyanomethyl)phosphonate (3.39 g, 19.2 mmol) in dry DMF (20 mL) was mixed together and stirred under a nitrogen atmosphere for 1.5 h. 3-fluorobenzaldehyde (2.01 g, 16.2 mmol) was then added dropwise to the solution. After vigorously stirring for 90 minutes, the reaction flask was heated to 60 °C, and continued stirred for another 30 minutes. The reaction was then quenched with water (70 mL), before the organic layer was washed with water (2x60 ml). This caused a big emulsion, and an unspecified amount of NaCl was added to break up the emulsion. The organic layer was washed with brine (70 mL), and dried over sodium sulphate. The solvent was removed under reduced pressure, giving the crude product as white crystals in 85% yield. Purification with flash column chromatography (ethyl acetate/n-pentane, 1:7), gave white crystals in 68% yield. ^{1}H NMR (400 MHz, CDCl3) δ (ppm): 7.42 - 7.36 (m, 2H), 7.35 (d, J = 17

Hz) 7.23 (d, J = 7.9 Hz, 1H), 7.17 - 7.10 (m, 2H), 5.89 (d, J = 17 Hz, 1H). ^{13}C NMR (100 MHz, CDCl3) δ (ppm): 164 - 162 (d, J = 248 Hz), 149 (d, J = 3.02 Hz), 136 (d, J = 8.05 Hz), 131 (d, J = 8.14 Hz), 124 (d, J = 2.87), 118 (d, J = 21.2 Hz), 114 (d, J = 22.6 Hz), 98.0. ASAP+ HRMS: Calculated for C9H7FN ([M]+): 147.0484. Found: 147.0481.

6.5 Synthesis of 3-(3-Fluorophenyl)propan-1-amine

The title compound **1b** was synthesized using a procedure from Arutyunyan *et.al* [8]. **2** (1.47 g, 9.98 mmol) in dry diethyl ether (50 mL) was added dropwise to lithium aluminum hydride (1.94 g, 51.1 mmol) in dry diethyl ether (50 mL). The reaction was stirred under a N_2-atmosphere at 0 °C for 3.5 h. The reaction flask was then cooled down to -10 °C, before the reaction was quenched with water (2 mL). After an aquatic work-up with 15% NaOH (2 mL) and water (4 mL), the reaction flask was removed from the cooling bath and the mixture was stirred for 15 min. The water was then dried off with sodium sulphate, and all solids were filtered off. The solvent was removed under reduced pressure, giving **1b** as a bright yellow oil in 67% yield. The crude product were purified using ball tube distillation, giving **1b** as a colorless oil in 18% yield. ^{1}H NMR (400 MHz, CDCl3) δ (ppm): 7.21 (q, J = 7.47 Hz, 1H), 7.95 (d, J = 7.47 Hz, 1H), 6.90 - 6.83 (m, 2H), 2.70 (t, J = 7.1 Hz, 2H), 2.64 (t, J = 7.9 Hz, 2H), 1.78 - 1.71 (m, 2H), 1.45 (br, 2H) ^{13}C NMR (100 MHz, CDCl3) δ (ppm): 164.2 - 161.6 (d, J = 246 Hz), 144.7 (d, 7.42 Hz), 129.7 (d, J = 8.8 Hz), 124.0 (d, J = 2.95 Hz), 115.1 (d, J = 21 Hz), 41.6, 35.0, 33.0. ASAP+ HRMS: Calculated for C9H13FN+ ([M + H]+): 154.1032. Found: 154.1031.

6.6 Synthesis of *Z*- and *E*-3-(2-Fluorophenyl)acrylonitrile

The title compound **2c** was synthesized using a procedure from Van Wagenen *et.al.* [9]. Sodium hydride (471 mg, 19.6 mmol) in dry DMF (40 mL) and diethyl(cyanomethyl)phosphonate (3.45 g, 19.5 mmol) in dry DMF (20 mL) was mixed together and stirred under a nitrogen atmosphere for 1.5 h. 3-fluorobenzaldehyde (2.03 g, 16.4 mmol) was then added dropwise to the solution. After vigorously stirring for 90 minutes, the reaction flask was heated to 60 °C, and continued stirred for another 30 minutes. The temperature of the oil bath varied from 50-80 °C during this time. The reaction was quenched with water (70 mL), before the organic

layer was washed with water (2x60 ml), causing a white, difficult emulsion. After some time, the organic layer was washed with brine (70 mL), and dried over sodium sulphate. The solvent was removed under reduced pressure, giving the crude product as white crystals in 68% yield. Purification with flash column chromatography (ethyl acetate/n-pentane, 1:7), gave white crystals in 53% yield. ^{1}H NMR (400 MHz, CDCl3) δ (ppm): 7.48 (d, J = 17 Hz, 1H), 7.46 - 7.39 (m, 2H), 7.20 (t, J = 7.6 Hz, 1H), 7.13 (t, 9.28, 1H), 6.04 (d, J = 17 Hz, 1H). ^{13}C NMR (100 MHz, CDCl3) δ (ppm): 162 - 160 (d, J = 255 Hz), 143 (d, J = 2.43 Hz), 133 (d, 22), 129 (d, J = 2.9 Hz), 125 (d, J = 3.70), 122 (d, J = 11 Hz), 118, 116 (d, J = 22.4 Hz), 99.3 (d, J = 9.35 Hz). ASAP+ HRMS: Calculated for C9H7FN+ ([M + H]+): 148.0653. Found: 148.0561.

6.7 Synthesis of 3-(2-Fluorophenyl)propan-1-amine

The title compound **1c** was synthesized using a procedure from Arutyunyan *et.al* [8]. **2** (1.12 g, 7.69 mmol) in dry diethyl ether (50 mL) was added dropwise to lithium aluminum hydride (1.89 g, 49.8 mmol) in dry diethyl ether (50 mL). The reaction was stirred under a N_2-atmosphere at 0 °C for 4 h. The reaction flask was then cooled down to -10 °C, before the reaction was quenched with water (1.5 mL). After an aquatic work-up with 15% NaOH (1.5 mL) and water (3 mL), the reaction flask was removed from the cooling bath and the mixture was stirred for 15 min. The water was then dried off with sodium sulphate, and all solids were filtered off. The solvent was removed under reduced pressure, giving **1c** as a bright yellow oil in 49% yield. The crude product were purified using ball tube distillation, giving **1c** as a colorless oil in 25% yield. ^{1}H NMR (400 MHz, CDCl3) δ (ppm): 7.21 - 7.11 (m, 2H), 7.07 - 6.95 (m, 2H), 2.69 (m, 4H), 1.74 (m, 2H), 1.33 (br, 2H) ^{13}C NMR (100 MHz, CDCl3) δ (ppm): 162.3 - 159.9 (d, J = 245 Hz), 130.6 (d, 5.25 Hz), 128.9 (d, J = 16 Hz), 127.5 (d, J = 8.14Hz), 123.9 (d, J = 3.47 Hz), 115.1 (d, J = 22 Hz), 41.7, 34.1, 26.27 (d, J = 3.01 Hz). ASAP+ HRMS: Calculated for C9H13FN+ ([M + H]+): 154.1032. Found: 154.1022.

6.8 Synthesis of 3-Bromo-N-(3-phenylpropyl)benzylamide)

The title compound **5** was synthesized using a procedure from M. Baumann [52]. To a stirring solution of 3-bromobenzoic acid (518 mg, 2.57 mmol) in dry DCM (20 mL), mono(1-

((dimethylamino)(dimethyliminio)methyl)-1H-[1,2,3]triazolo[4,5-b]pyridine-4-ium 3-oxide) mono(hexafluorophosphate(V)) (1.15 g, 3.02 mmol) (HATU), and N-ethyl-N-isopropylpropan-2-amine (965 mg, 7.46 mmol) were added. The reaction was stirring under N_2-atmosphere for 40 min in rt, before 3-phenylpropan-1-amine (330 mg, 2.44 mmol) was added via a syringe. The reaction was kept stirring for 48 h in rt, before the solvent was removed under reduced pressure. The residue was then dissolved in water (20 mL) and extracted with ethyl acetate (4 x 20 mL). The combined organic layer were washed with 1M $NaHSO_4$ (30 mL), water (30 mL), $NaHCO_3$ (30 mL) and saturated NaCl (30 mL). After drying over sodium sulphate, the remaining solvent was removed under reduces pressure, giving the crude product of **5** as red, partly crystalized oil in 122% yield. Purification with flash column chromatography (pentane/ethyl acetate, 3:1), gave **5** as white crystals in 54% yield. ^{1}H NMR (400 MHz, CDCl3) δ (ppm): 7.74 (s, 1H), 7.60 (d, J = 7.9 Hz, 1H), 7.56 (d, J = 8.1, 1H), 7.33 - 7.20 (m, 6H), 7.97 (s, 1H), 3.51 (q, J = 5.90 Hz, 2H) 2.74 (t, J = 7.31 Hz, 2H), 1.98 (m, 2H). ^{13}C NMR (100 MHz, CDCl3) δ (ppm): 166.9, 141.4, 136.6, 134.4, 130.0, 128.6, 128.4, 126.3, 125.5, 122.7, 40.10, 33.67, 30.99. ASAP+ HRMS: Calculated for C9H13FN+ ([M + H]+): 154.1032. Found: 154.1022.

References

[1] B. Spellberg, J. Bartlett, and D. Gilbert, "The future of antibiotics and resistance", *New Engl. J. Med.*, vol. 368, 2013.

[2] M. Kandeel, A. Kato, Y. Kitamura, and Y. Kitade, "Thymidylate kinase: The lost chemotherapeutic target", *Nucleic Acids Symposium Series*, vol. 53, no. 1, 2009.

[3] L. Song, R. Merceron, B. Gracia, A. L. Quintana, M. D. P. Risseeuw, F. Hulpia, P. Cos, J. A. Aínsa, H. Munier-Lehmann, S. N. Savvides, and S. Van Calenbergh, "Structure guided lead generation toward nonchiral m. tuberculosis thymidylate kinase inhibitors", *Journal of Medicinal Chemistry*, vol. 61, no. 7, 2018.

[4] "Malaria", *Store medisinske leksikon*, 2018, Accessed: 2019-01-18. [Online]. Available: https://sml.snl.no/malaria.

[5] K. Sinha and G. S. Rule, "The structure of thymidylate kinase from candida albicans reveals a unique structural element", *Biochemistry*, vol. 56, no. 33, 2017.

[6] J. Y. Choi, M. S. Plummer, J. Starr, C. R. Desbonnet, H. Soutter, J. Chang, J. R. Miller, K. Dillman, A. A. Miller, and W. R. Roush, "Structure guided development of novel thymidine mimetics targeting pseudomonas aeruginosa thymidylate kinase: From hit to lead generation", *Journal of Medicinal Chemistry*, vol. 55, no. 2, 2012.

[7] X. Zhu, M. Zhang, J. Liu, J. Ge, and G. Yang, "Ametoctradin is a potent qo site inhibitor of the mitochondrial respiration complex iii", *Journal of Agricultural and Food Chemistry*, vol. 63, no. 13, 2015.

[8] N. Arutyunyan, L. Akopyan, N. Akopyan, G. Gevorgyan, G. Stepanyan, R. Paronikyan, M. Malakyan, R. Agdzhoyan, S. A. Badzhinyan, and A. A. Shakhatuni, "Synthesis, antibacterial, and antioxidant activity of [3-(4-chlorophenyl)-3-(4-fluorophenyl)propyl]-substituted ammonium oxalates", *Pharmaceutical Chemistry Journal*, vol. 46, no. 6, 2012.

[9] B. Van Wagenen, S. Moe, M. Balandrin, E. DelMar, and E. Nemeth, "Calcium receptor-active compounds", *US6211244*, 2001.

[10] C. K. Lee and J. Y. Shim, "An efficient synthesis of α,β-unsaturated carboxylic acids and nitriles", *OPPIAK*, vol. 22, no. 1, 1990.

[11] J. Besida and R. F. C. Brown, "Methyleneketenes and methylenecarbenes. xviii. a pyrolytic synthesis of aniline from trimethylsilyl (e,e)-2-cyanohexa-2,4-dienoate", *AJCHAS*, vol. 35, no. 7, 1982.

[12] E. G. Mckenna and B. J. Walker, "Wittig reactions of ylide anions derived from stabilised ylides", *J. Chem. Soc., Chem. Commun.*, 1989.

[13] L. Kürti and B. Czakó, *Strategic Applications of Named Reactions in Organic Synthesis - Background and Detailed Mechanisms*, 1. San Diego, US: Elsevier Academic Press, 2005, vol. 1.

[14] B. Maryanoff and A. Reitz, "The wittig olifination reaction and modifications involving phosphoryl-stabilized carbanions. stereochemistry, mechanism, and selected synthetic aspects.", *Chem. Rev*, vol. 89, 1989.

[15] S. Kelly, *Alkene synthesis*, 1st ed., B. Trost and I. Fleming, Eds. Oxford, UK: Pergamon, 1991.

[16] E. Vedejs and M. Peterson, "Stereochemistry and mechanism in the wittig reaction", *Top. Stereochem.*, vol. 21, 1994.

[17] I. Gosney and D. Lloyd, *One or more C=C bond(s) formed by condensation: Condensation of P, As, Sb, Bi, Si or metal functions*. Cambridge, UK: Pergamon, 1992, vol. 1.

[18] B. H. Hoff, "Acetonitrile as a building block and reactant", *Synthesis*, vol. 50, no. 15, 2018.

[19] S. Yamashita, K. Iso, K. Kitajima, M. Himuro, and M. Hirama, "Total synthesis of cortistatins a and j", *The Journal of Organic Chemistry*, vol. 76, no. 8, 2011.

[20] A. C. O. Hann and A. Lapworth, "Optically active esters of β - ketonic and β - aldehydic acid. part iv. condensation of aldehydes with menthyl acetoacetate.", *J. Chem. Soc.*, vol. 85, 1904.

[21] G. Jones, "Knoevenagel condensation", *Org. React.*, vol. 15, 1967.

[22] J. L. Van der Baan and F. Bickelhaupt, "Knoevenagel reaction of malononitrile with cyclic β -keto esters. ii. mechanism of formation of heterocyclic reaction products.", *Tetrahedron*, vol. 30, 1974.

[23] J. A. Cabello, J. M. Campello, A. Garcia, D. Luna, and J. M. Marinas, “Knoevenagel condensation in the heterogeneous phase using aluminum phosphate-aluminum oxide as a new catalyst.”, *J. Org. Chem.*, vol. 49, 1984.

[24] S. Kinastowski and W. Mroczyk, “Kinetic investigations on aldolic stage of knoevenagel’s reaction.”, *Pol. J. Chem.*, vol. 58, 1984.

[25] R. Tanikaga, N. Konya, and A. Kaji, “Stereochemistry of amine-catalyzed knoevenagel reactions”, *Chem. Lett*, 1985.

[26] R. Tanikaga, N. Konya, T. Tamura, and A. Kaji, “Stereochemistry in the knoevenagel reaction of methyl (arylsulfinyl)acetate and aldehydes”, *J. Chem. Soc., Perkin Trans. 1*, 1987.

[27] M. Tanaka, O. Oota, H. Hiramatsu, and K. Fujiwara, “The knoevenagel reactions of aldehydes with carboxy compounds. i. reactions of p-nitrobenzaldehyde with active methine compounds.”, *Bull. Chem. Soc. Jpn.*, vol. 61, 1988.

[28] S. Kinastowski and W. Mroczyk, “The mechanism of the knoevenagel reaction of malonic ester with benzaldehyde, catalized by pyrrolidine.”, *Bull. Pol. Acad. Sci., Chem*, vol. 37, 1989.

[29] L. F. Tietze and U. Beifuss, *The Knoevenagel Reaction*, B. Trost and I. Fleming, Eds. Oxford, UK: Pergamon, 1991, vol. 2.

[30] W. Mroczyk, J. Grabarkiewicz-Szczesna, and S. Kinastowski, “Mechanism of knoevenagel reaction of malonic ester with benzaldehyde catalyzed by pyrrolidine: Kinetic studies of the deamination stage.”, *Roczniki Akademii Rolniczej w Poznaniu*, vol. 281, 1995.

[31] A. Bojilova, R. Nikolova, C. Ivanov, N. A. Rodios, A. Terzis, and C. P. Raptopoulou, “A comparative study of the interaction of salicylaldehydes with phosphonoacetates under knoevenagel reaction conditions. synthesis of 1,2-benzoaxphosphorins and their dimers.”, *Tetrahedron*, vol. 52, 1996.

[32] D. Bogdal, “Influence of microwave irradiation on the rate of coumarin synthesis by knoevenagel condensation”, in *ECHET98: Electronic Conference on Heterocyclic Chemistry, June 29-July 24, 1998*, 1998.

[33] V. Boucard, “Kinetic study of knoevenagel condensations applied to the synthesis of poly[bicarbazolylene-alt-phenylenebis(cyanovinylene)]s.”, *Macromolecules*, vol. 34, 2001.

[34] H. A. A. Medien, "Kinetic studies of condensation of aromatic aldehydes with meldrum's acid. z.", *Naturforsch., B: Chem. Sci.*, vol. 57, 2002.

[35] E. pivonka Don and R. Empfield James, "Real-time in situ raman analysis of microwave-assisted organic reactions.", *Appl. Spectrosc*, vol. 58, 2004.

[36] P. Furet, B. Gay, G. Caravatti, C. Garcia-Echeverria, R. J., J. Schoepfer, and H. Fretz, "Structure-based design and synthesis of high affinity tripeptide ligands of the grb2-sh2 domain", *J. Med. Chem.*, vol. 41, 1998.

[37] M. Szostak, B. Sautier, M. Spain, and D. J. Procter, "Electron transfer reduction of nitriles using smi2-et3n-h2o: Synthetic utility and mechanism", *Org. Lett*, vol. 16, 2014.

[38] L.-Q. Sun, K. Takaki, J. Chen, L. Iben, J. O. Knipe, L. Pajor, C. D. Mahle, E. Ryan, and C. Xu, "N-2-[2-(4-Phenylbutyl)benzofuran-4-yl]cyclopropylmethylacetamide: An orally bioavailable melatonin receptor agonist", *Bioorg. Med. Chem. Lett.*, vol. 14, 2004.

[39] I. L. Scott, V. A. Kuksa, and R. Kubota, "Amine derivative compounds for treating ophtalmic and disorders", *UK Pat App GB2463151A*, 2010.

[40] T. G. Solomons, C. B. Fryhle, and S. A. Snyder, *Organic Chemistry, International Student Version*, 11th ed. Singapore: John Wiley & Sons, 2011.

[41] F. A. Carey and R. J. Sundberg, *Advanced organic chemistry - Part B: Reactions and synthesis*, 5th ed. Virginia, US: Springer, 2007.

[42] V. Micovic and M. Mihailovic, "The reduction of acid amides with lithium aluminum hydride", *The Journal of Organic Chemistry*, vol. 18, no. 9, 1953.

[43] T. O. C. Merlic Group at UCLA, "Fieser reaction", Downloaded in January 2019.

[44] E. Valeur and M. Bradley, "Amide bond formation: Beyond the myth of coupling reagents", *Chem. Soc. Rev*, vol. 38, 2009.

[45] T. A. Bakka, M. B. Strøm, J. H. Andersen, and O. R. Gautun, "Methyl propiolate and 3-butynone: Starting points for synthesis of amphiphilic 1,2,3-triazole peptidomimetics for antimicrobial evaluation", *Bioorganic & Medicinal Chemistry*, vol. 25, no. 20, 2017.

[46] J. Hachmann and M. Lebl, "Search for optimal coupling reagent in multiple peptide synthesizer", *Peptide Science*, vol. 84, no. 3, 2006.

[47] D. C. Pryde, A. S. Cook, D. J. Burring, L. H. Jones, S. Foll, M. Y. Platts, V. Sanderson, M. Corless, A. Stobie, D. S. Middleton, L. Foster, L. Barker, P. V. D. Graaf, P. Stacey, C. Kohl, S. Coggon, and K. Beaumont, "Novel selective inhibitors of neutral endopeptidase for

the treatment of female sexual arousal disorder", *Bioorganic & Medicinal Chemistry*, vol. 15, no. 1, 2007.

[48] R. Monson, *Advanced organic synthesis: methods and techniques*. New York, US and London, UK: Academic Press, 1971.

[49] H. C. Brown and G. Zweifel, "Convenient new procedures for the hydroboration of olefins", *Journal of the American Chemical Society*, vol. 81, no. 15, 1959.

[50] J. B. Brenneman, "Heterocyclic carboxylic acids as activators of soluble guanylate cyclase", WO 2016/014463 A1, 2016.

[51] M. D. Alexander, "Mk2 inhibitors and uses thereof", WO 2014/149164 A1, 2014.

[52] M. Baumann, "Synthesis of bicyclic cxcr4 antagonists", PhD thesis, UiB, Norway, 2016.

[53] F. Fang, Y. Li, and S.-K. Tian, "Stereoselective olefination of n-sulfonyl imines with stabilized phosphonium ylides for the synthesis of electron-deficient alkenes", *Eur. J. Org. Chem*, 2011.

[54] M. Döbele, S. Vanderheiden, N. Jung, and S. Bräse, "Synthesis of aryl fluorides on a solid support and in solution utilizing a fluorinated solvent", *Angewandte Chemie International Edition*, 2010.

[55] T. Nomura, T. Iwaki, T. Yasukata, K. Nishi, Y. Narukawa, K. Uotani, T. Hori, and H. Miwa, "A new type of ketolides bearing an n-aryl-alkyl acetamide moiety at the c-9 iminoether synthesis and structure–activity relationships", *Bioorganic & Medicinal Chemistry*, vol. 13, no. 24, 2005.

[56] H. Kurouchi, K. Kawamoto, H. Sugimoto, S. Nakamura, Y. Otani, and T. Ohwada, "Activation of electrophilicity of stable y-delocalized carbamate cations in intramolecular aromatic substitution reaction: Evidence for formation of diprotonated carbamates leading to generation of isocyanates", *The Journal of Organic Chemistry*, vol. 77, no. 20, 2012.

[57] H. Dong, M. Shen, J. E. Redford, B. J. Stokes, A. L. Pumphrey, and T. G. Driver, "Transition metal-catalyzed synthesis of pyrroles from dienyl azides", *Organic Letters*, vol. 9, no. 25, 2007.

[58] S. D. Banister, M. Manoli, M. R. Doddareddy, D. E. Hibbs, and M. Kassiou, "A σ1 receptor pharmacophore derived from a series of n-substituted 4-azahexacyclo[5.4.1.02,6.03,10.05,9.08,11]
3-ols (ahds)", *Bioorganic & Medicinal Chemistry Letters*, vol. 22, no. 19, 2012.

[59] J. B. Metternich, D. G. Artiukhin, M. C. Holland, M. von Bremen-Kühne, J. Neugebauer, and R. Gilmour, "Photocatalytic e - z isomerization of polarized alkenes inspired by the visual cycle: Mechanistic dichotomy and origin of selectivity", *The Journal of Organic Chemistry*, vol. 82, no. 19, 2017.

[60] R. P. Houghton, M. Voyle, and R. Price, "Reactions of co-ordinated ligands. part 10. rhodium-catalysed cyclisation of 3-(2-fluorophenyl)propanols to chromans", *J. Chem. Soc.*, 1984.

A. Experimental data of 2a

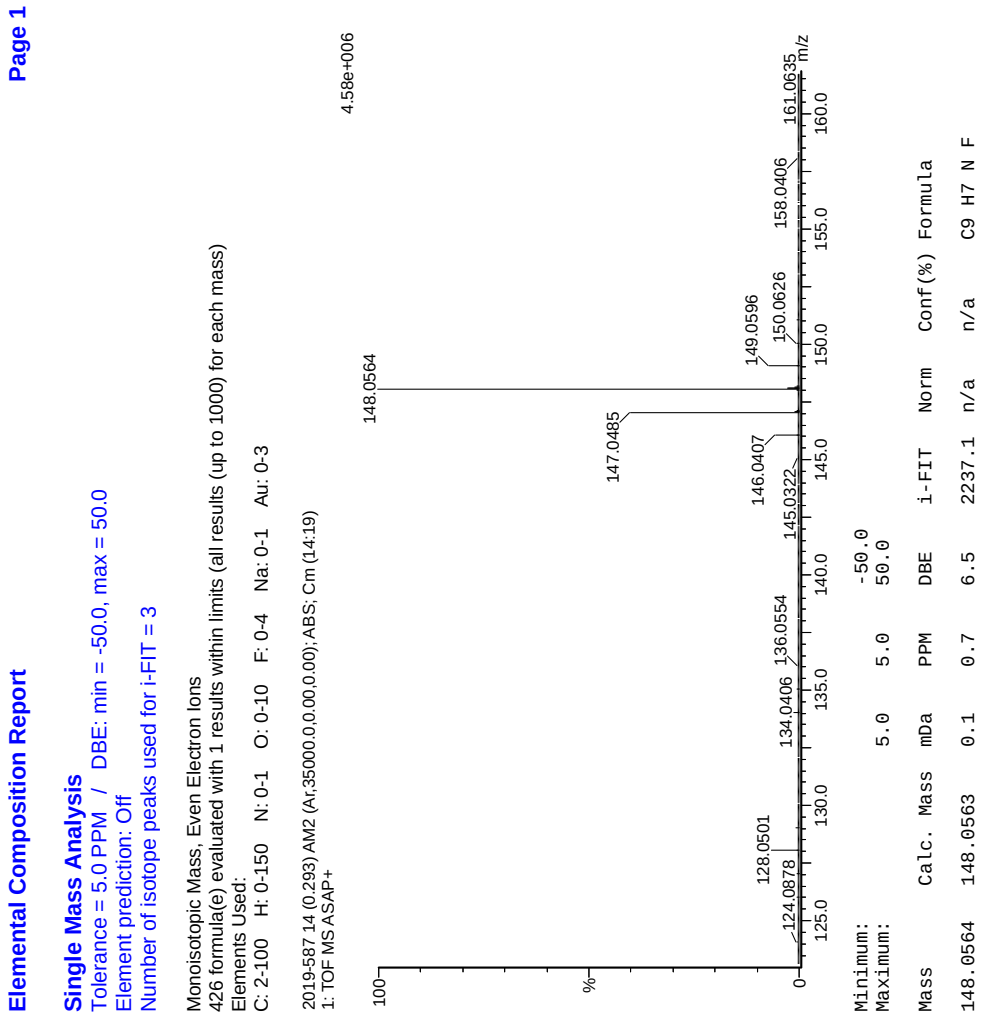

Figure A.1: MS spectrum of **2a**.

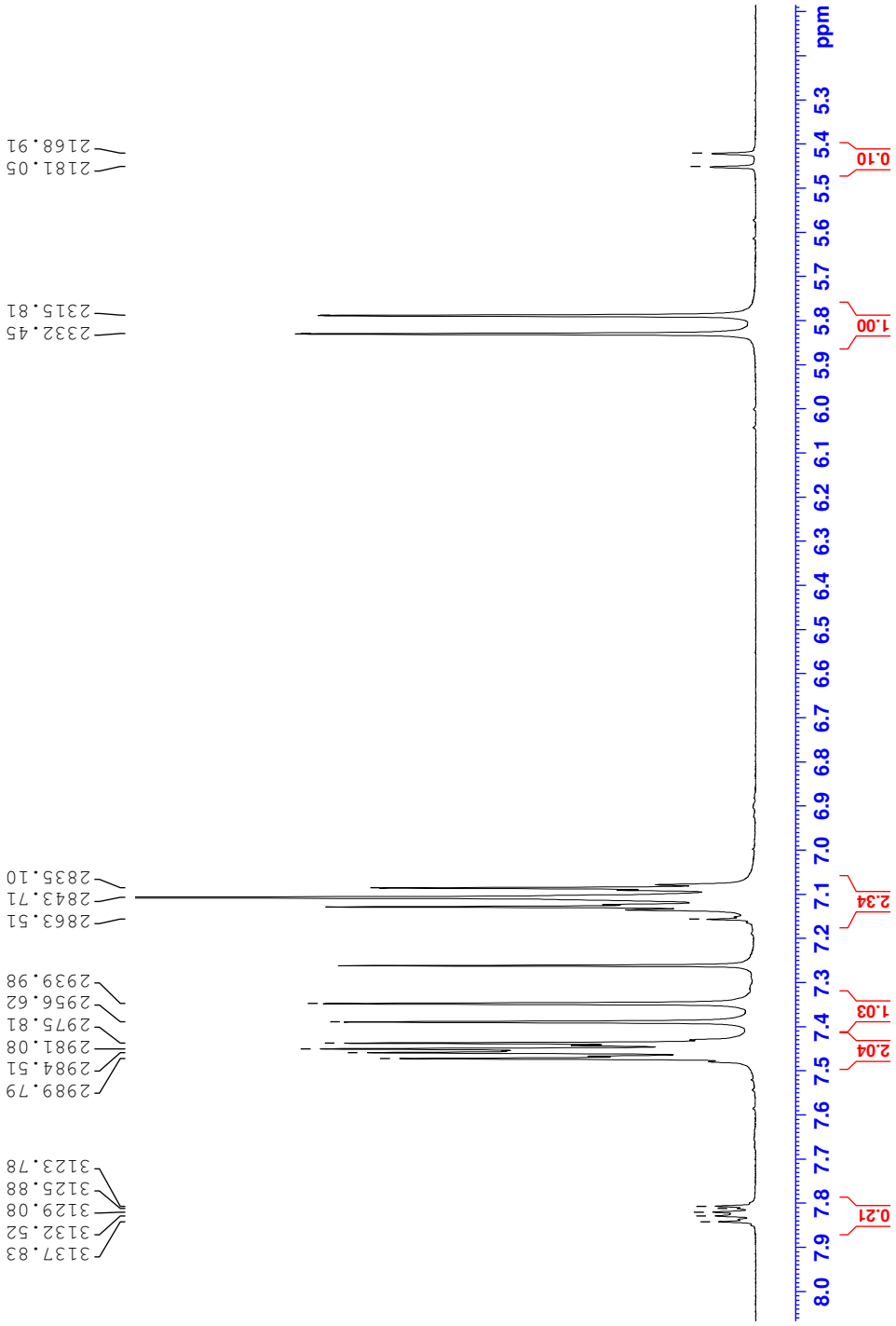

Figure A.2: ^{1}H-NMR spectrum of **2a**.

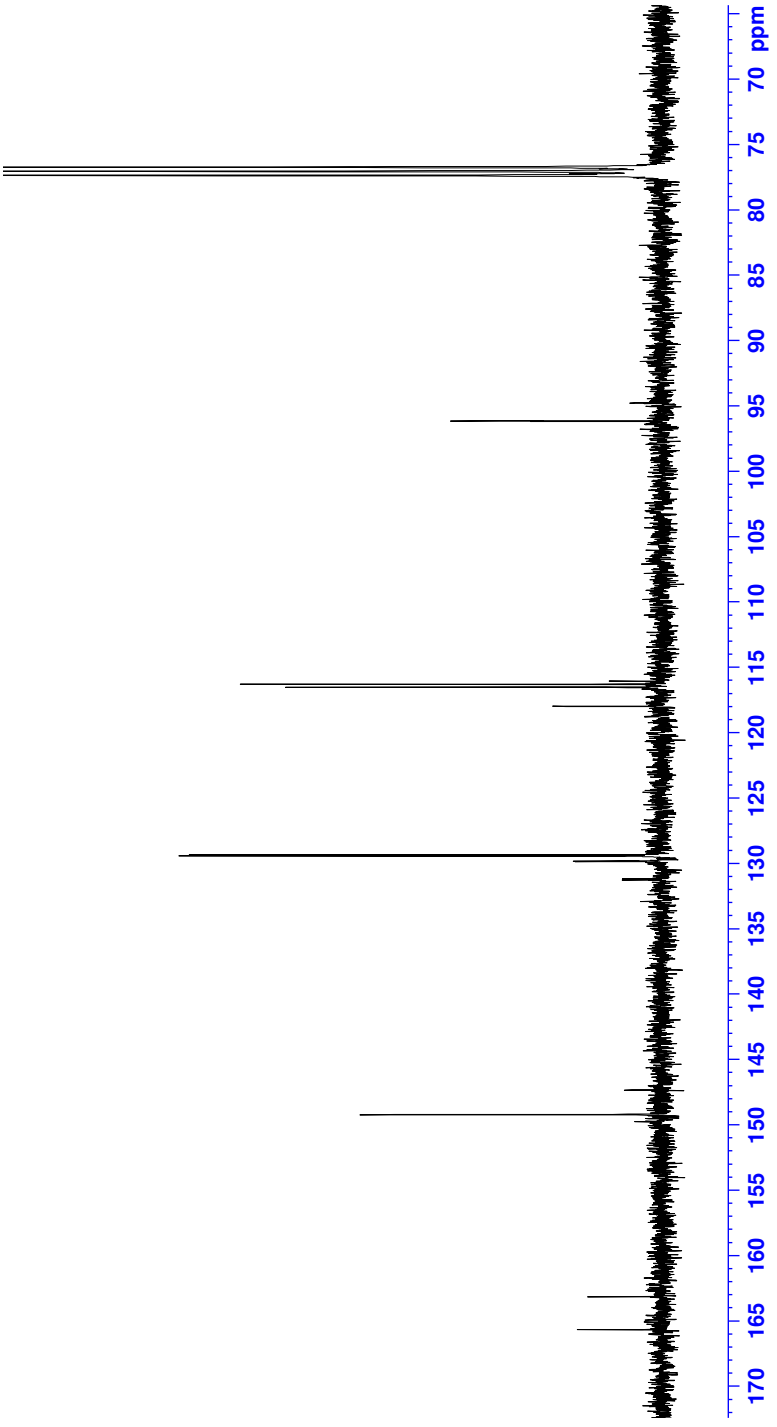

Figure A.3: ^{13}C-NMR spectrum of **2a**.

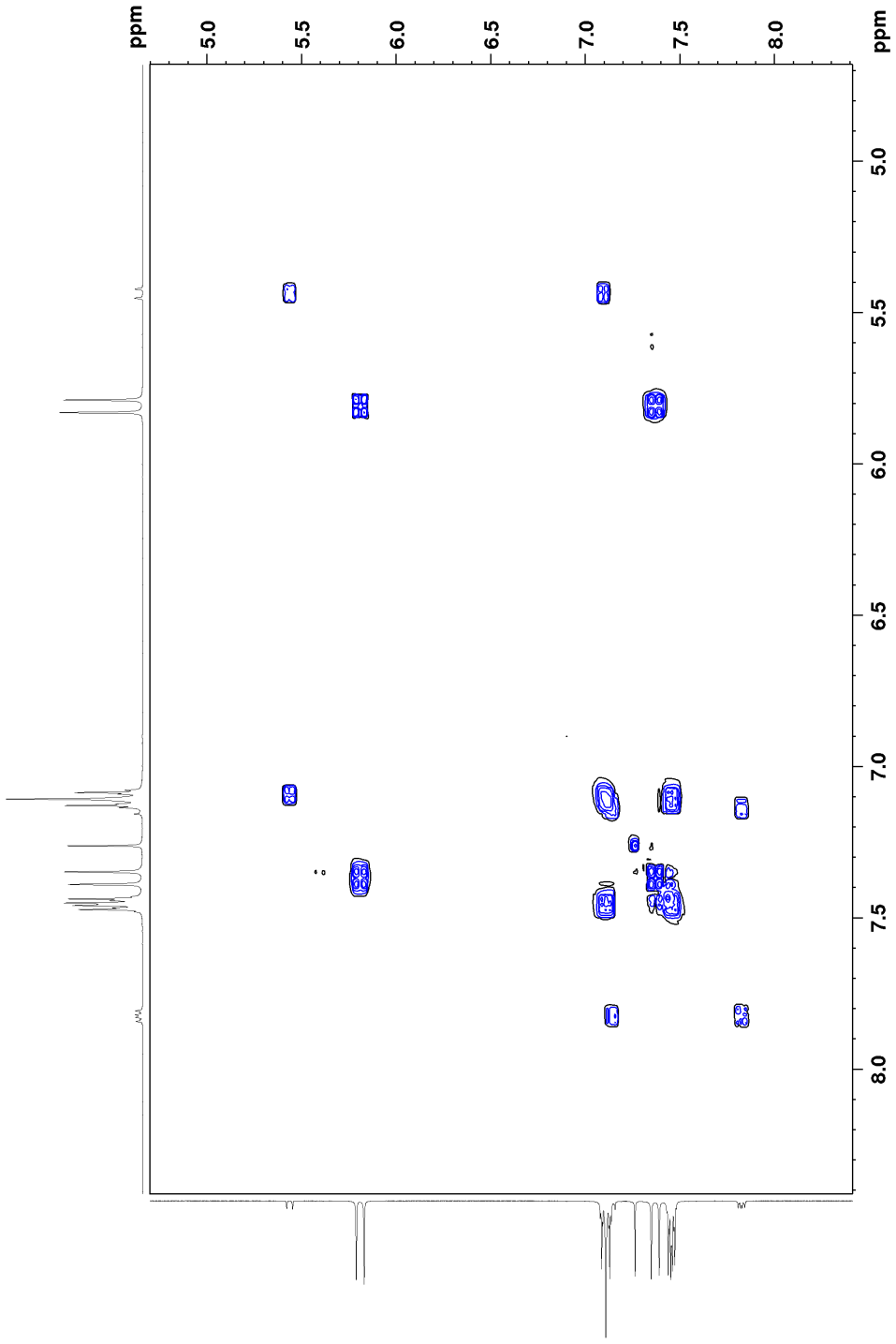

Figure A.4: COSY spectrum of **2a**.

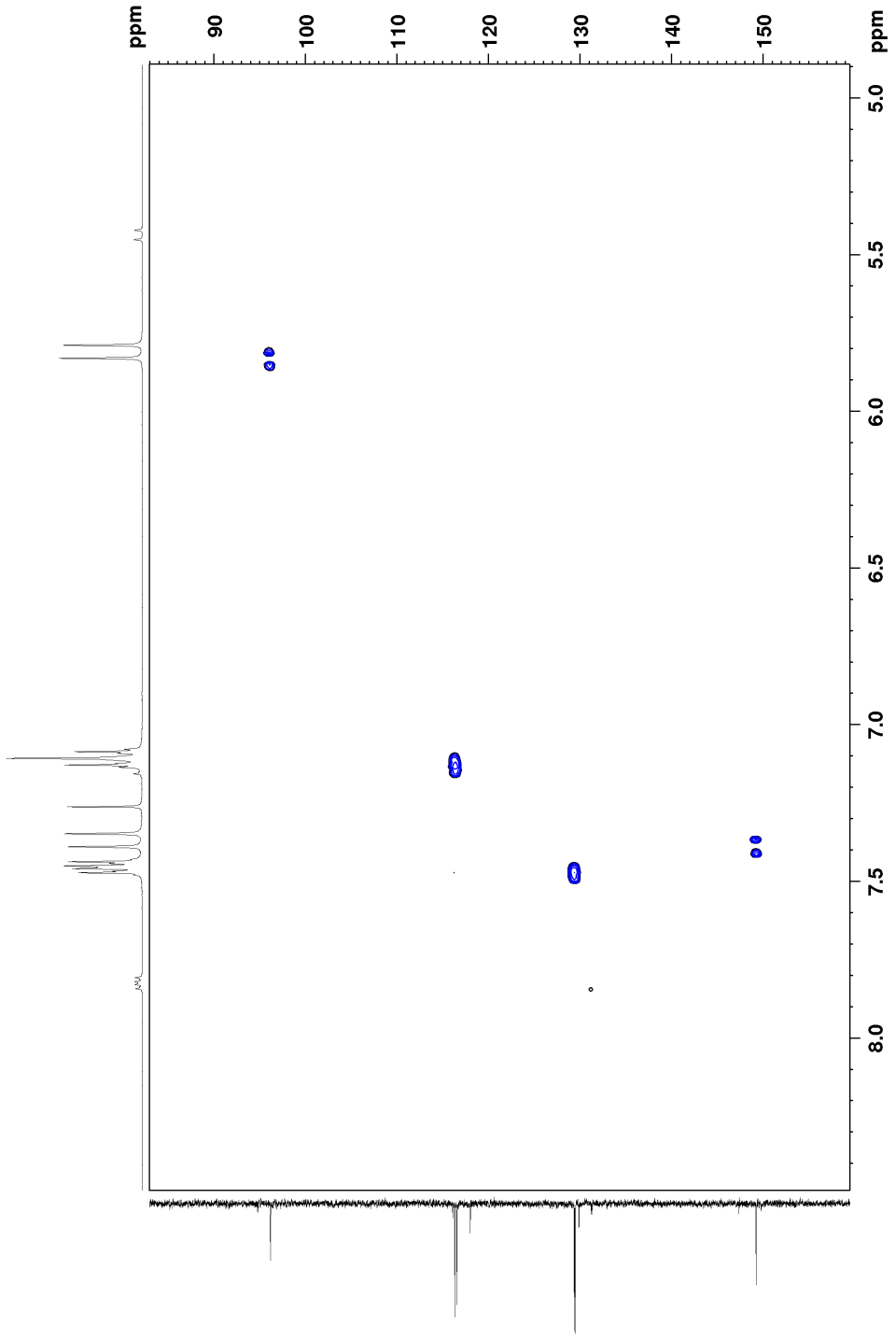

Figure A.5: HSQC spectrum of **2a**.

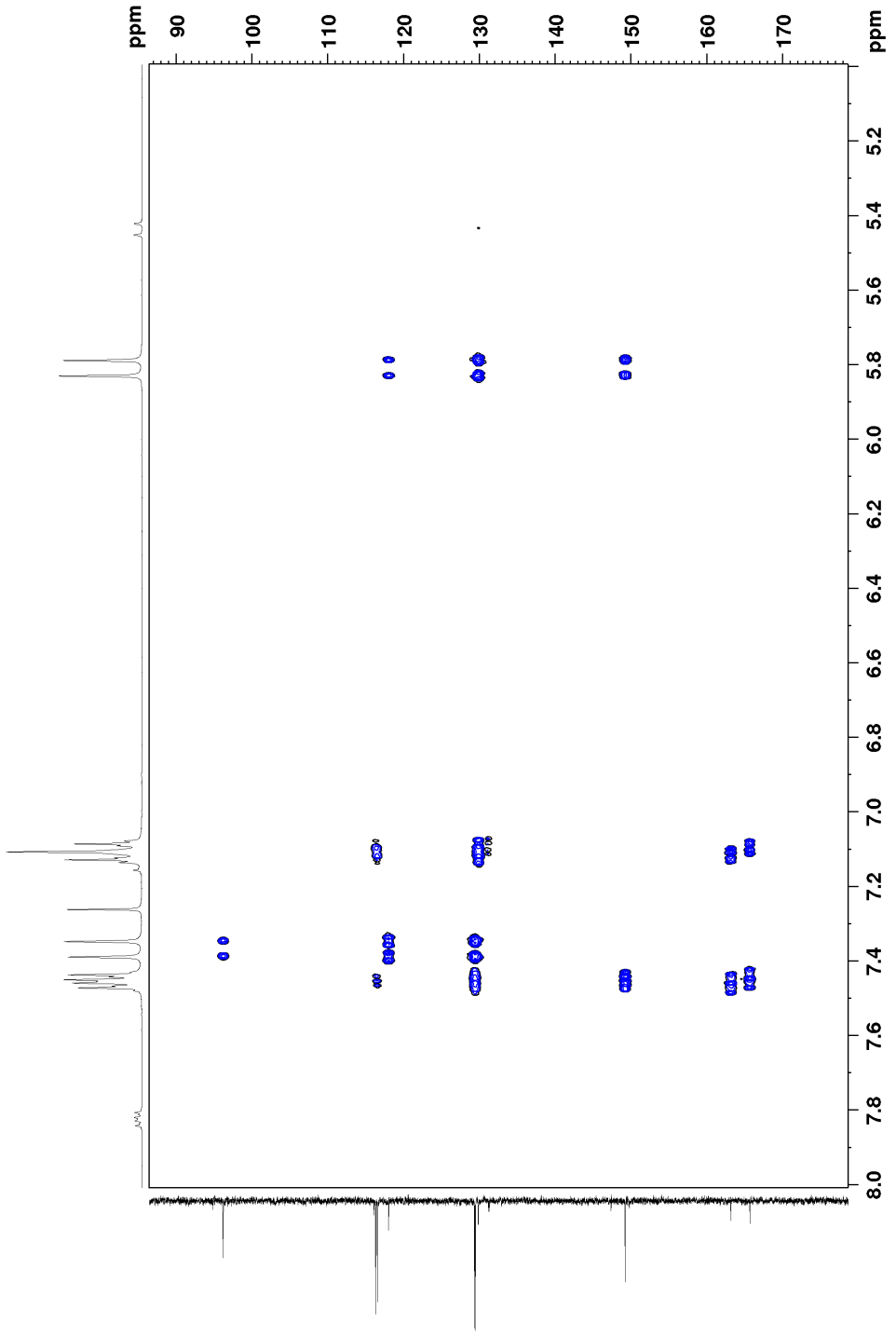

Figure A.6: HMBC spectrum of **2a**.

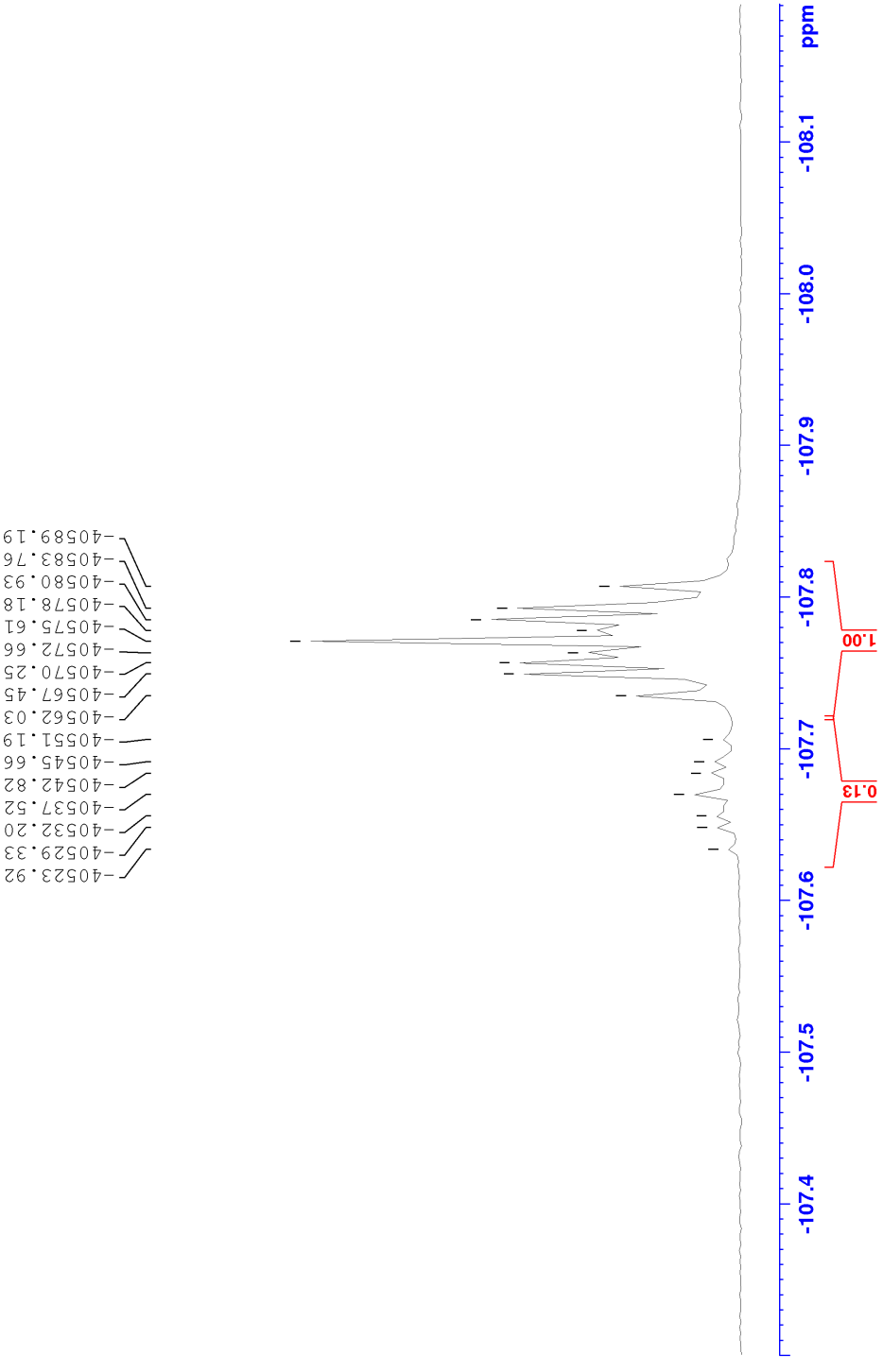

Figure A.7: ^{19}F-NMR spectrum of **2a**.

B. Experimental data of 1a

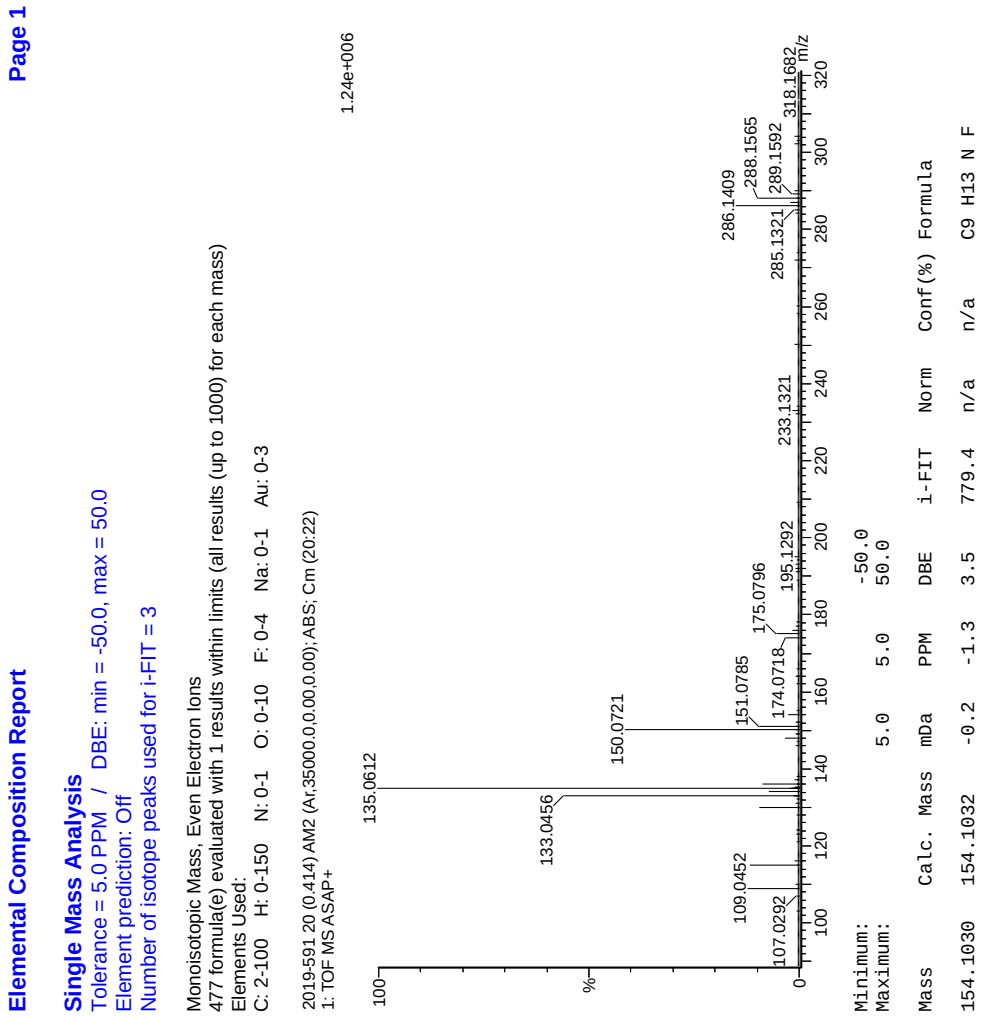

Figure B.1: MS spectrum of **1a**.

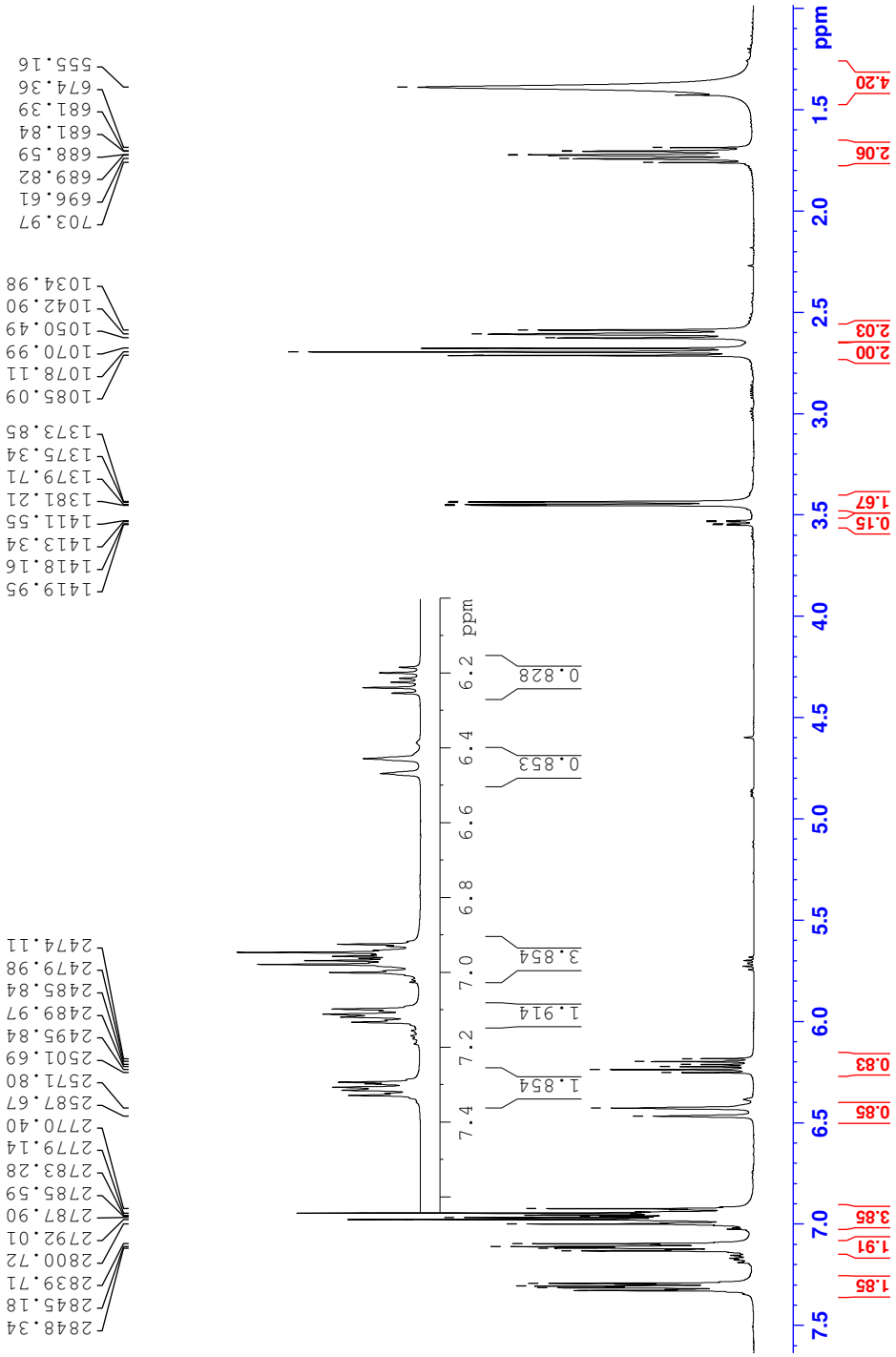

Figure B.2: ^{1}H-NMR spectrum of **1a**.

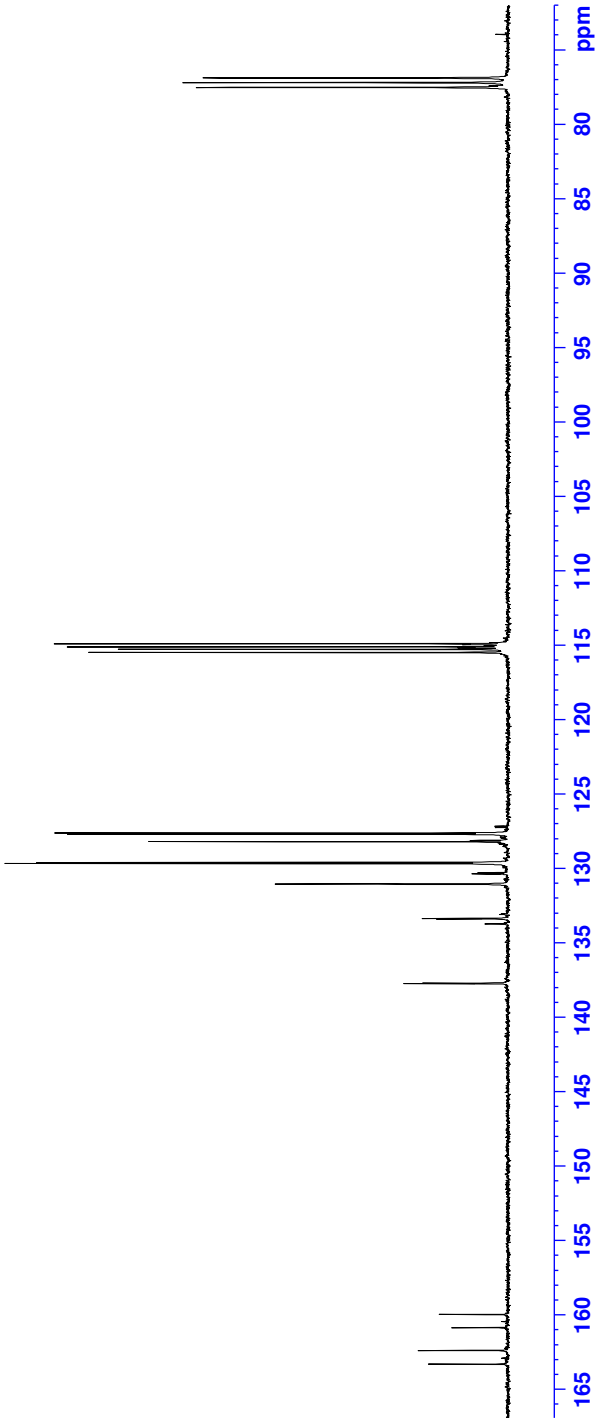

Figure B.3: ^{13}C-NMR spectrum of **1a**.

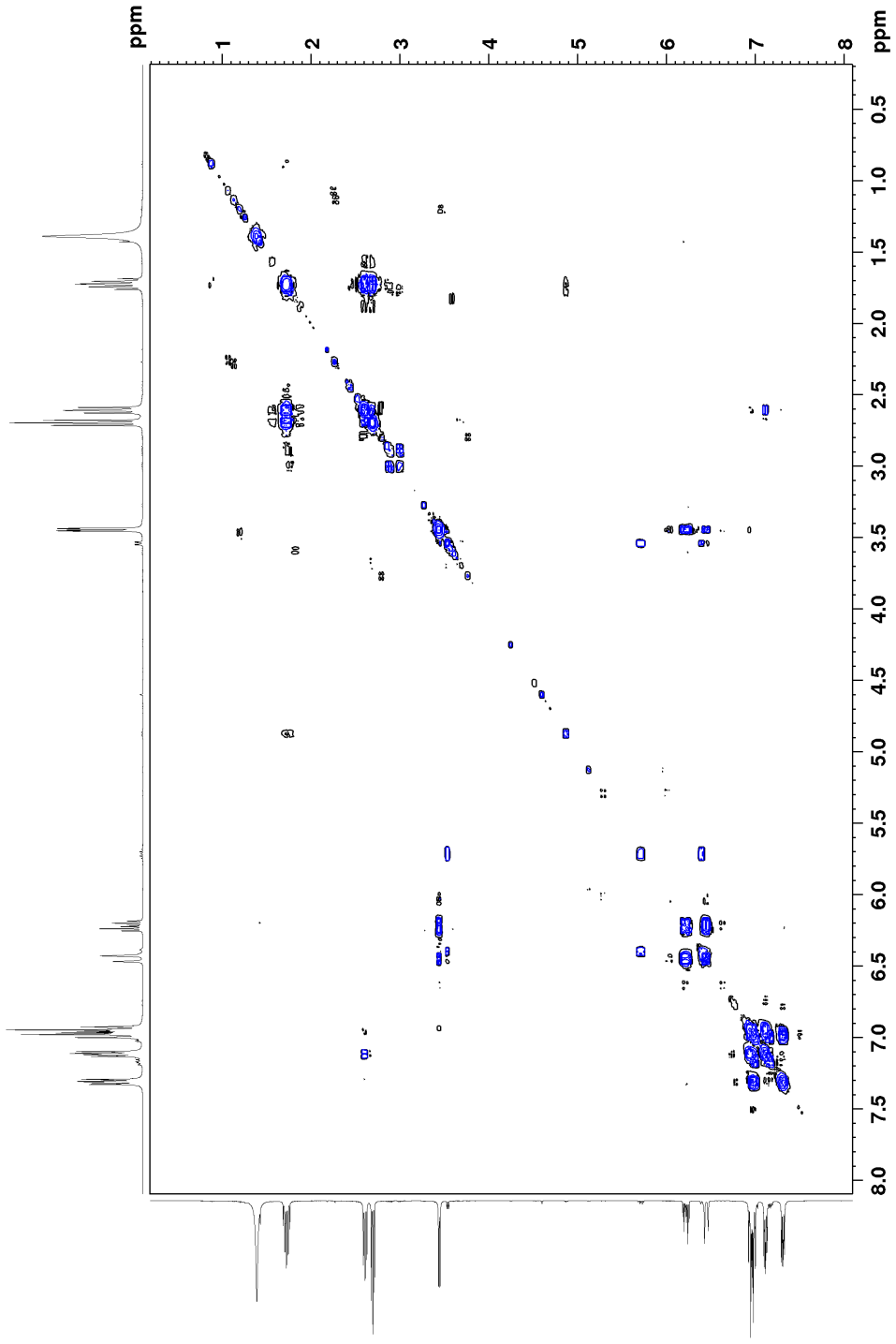

Figure B.4: COSY spectrum of **1a**.

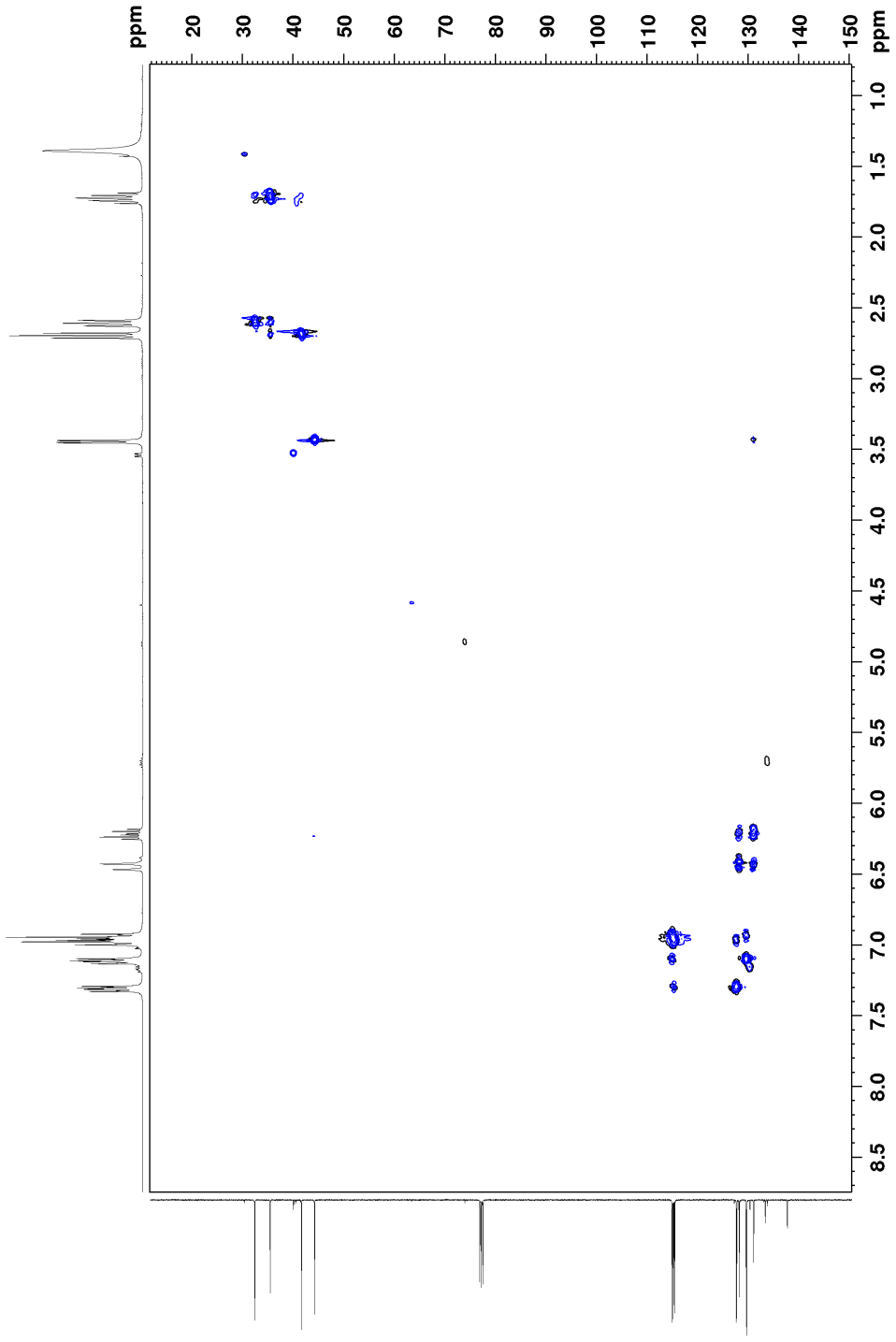

Figure B.5: HSQC spectrum of **1a**.

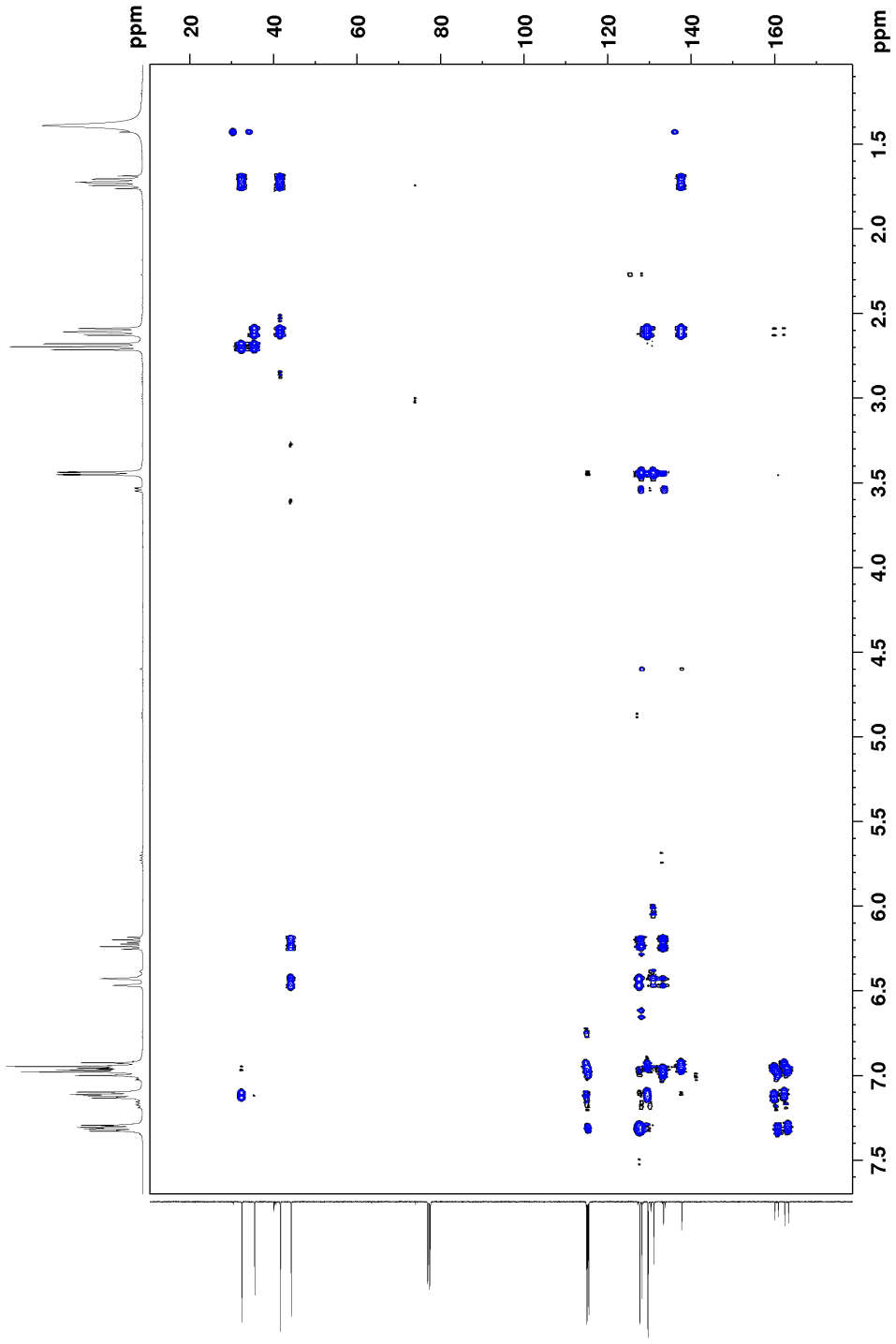

Figure B.6: HMBC spectrum of **1a**.

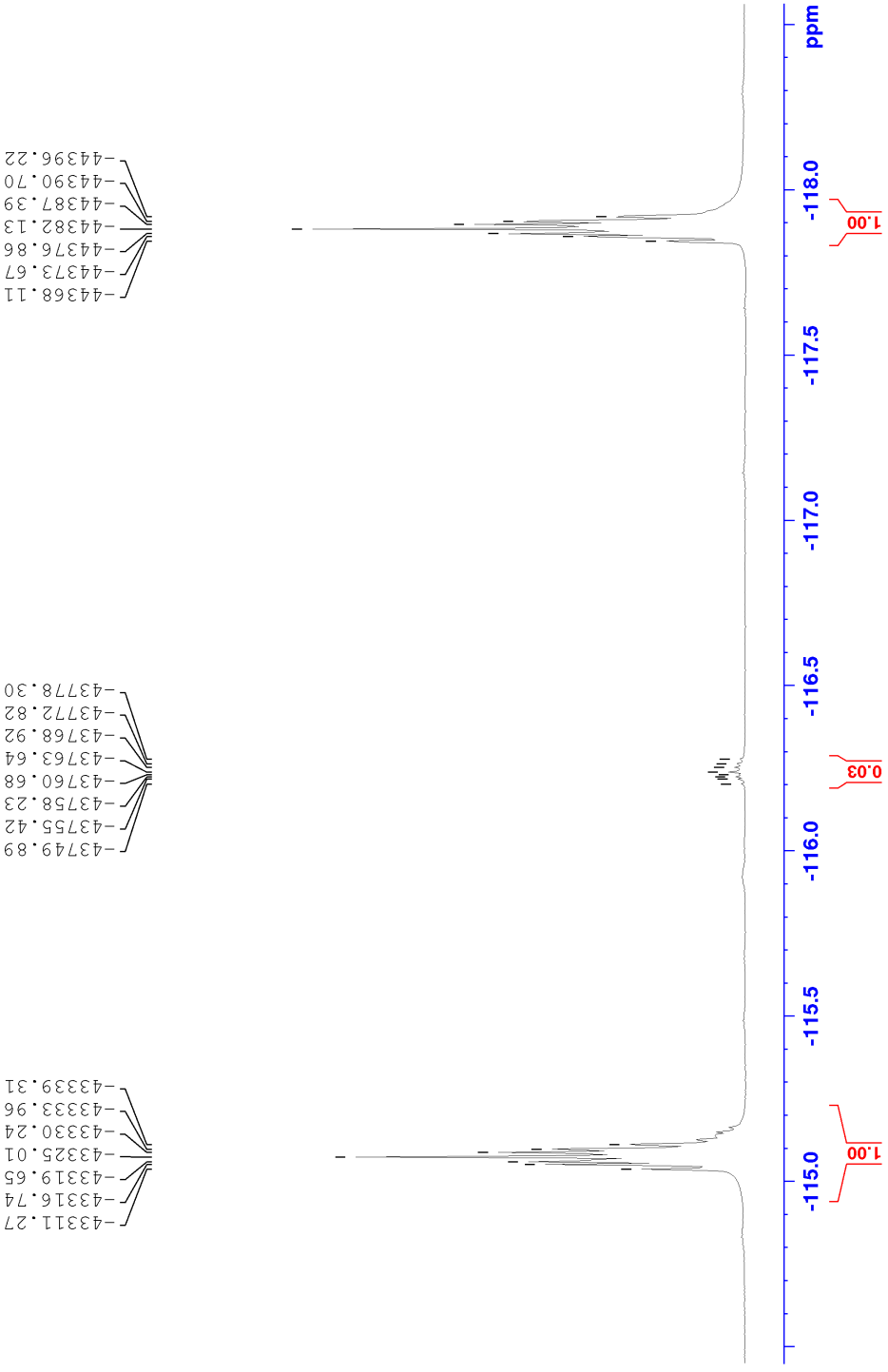

Figure B.7: ^{19}F-NMR spectrum of **1a**.

C. Experimental data of 2b

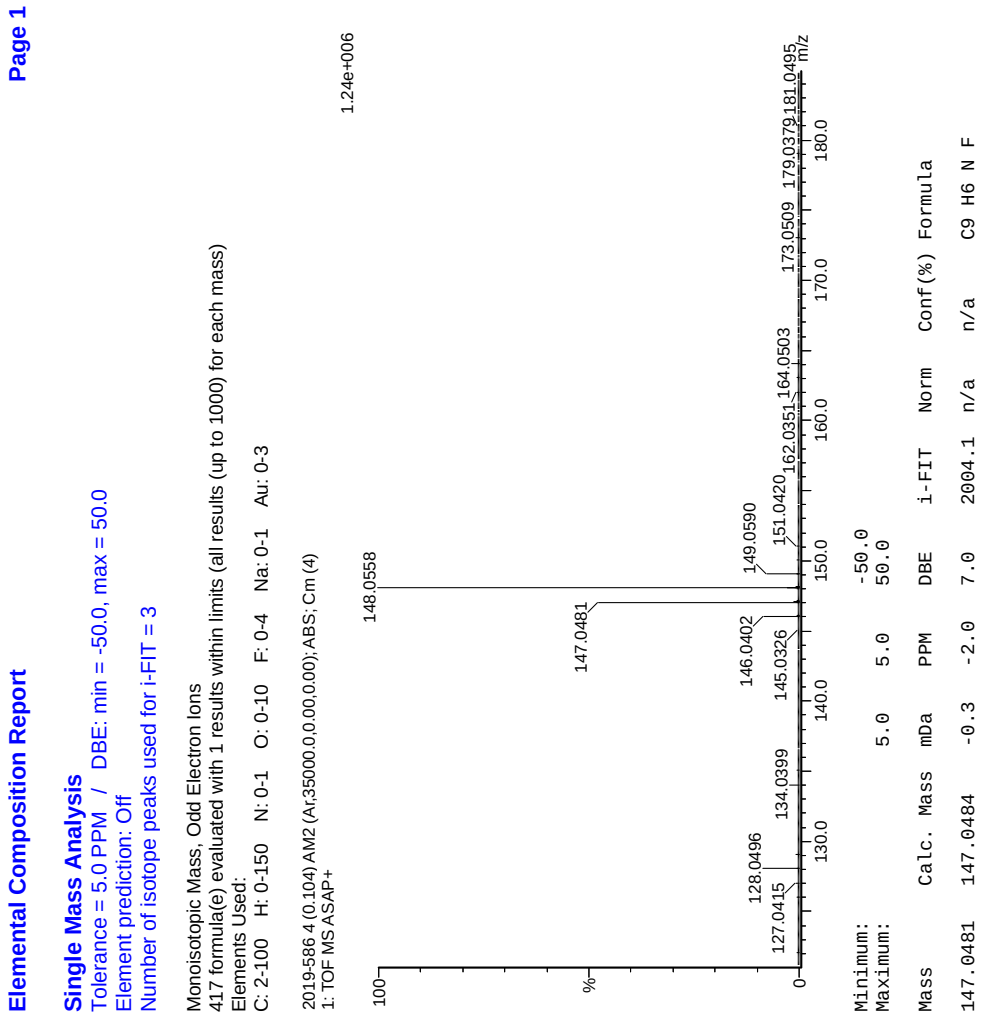

Figure C.1: MS spectrum of **2b**.

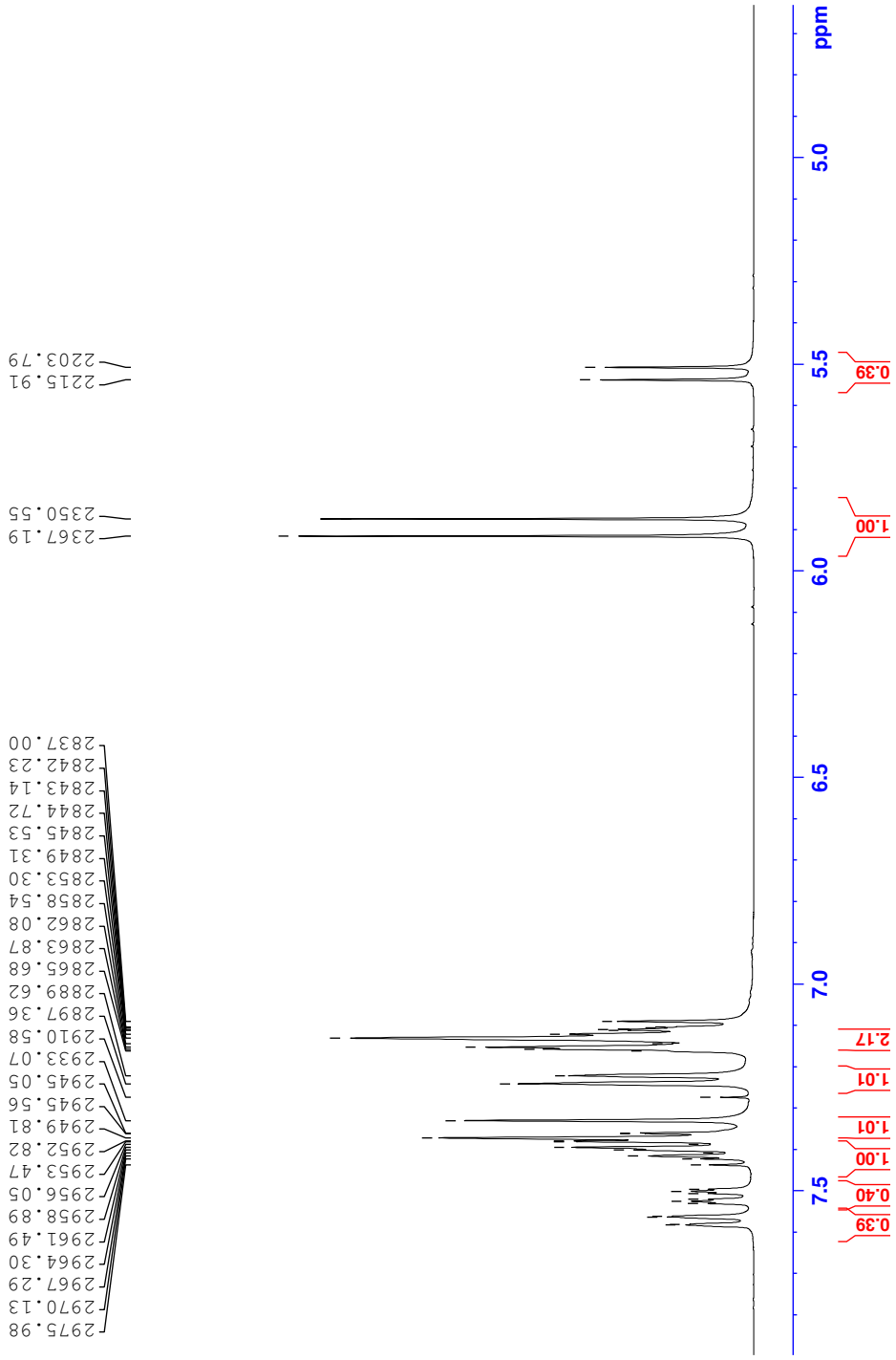

Figure C.2: ^{1}H-NMR spectrum of **2b**.

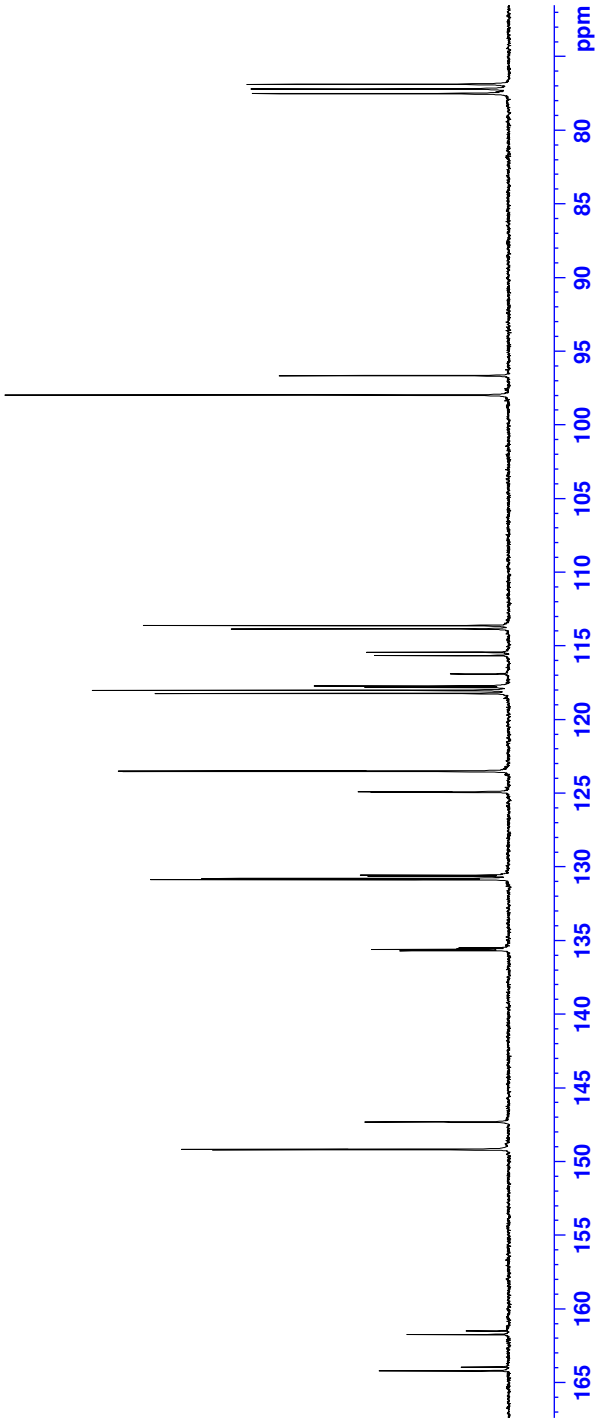

Figure C.3: ^{13}C-NMR spectrum of **2b**.

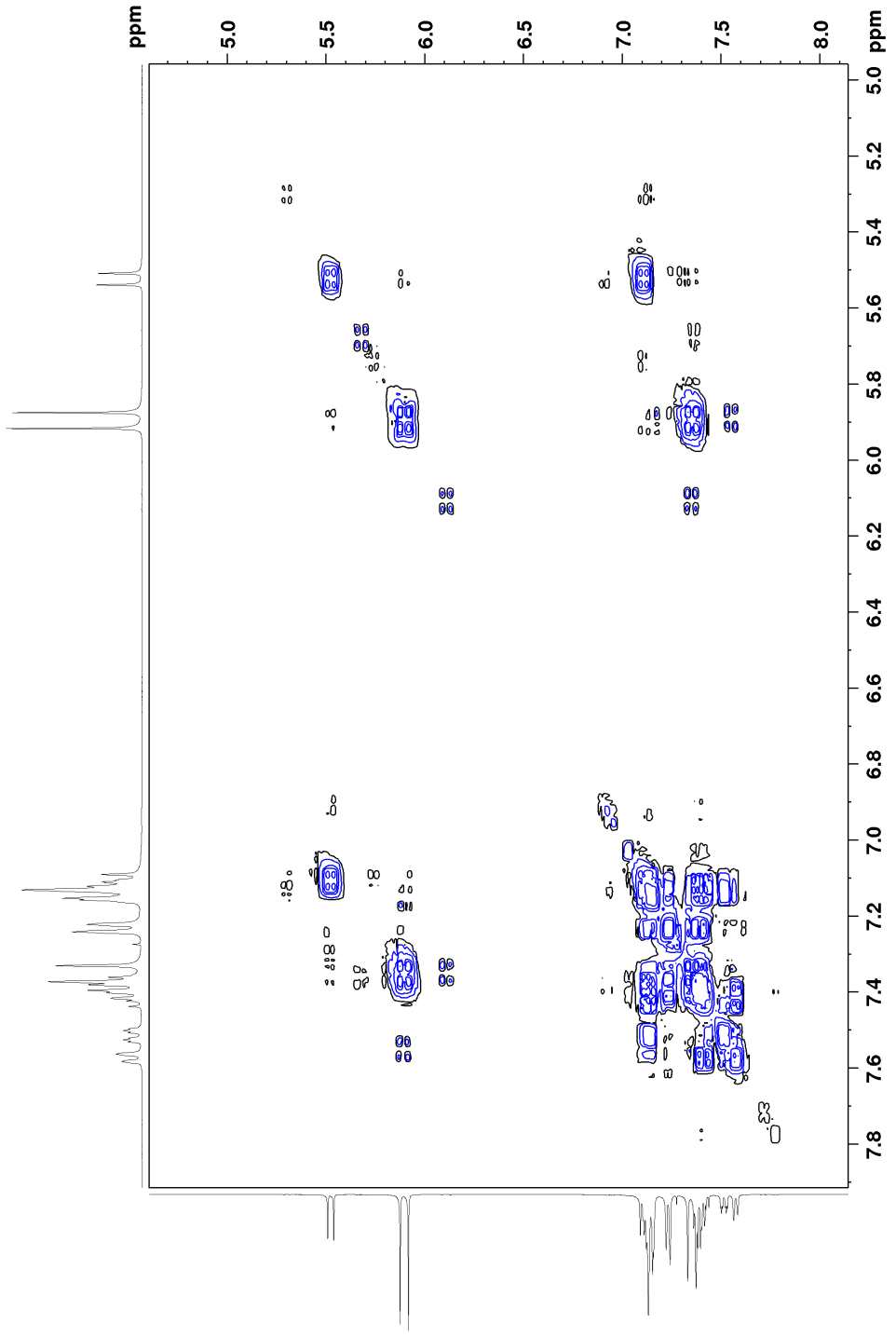

Figure C.4: COSY spectrum of **2b**.

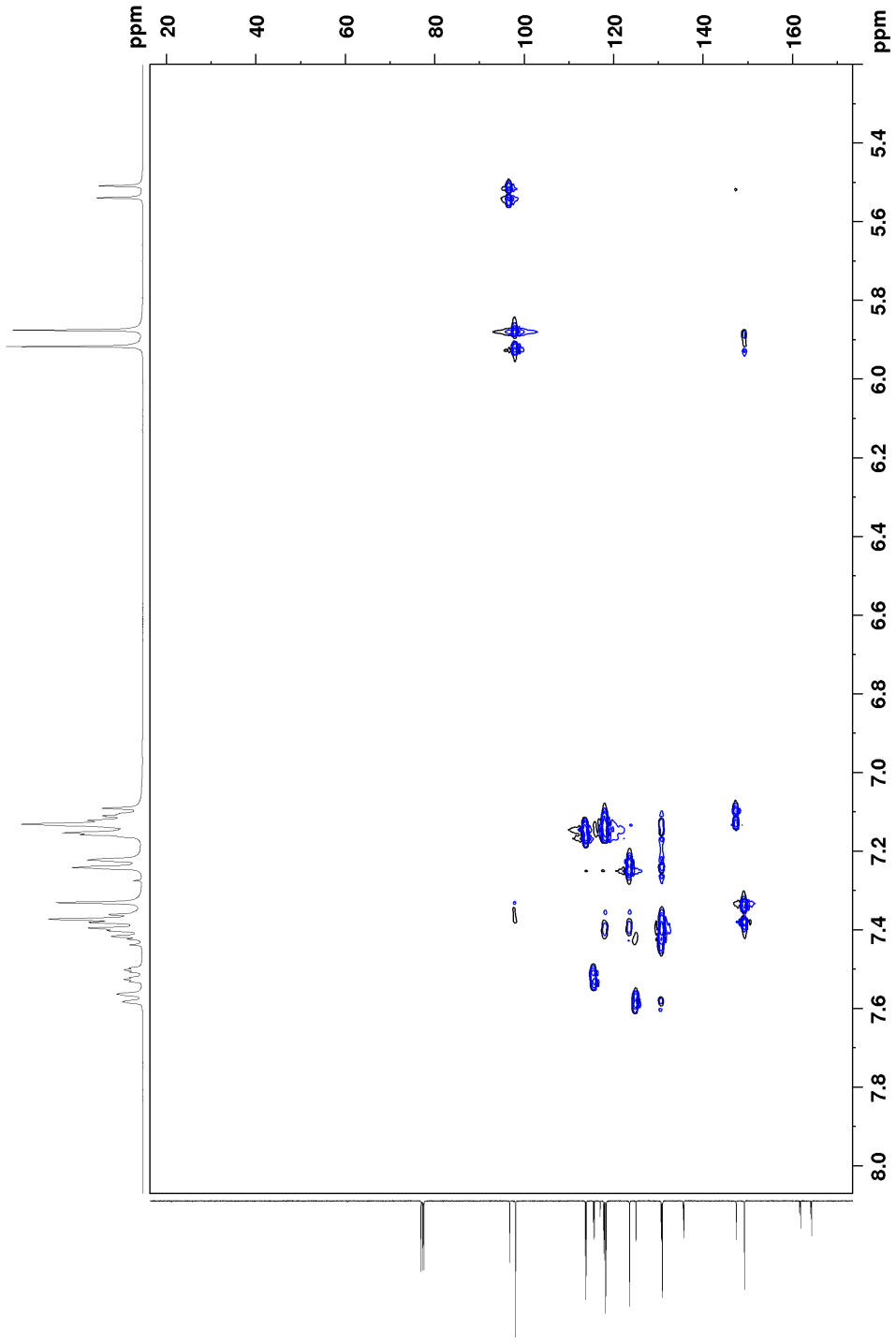

Figure C.5: HSQC spectrum of **2b**.

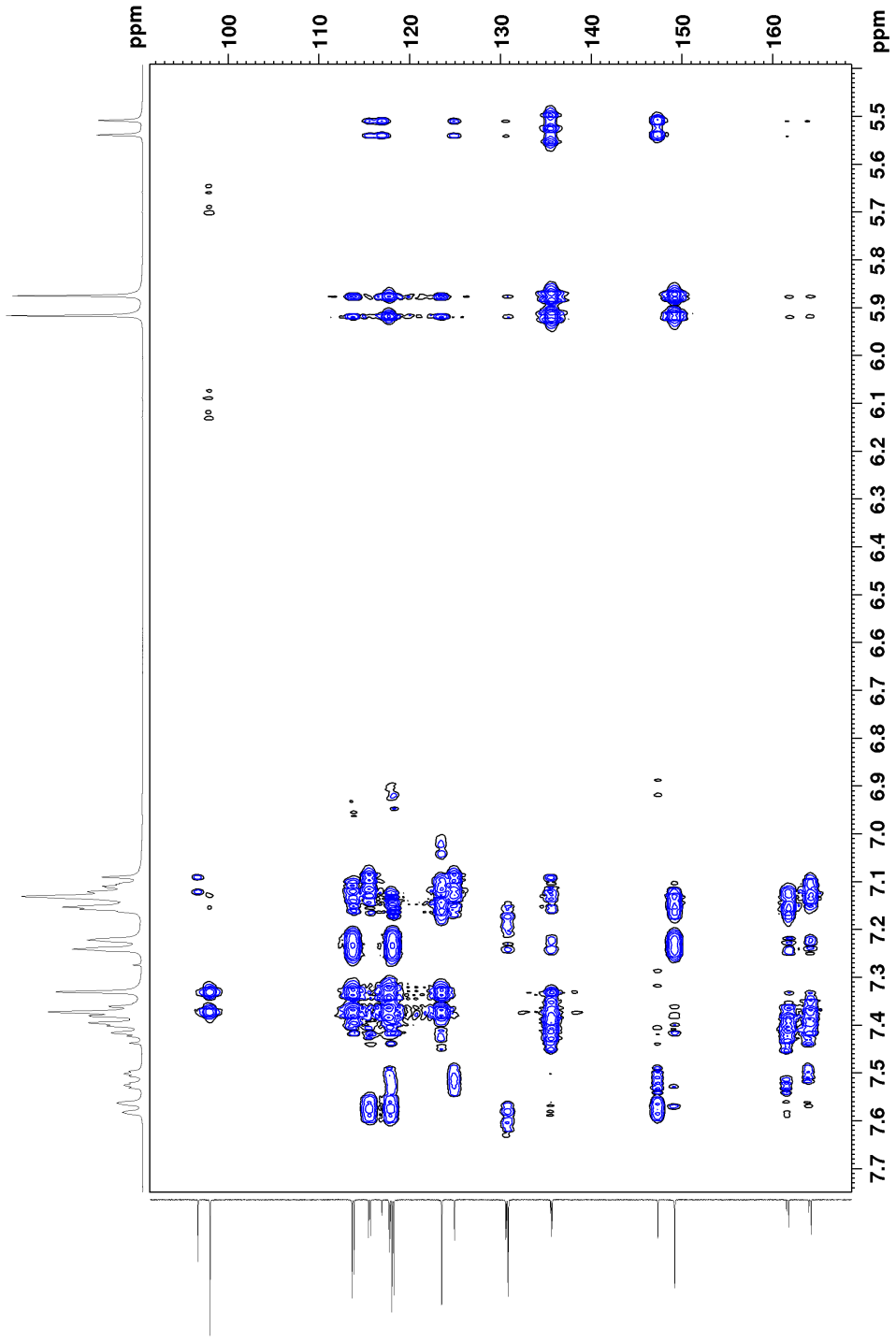

Figure C.6: HMBC spectrum of **2b**.

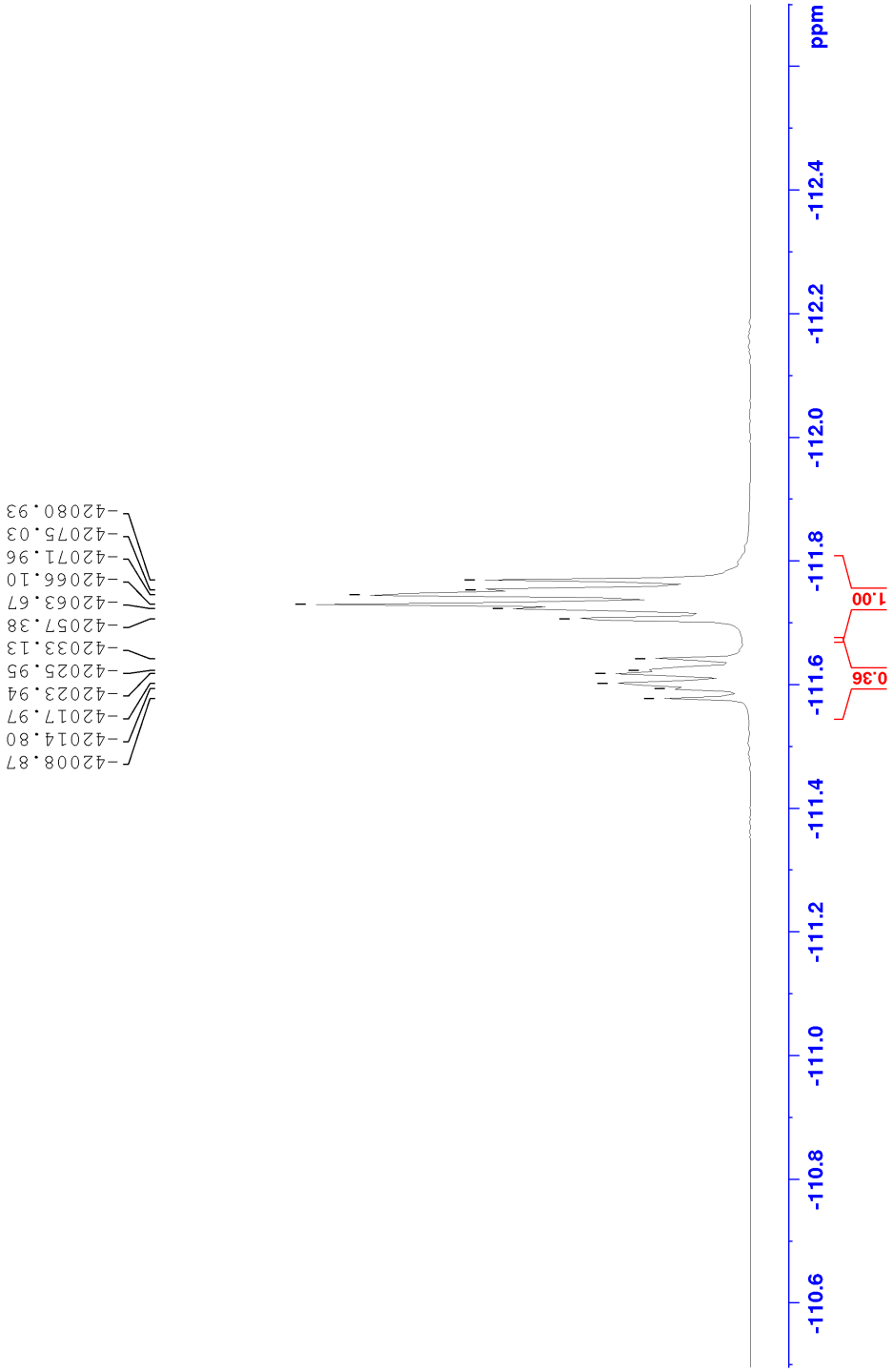

Figure C.7: ^{19}F-NMR spectrum of **2b**.

D. Experimental data of 1b

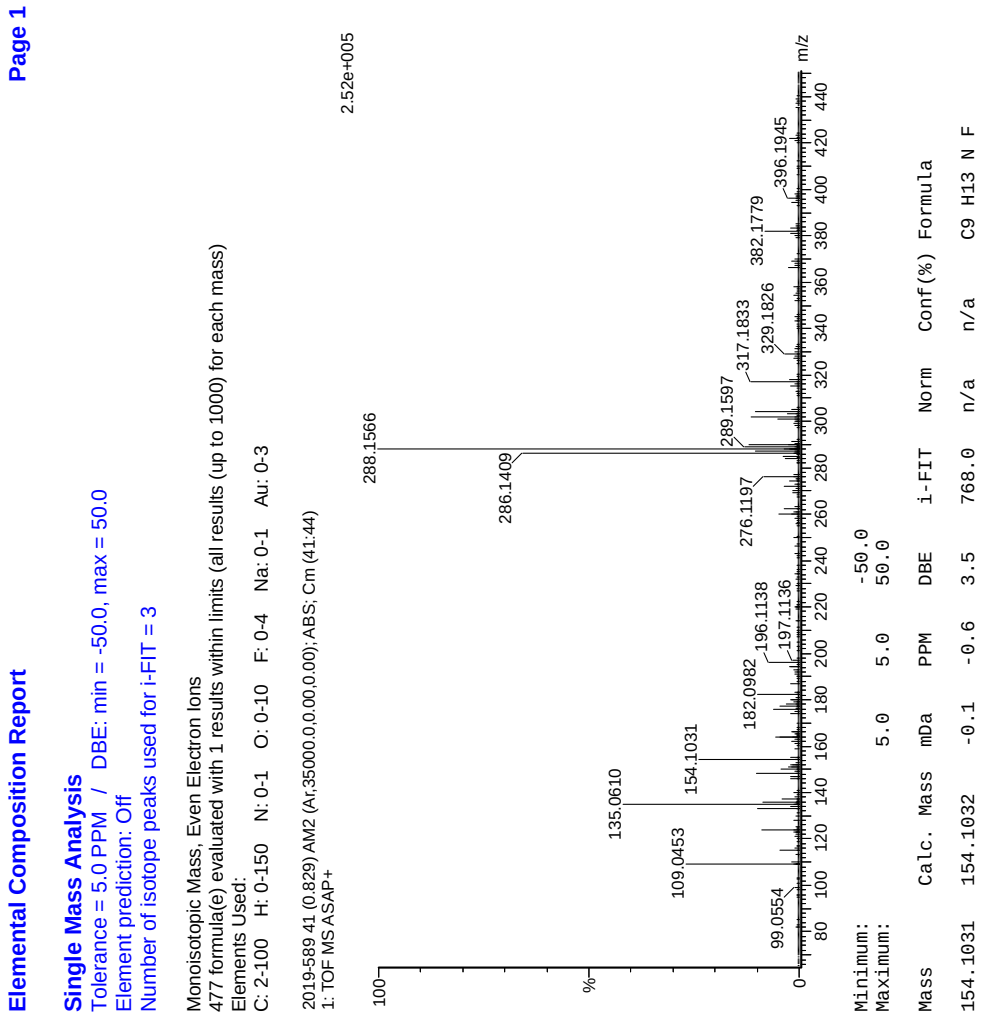

Figure D.1: MS spectrum of **1b**.

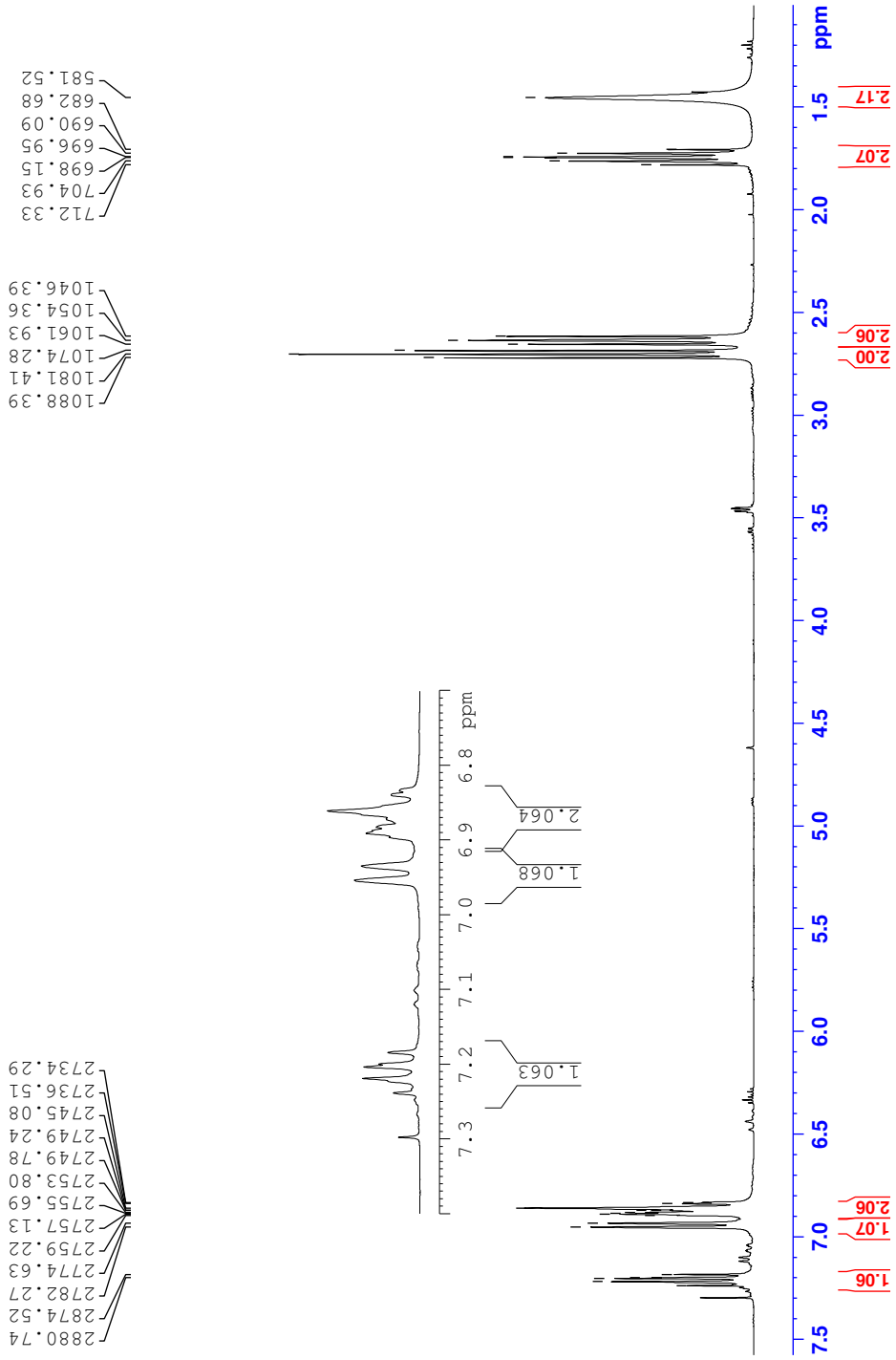

Figure D.2: ^{1}H-NMR spectrum of **1b**.

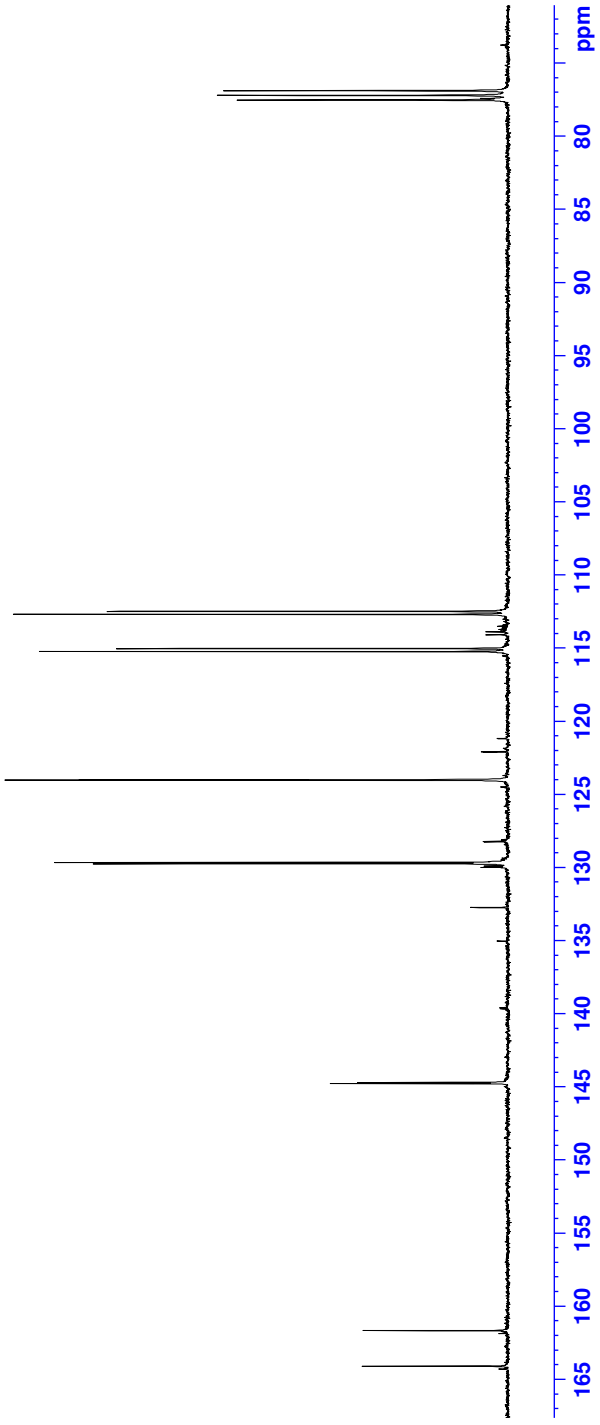

Figure D.3: ^{13}C-NMR spectrum of **1b**.

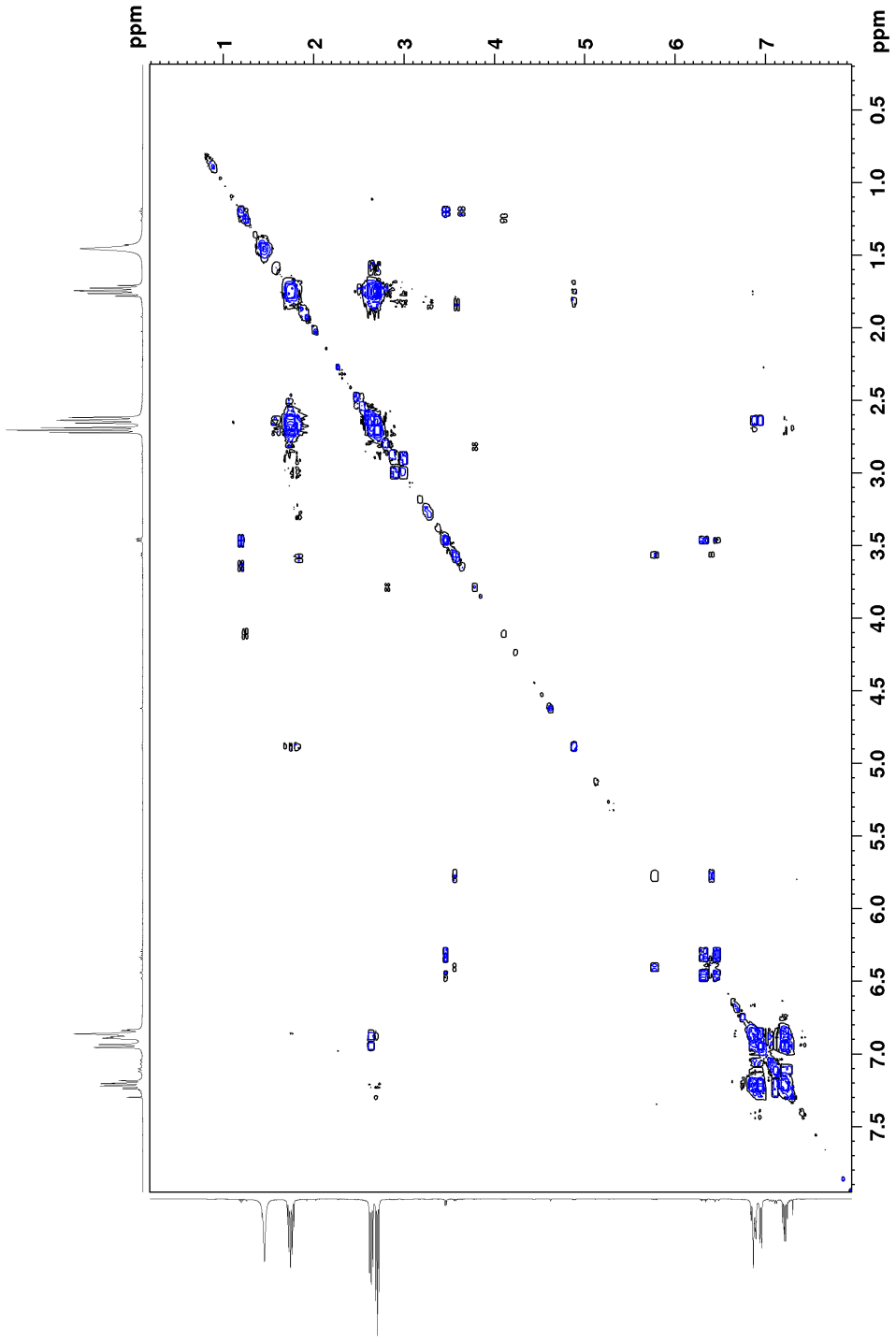

Figure D.4: COSY spectrum of **1b**.

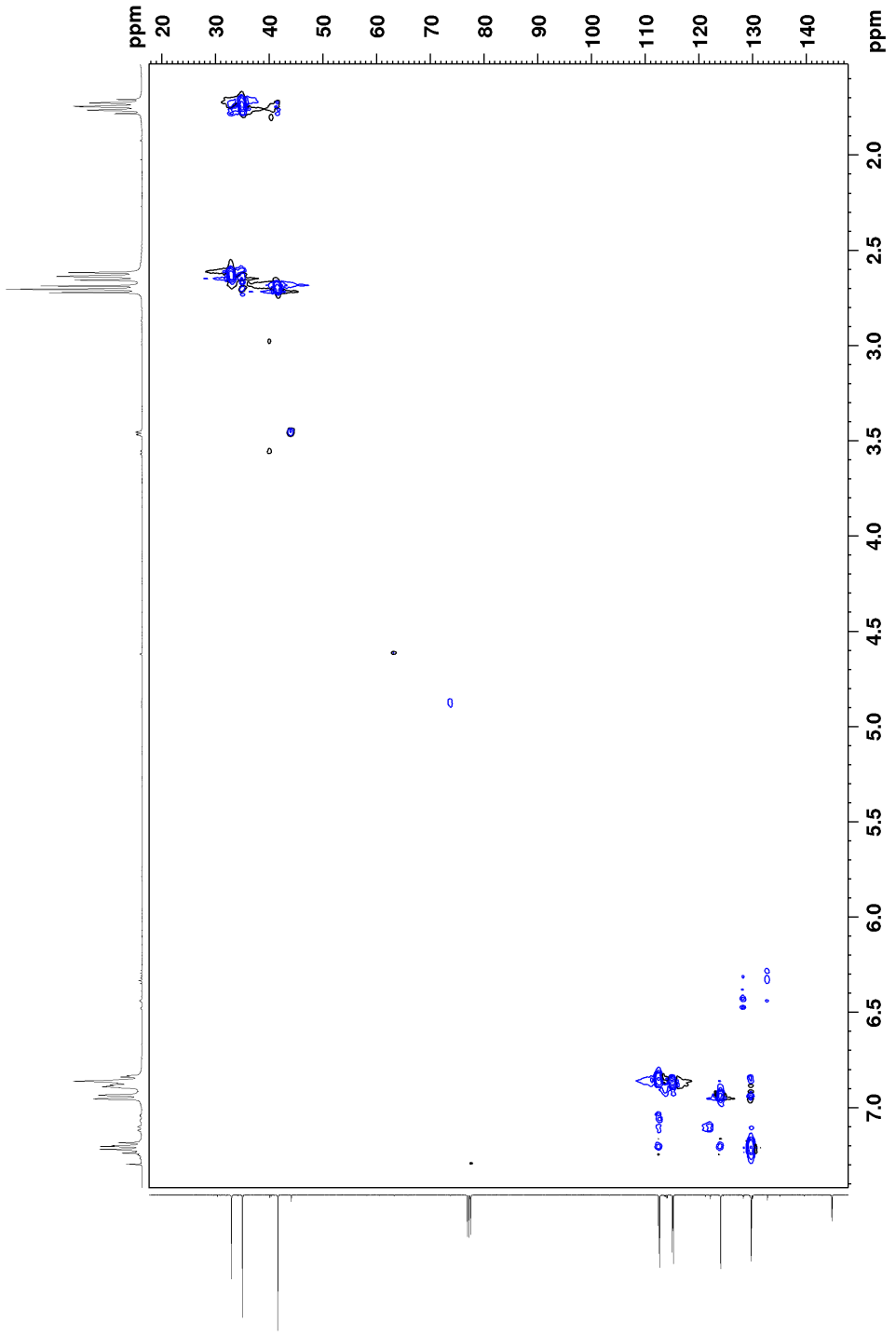

Figure D.5: HSQC spectrum of **1b**.

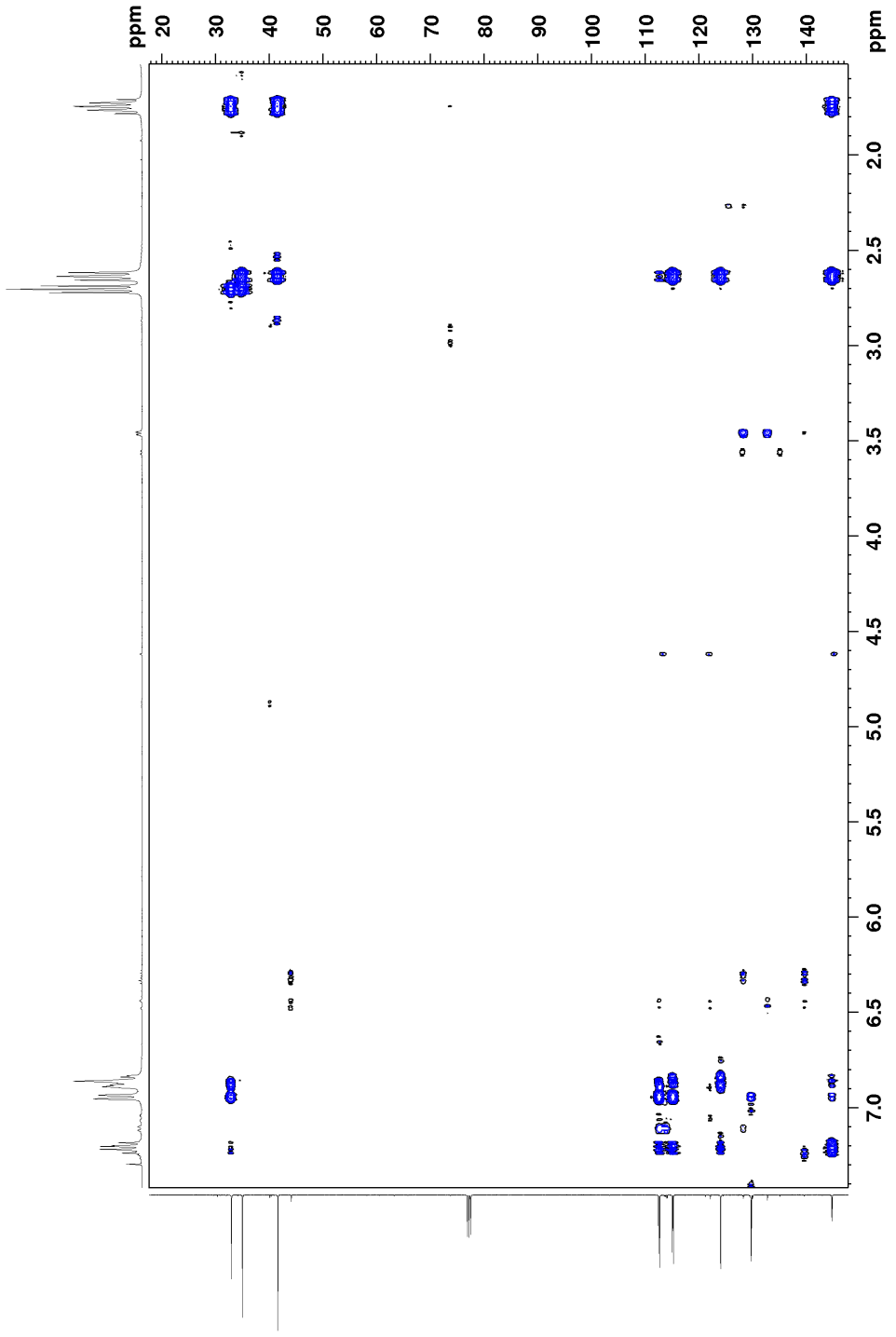

Figure D.6: HMBC spectrum of **1b**.

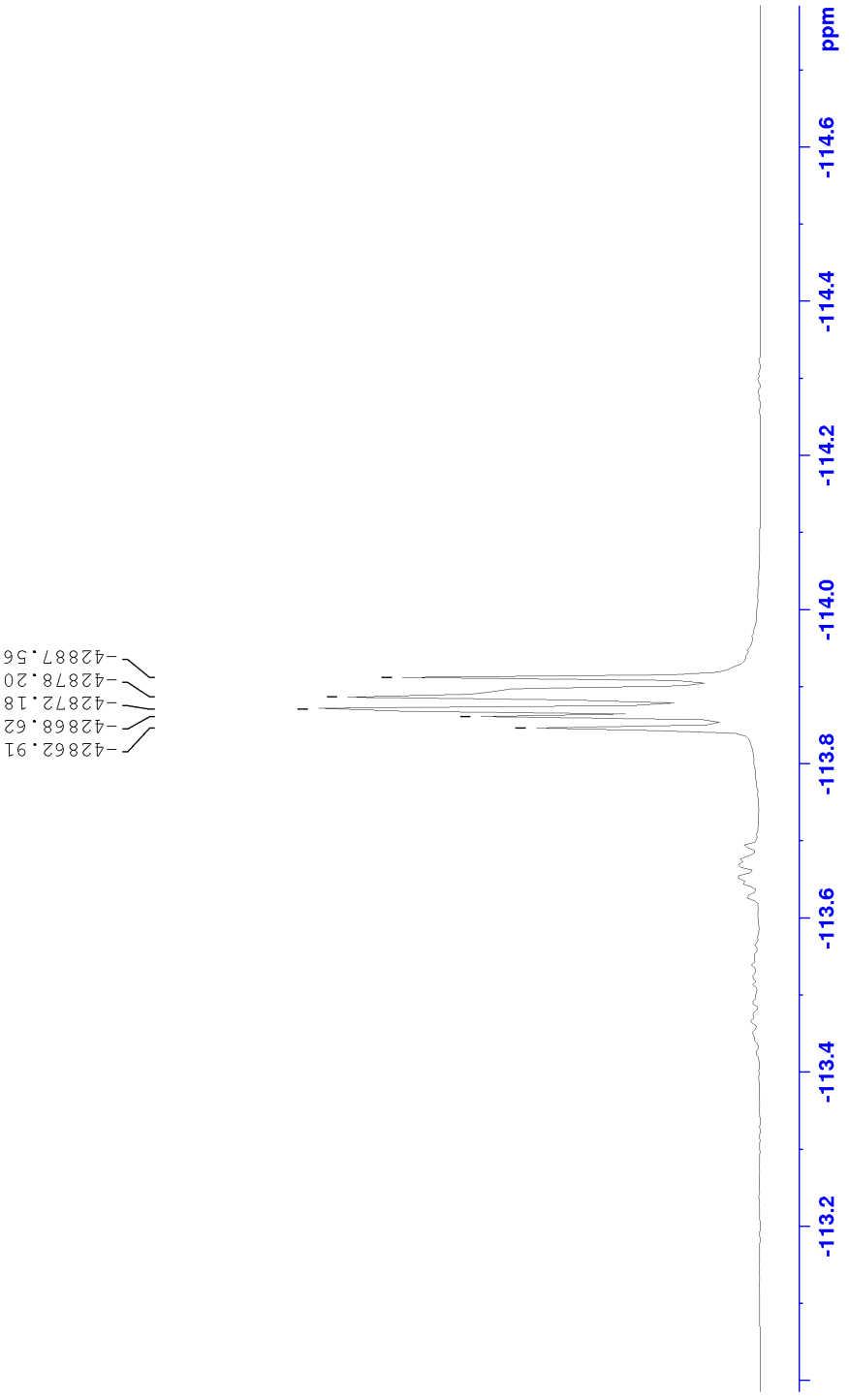

Figure D.7: ^{19}F-NMR spectrum of **1b**.

E. Experimental data of 2c

Figure E.1: MS spectrum of **2c**.

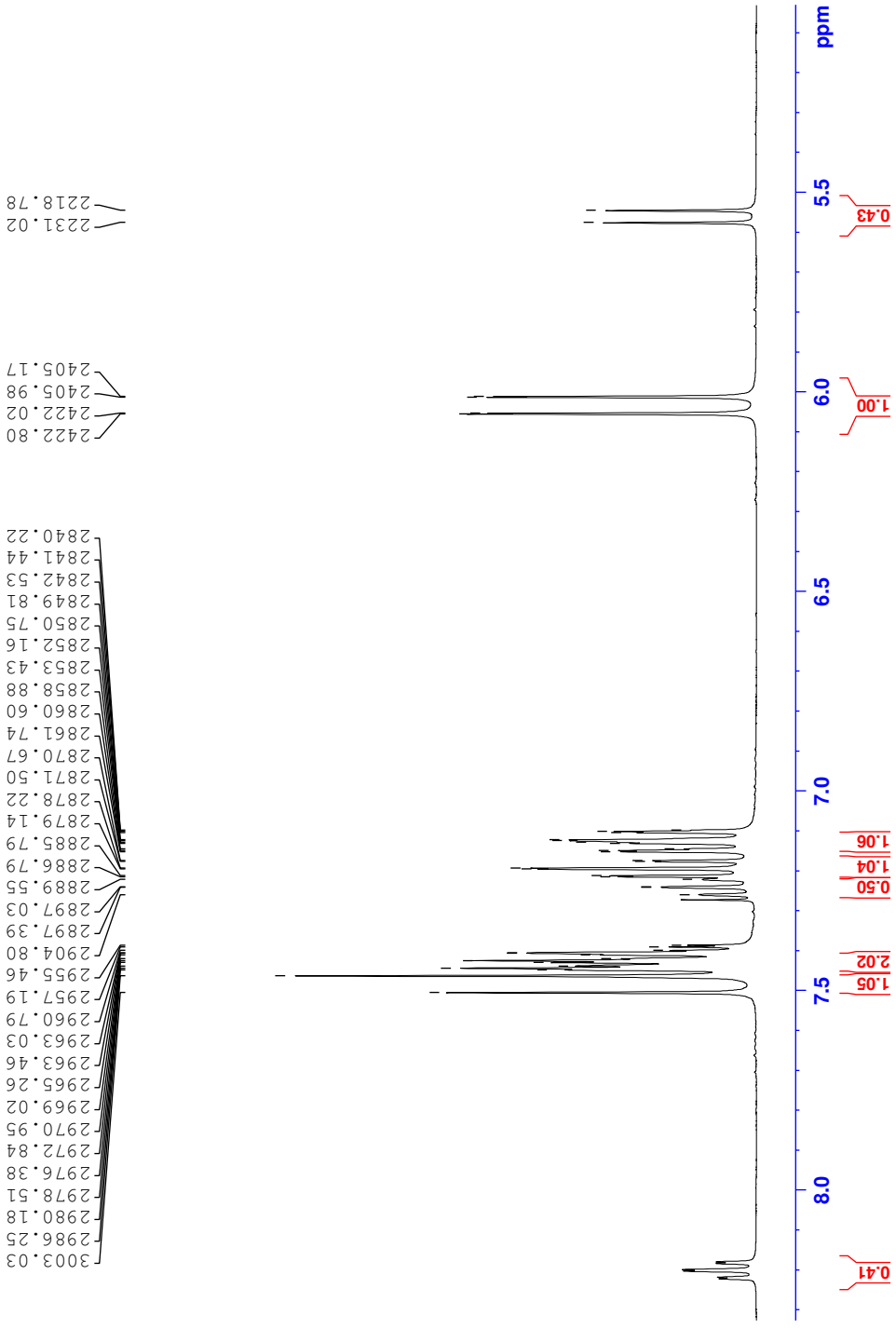

Figure E.2: ^{1}H-NMR spectrum of **2c**.

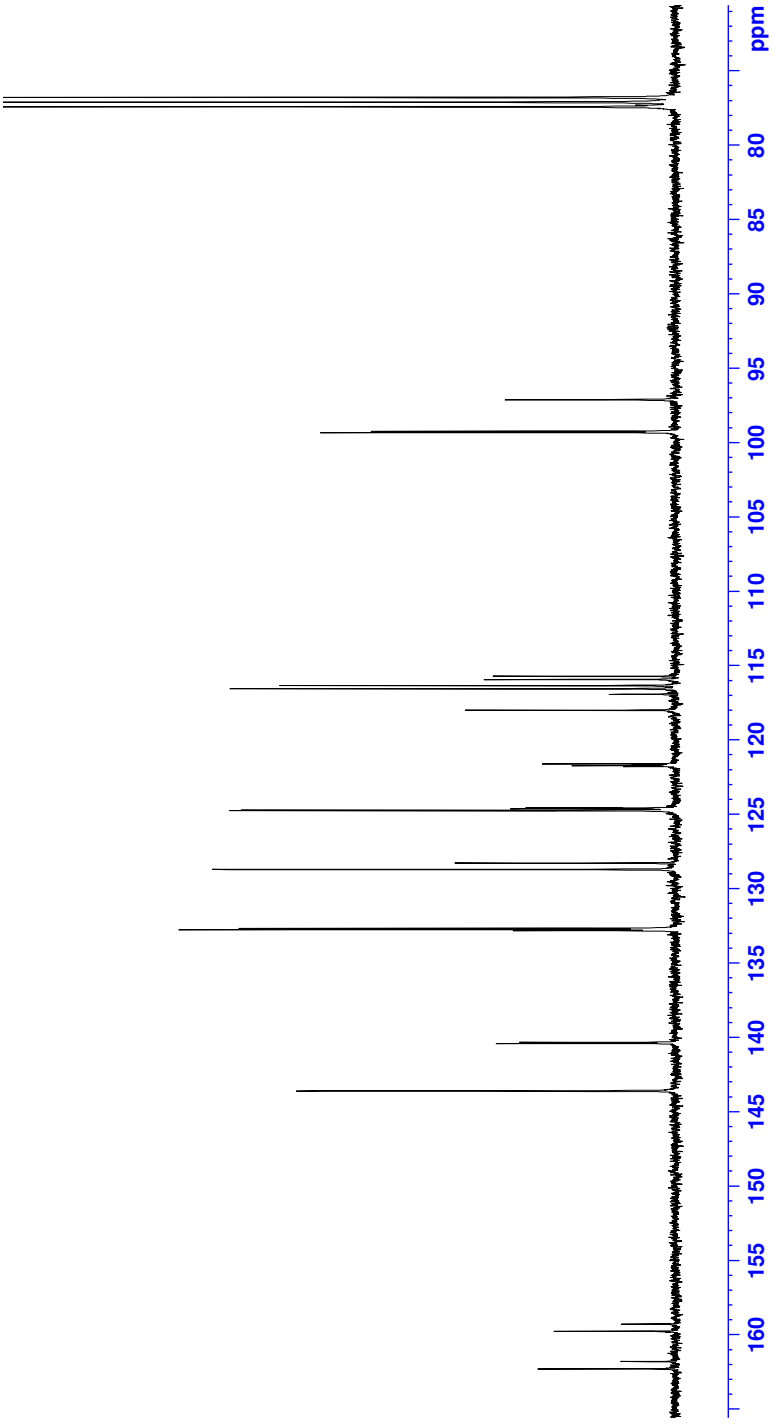

Figure E.3: ^{13}C-NMR spectrum of **2c**.

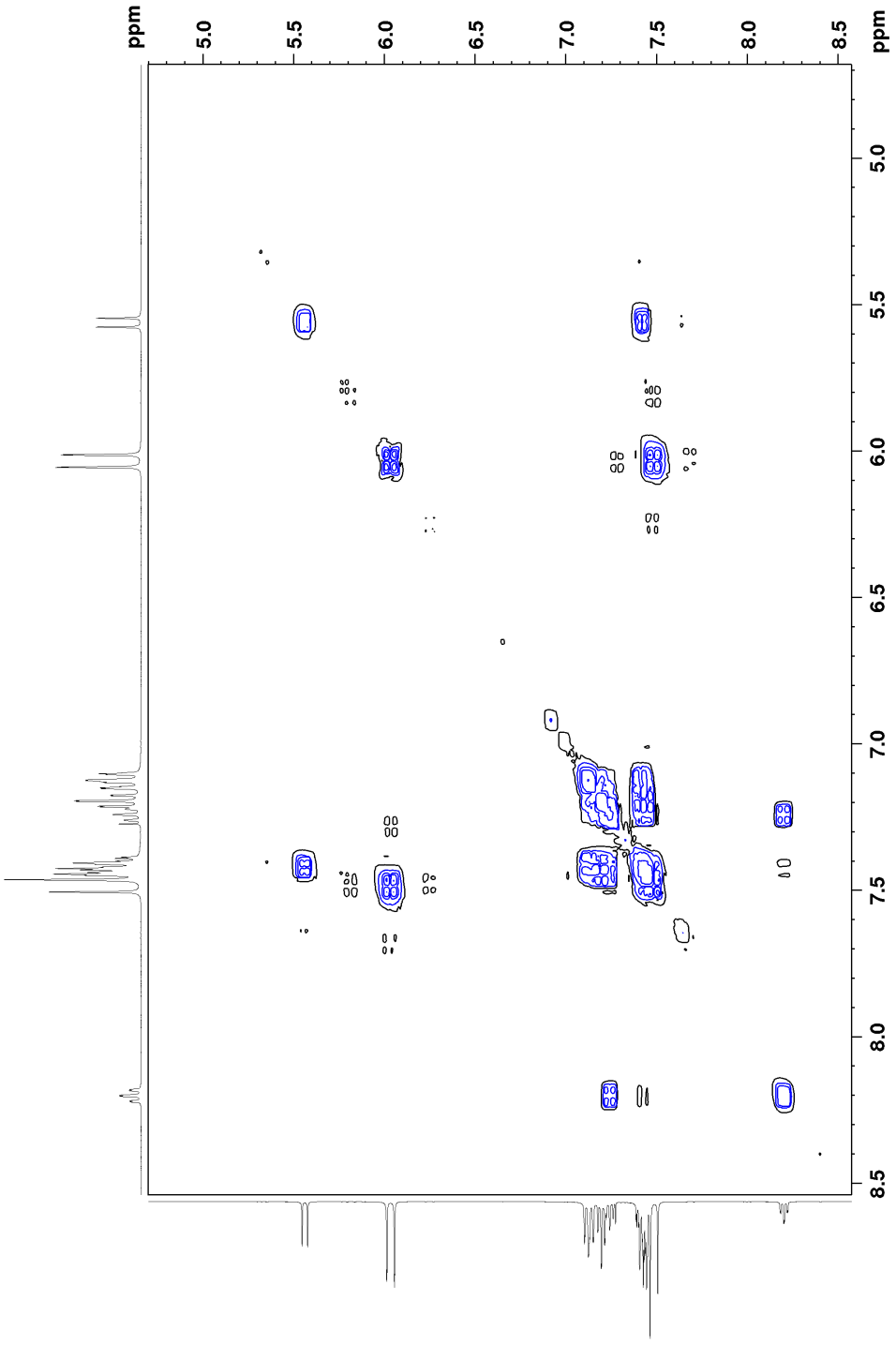

Figure E.4: COSY spectrum of **2c**.

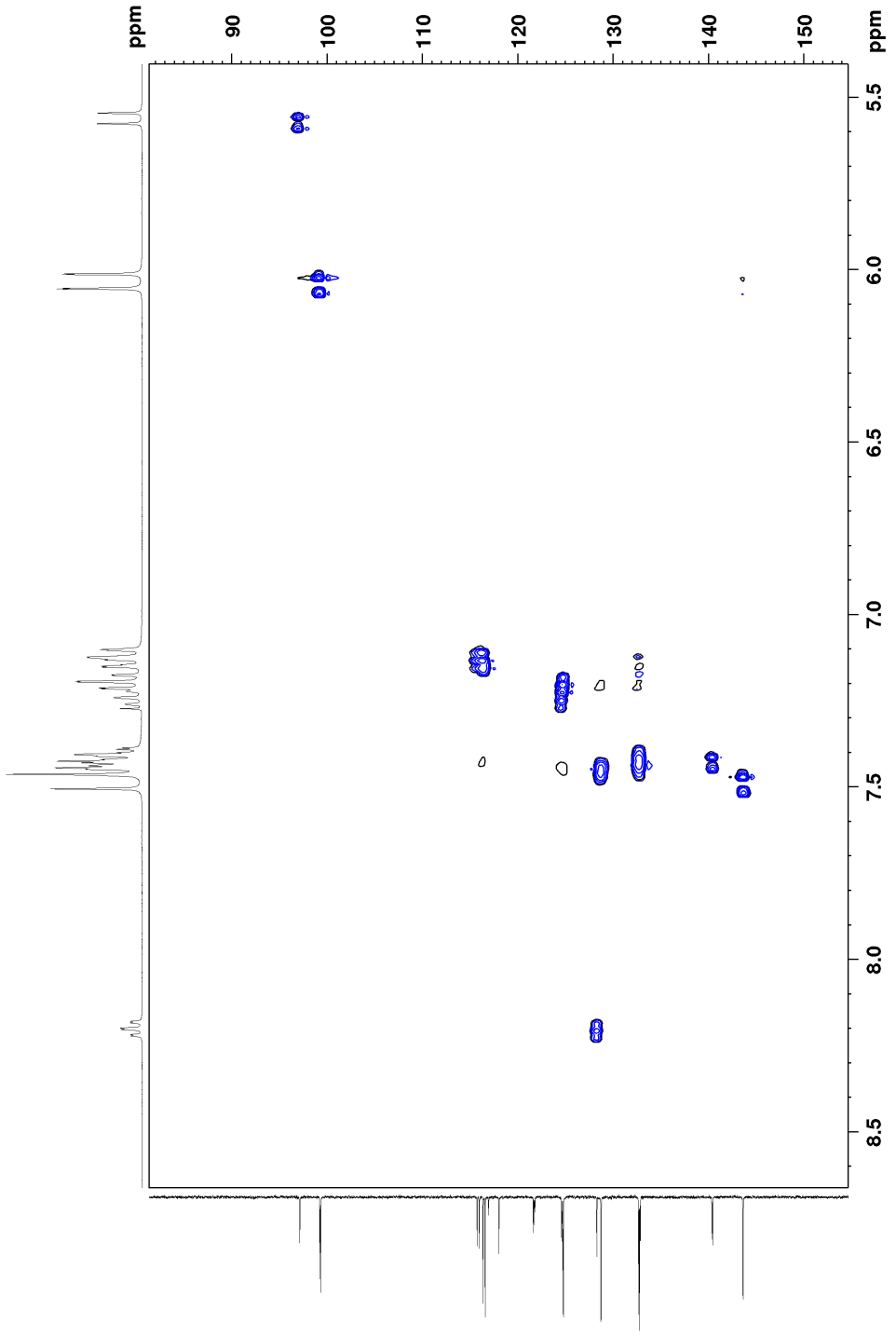

Figure E.5: HSQC spectrum of **2c**.

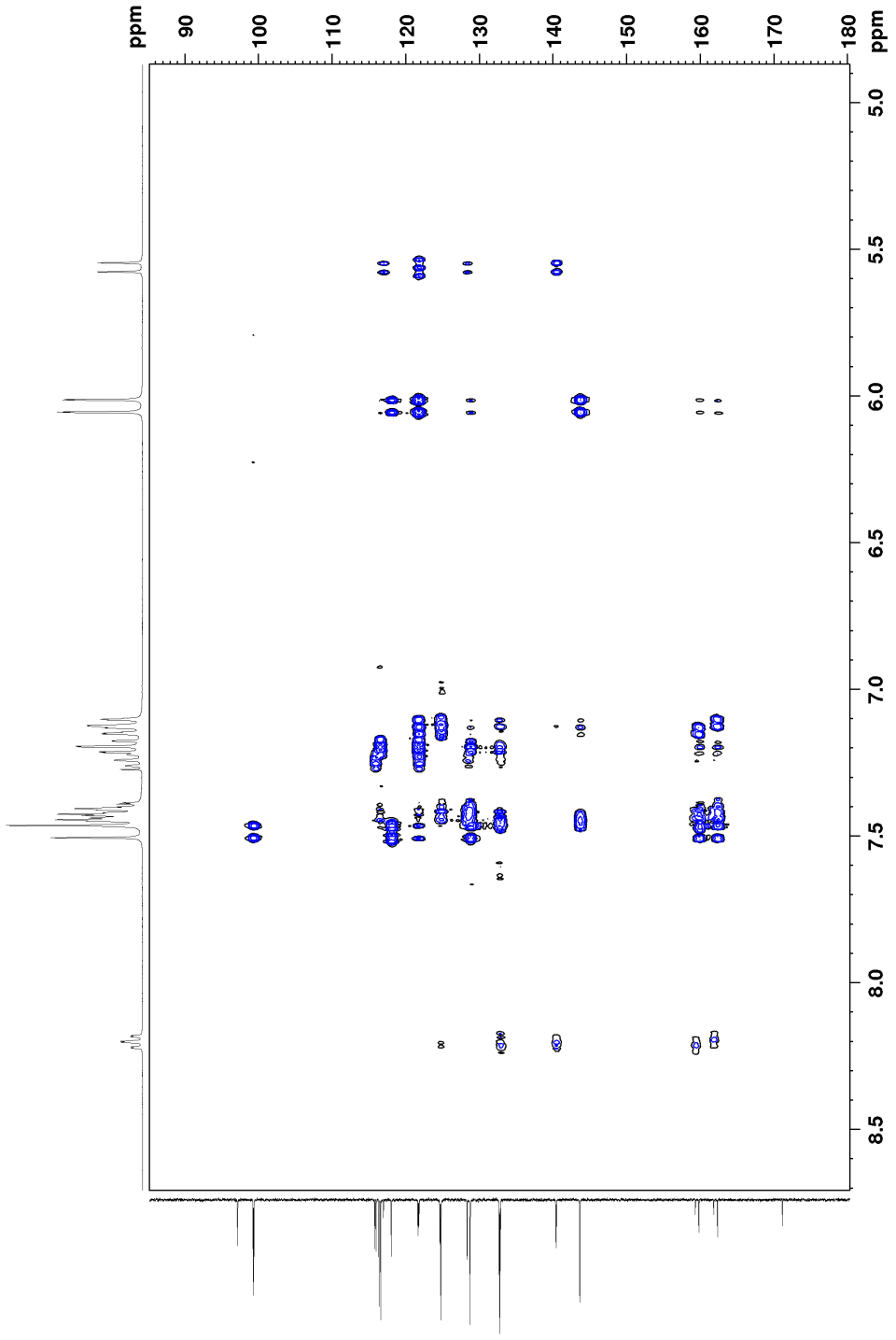

Figure E.6: HMBC spectrum of **2c**.

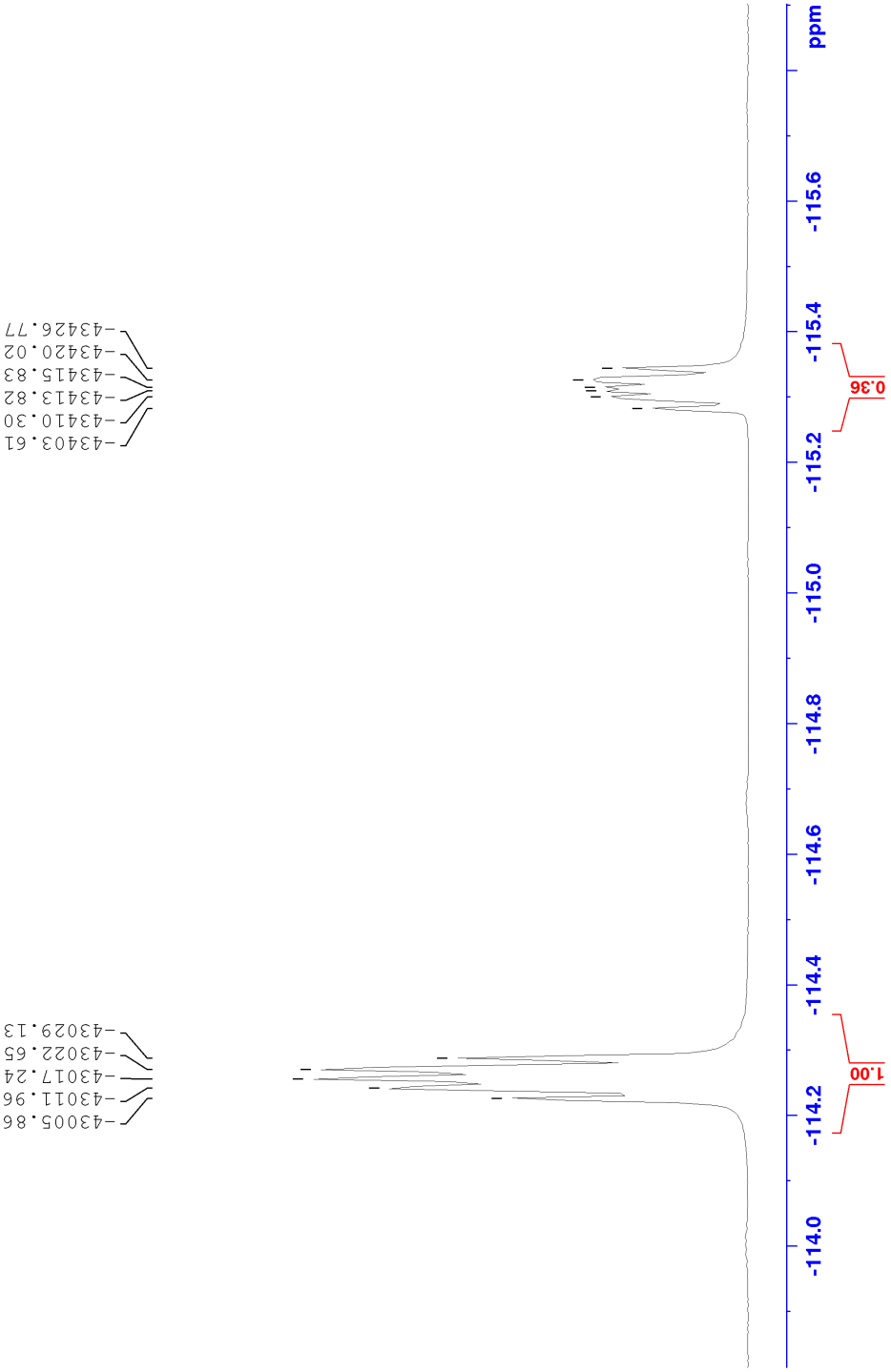

Figure E.7: ^{19}F-NMR spectrum of **2c**.

F. Experimental data of 1c

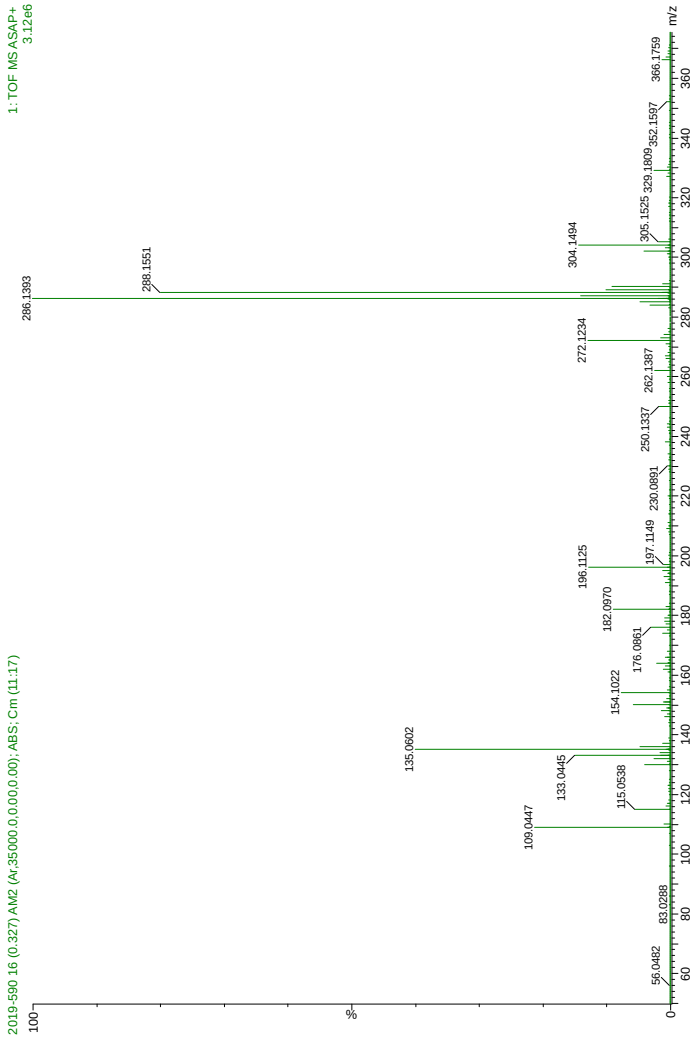

Figure F.1: MS spectrum of **1c**.

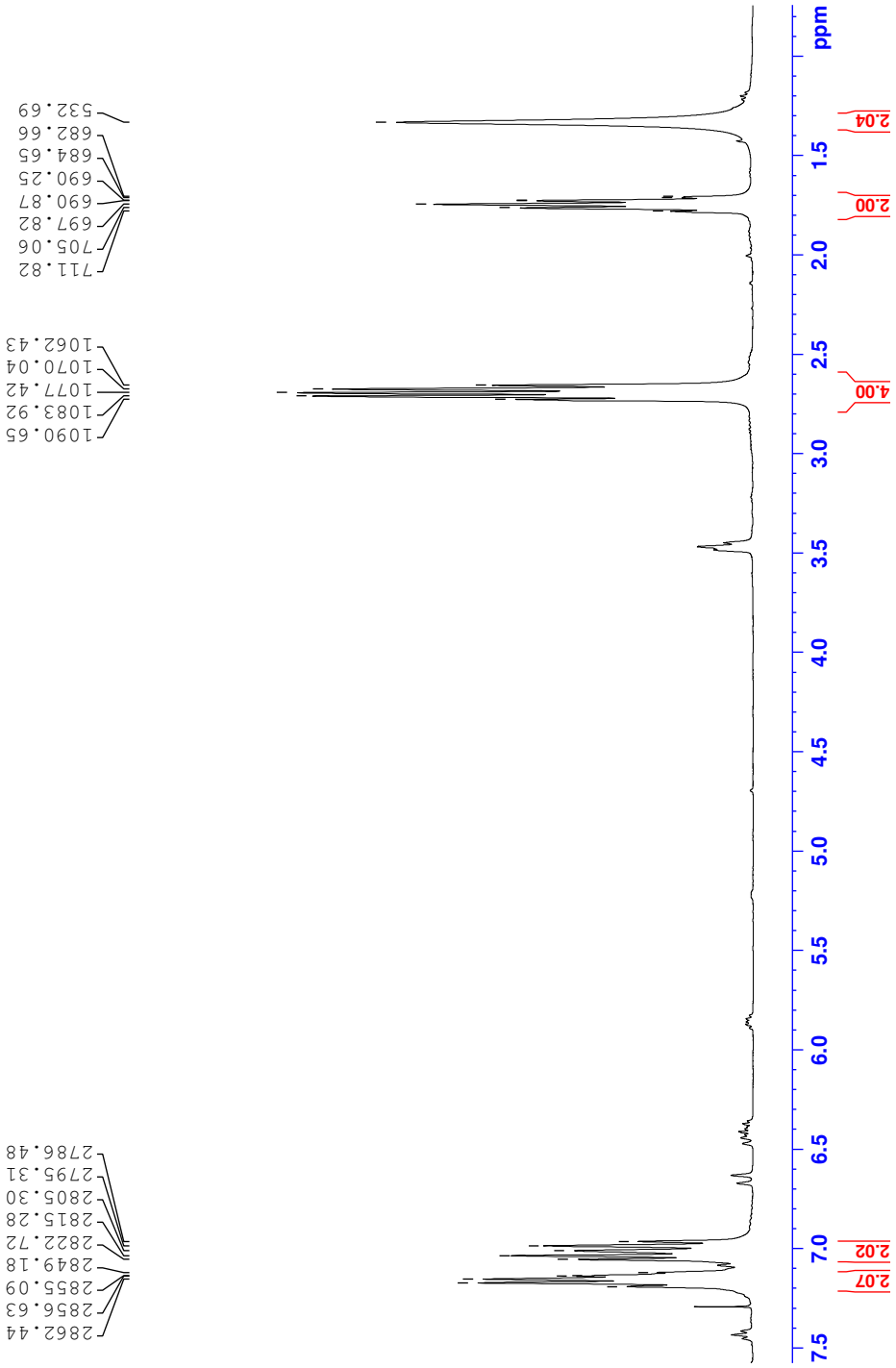

Figure F.2: ^{1}H-NMR spectrum of **1c**.

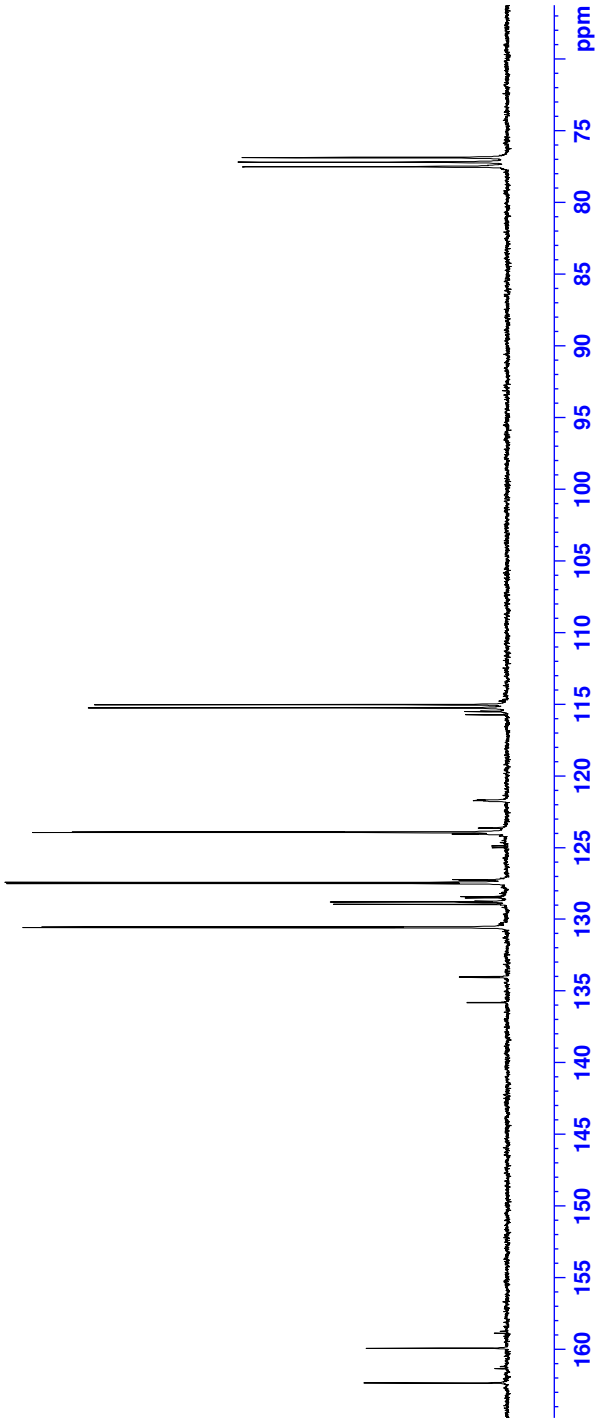

Figure F.3: ^{13}C-NMR spectrum of **1c**.

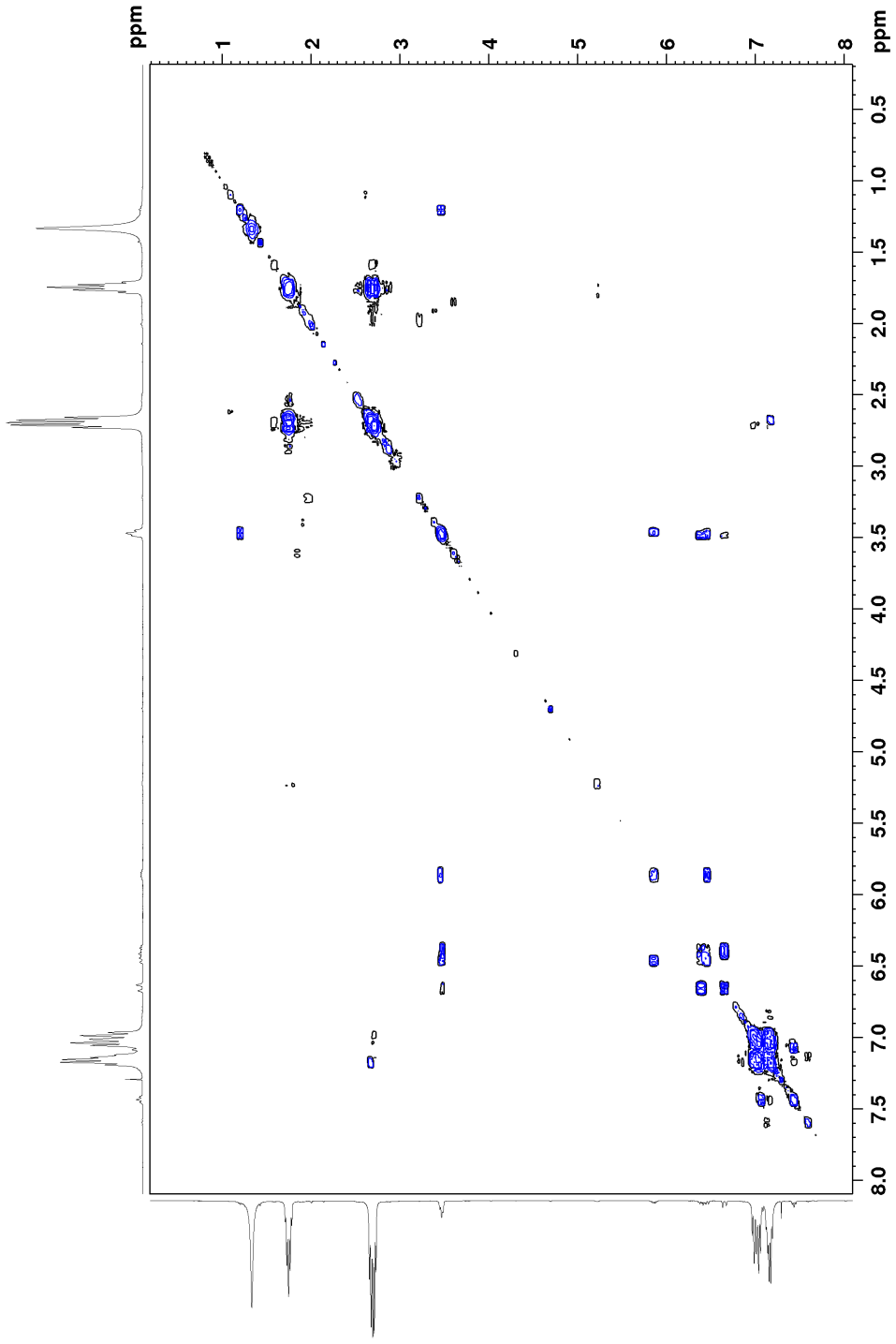

Figure F.4: COSY spectrum of **1c**.

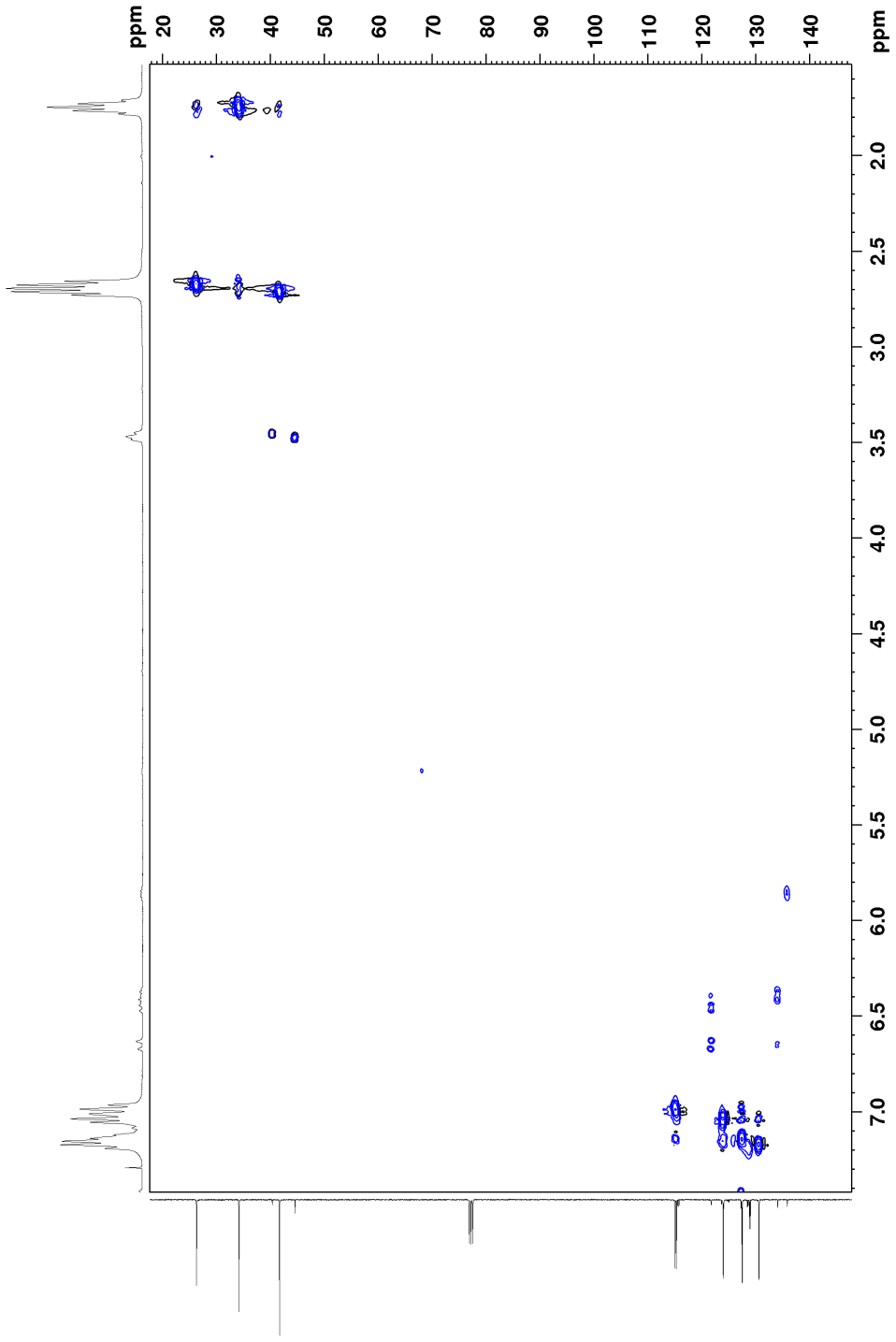

Figure F.5: HSQC spectrum of **1c**.

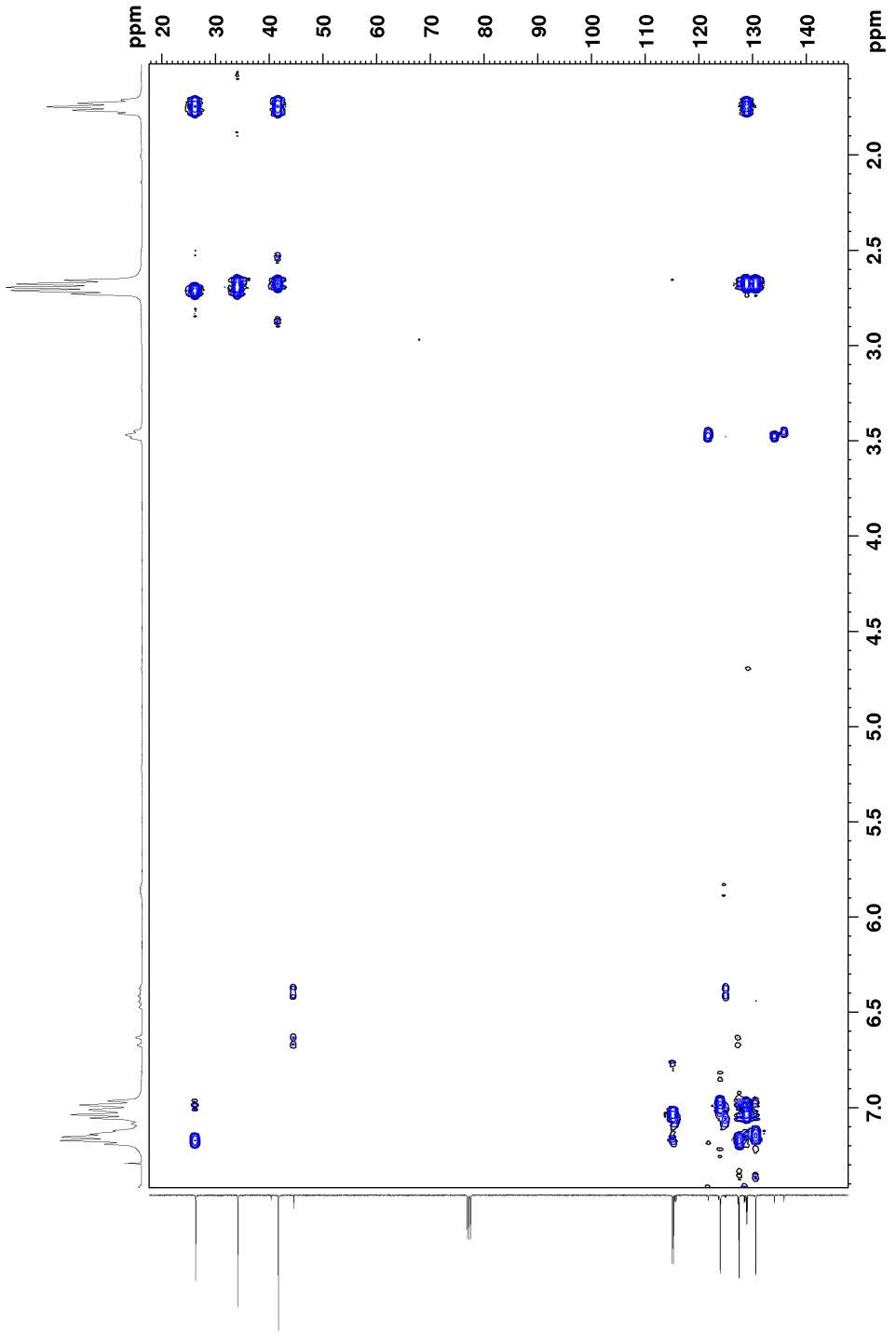

Figure F.6: HMBC spectrum of **1c**.

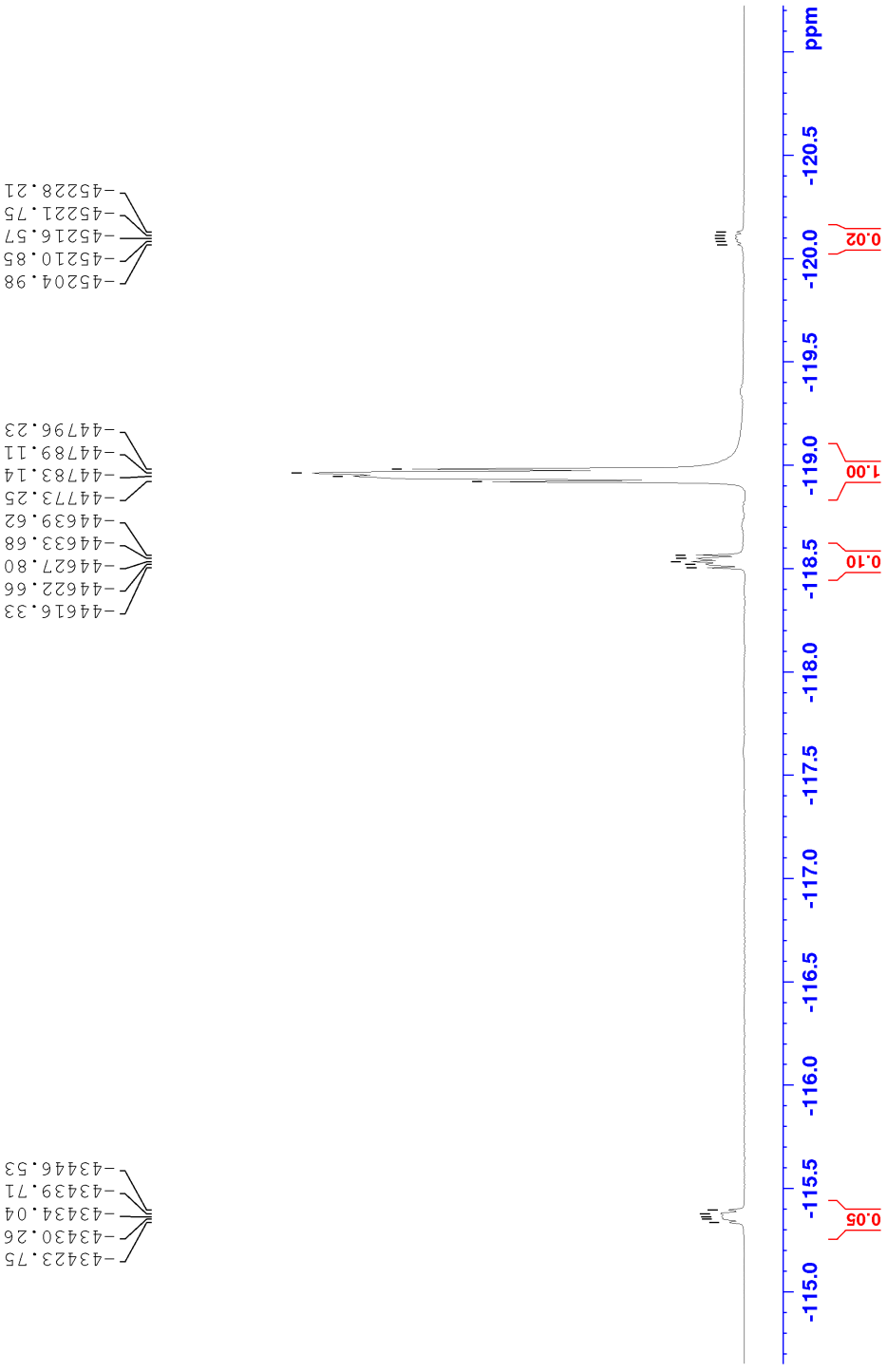

Figure F.7: ^{19}F-NMR spectrum of **1c**.

G. Experimental data of 5

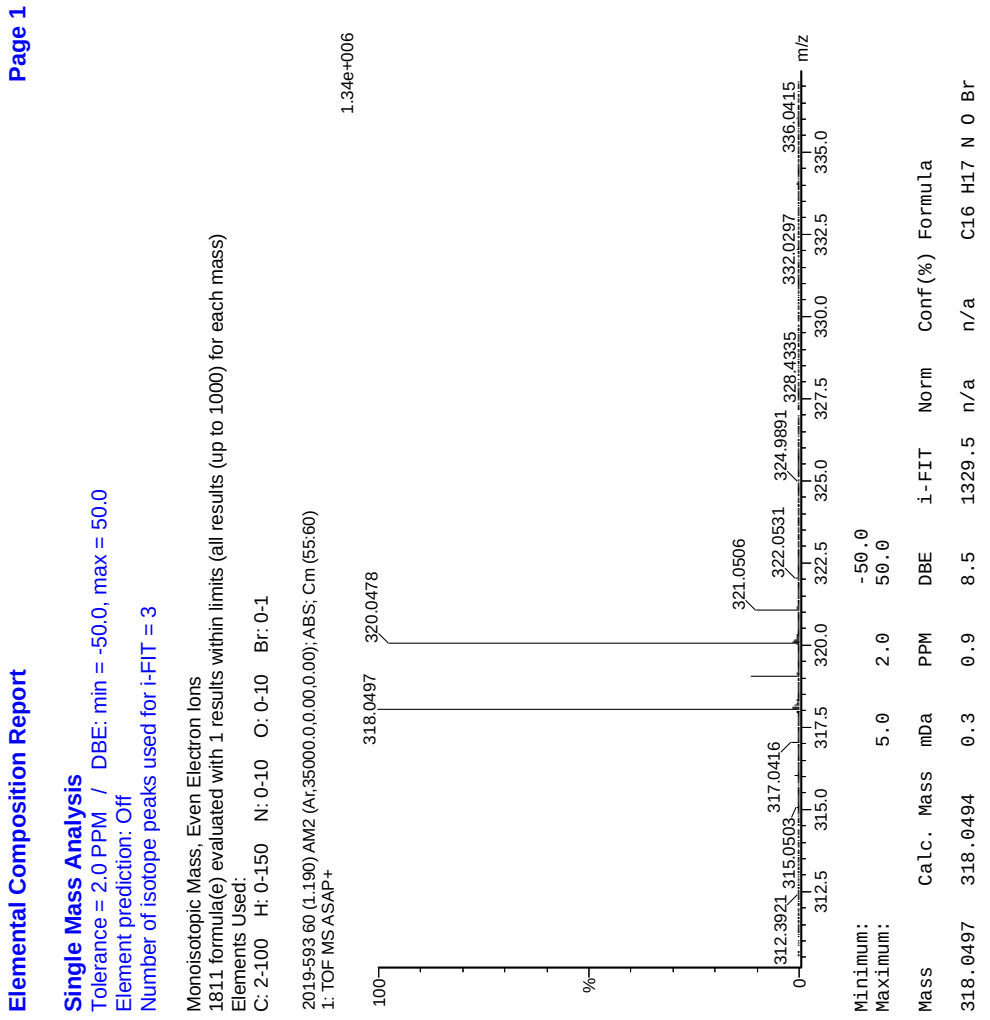

Figure G.1: MS spectrum of **5**.

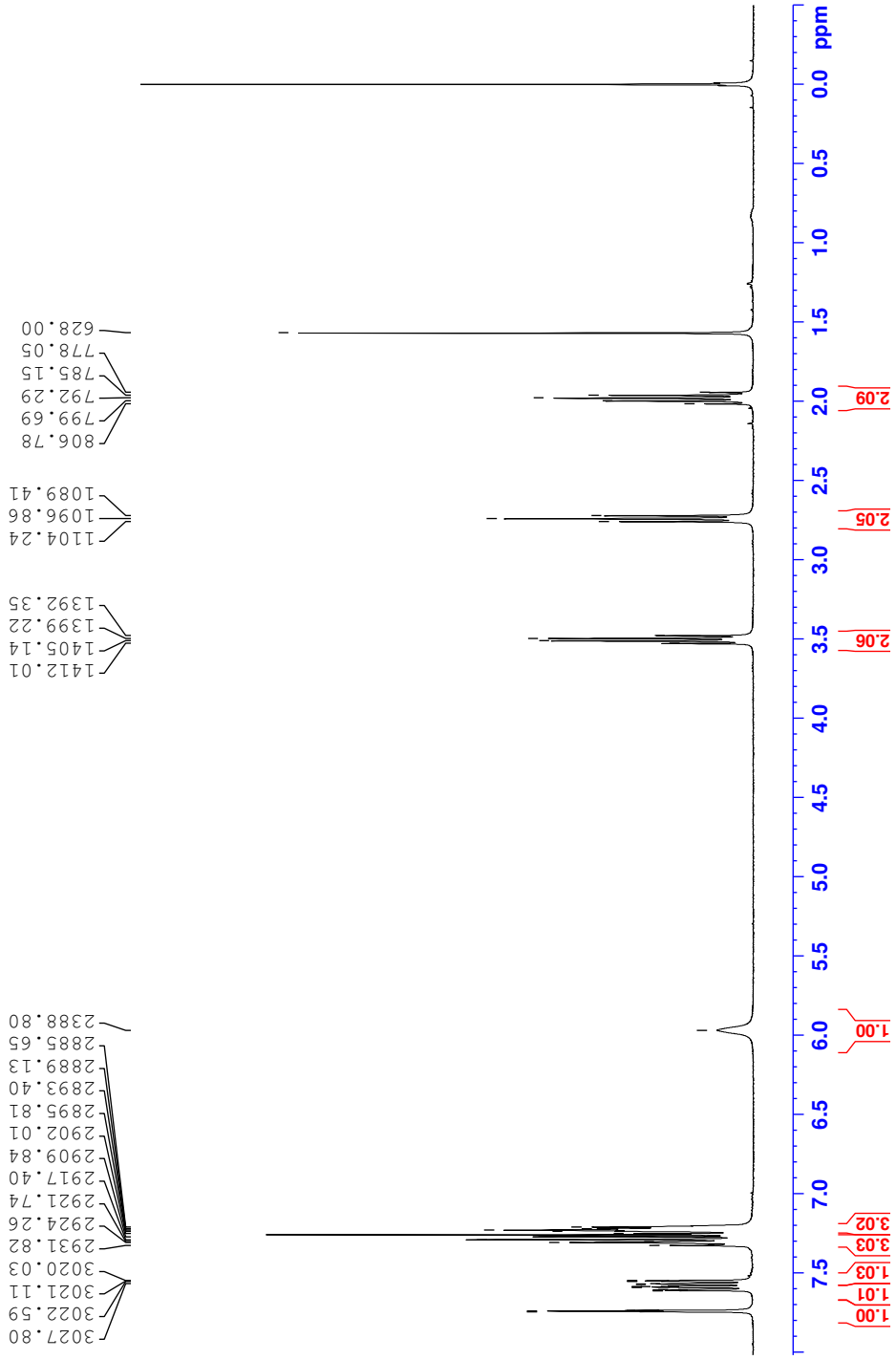

Figure G.2: ^{1}H-NMR spectrum of **5**.

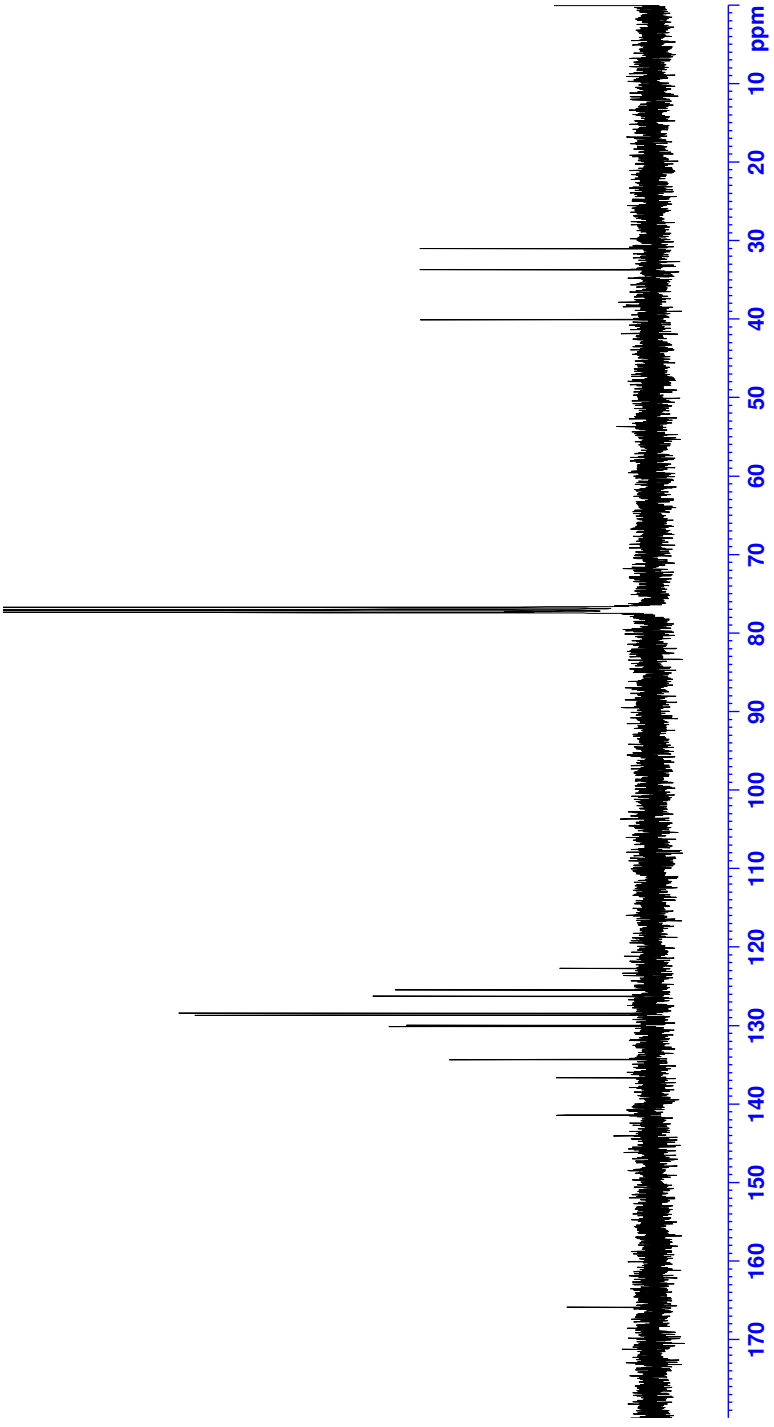

Figure G.3: ^{13}C-NMR spectrum of **5**.

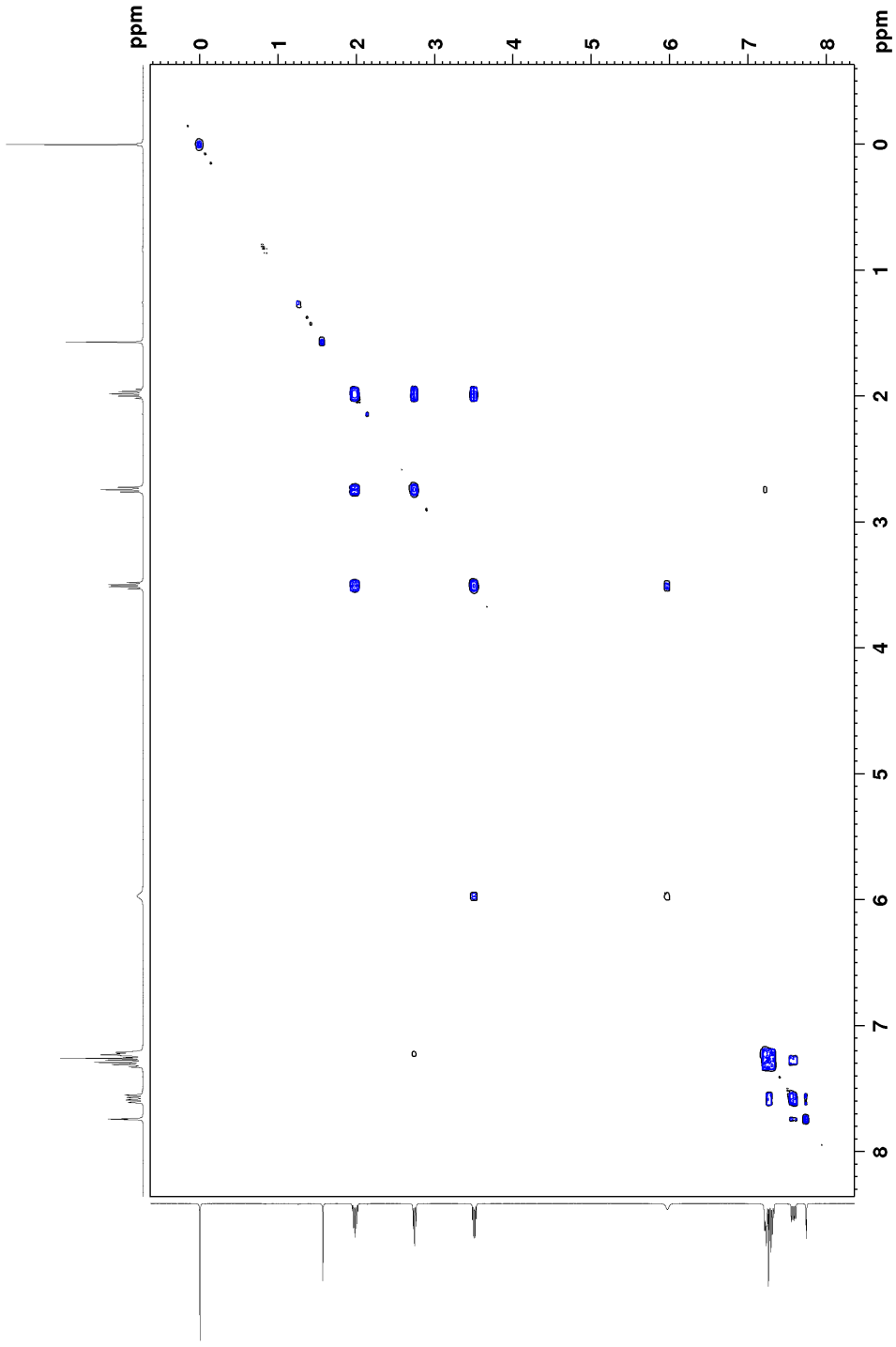

Figure G.4: COSY spectrum of **5**.

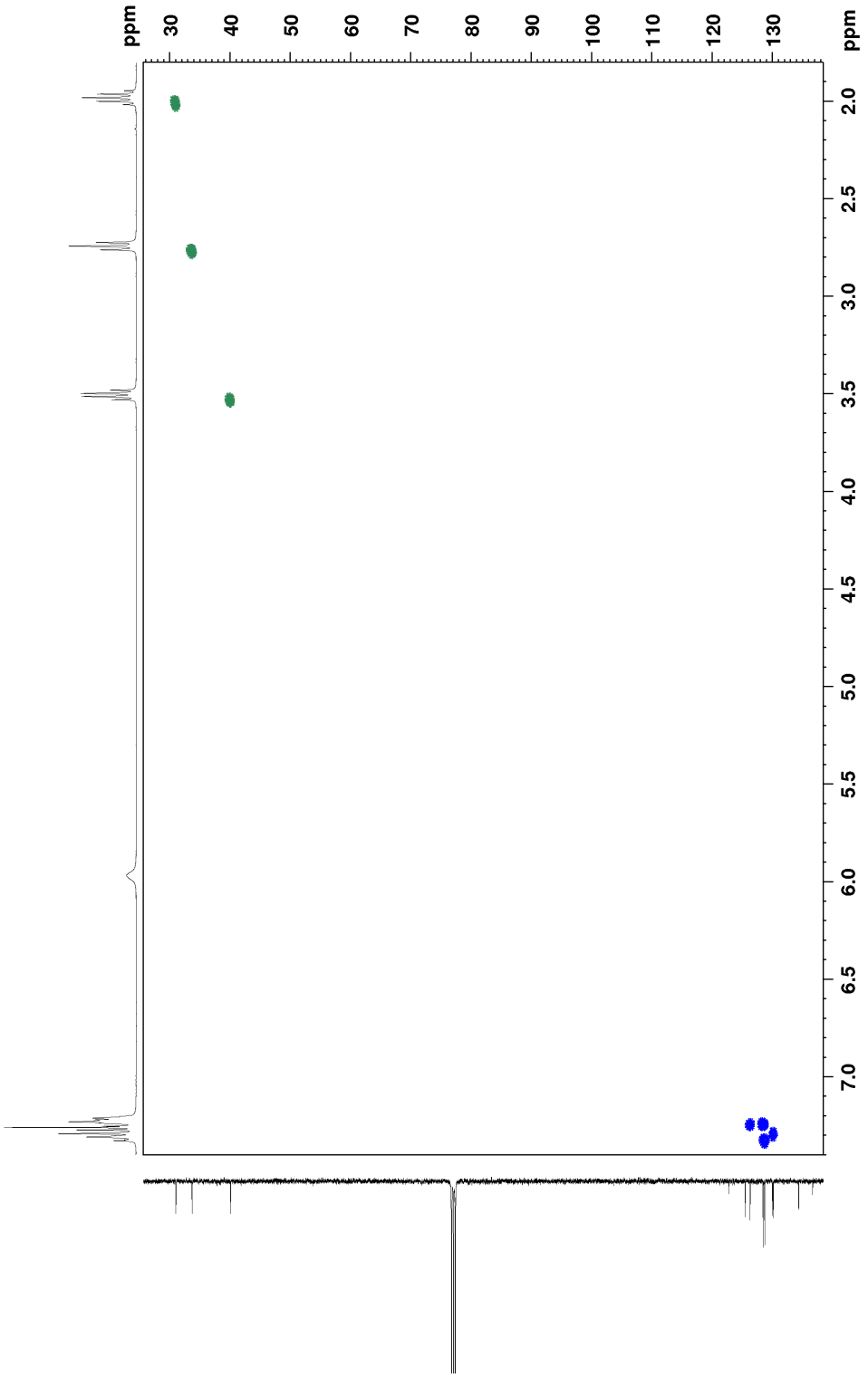

Figure G.5: HSQC spectrum of **5**.

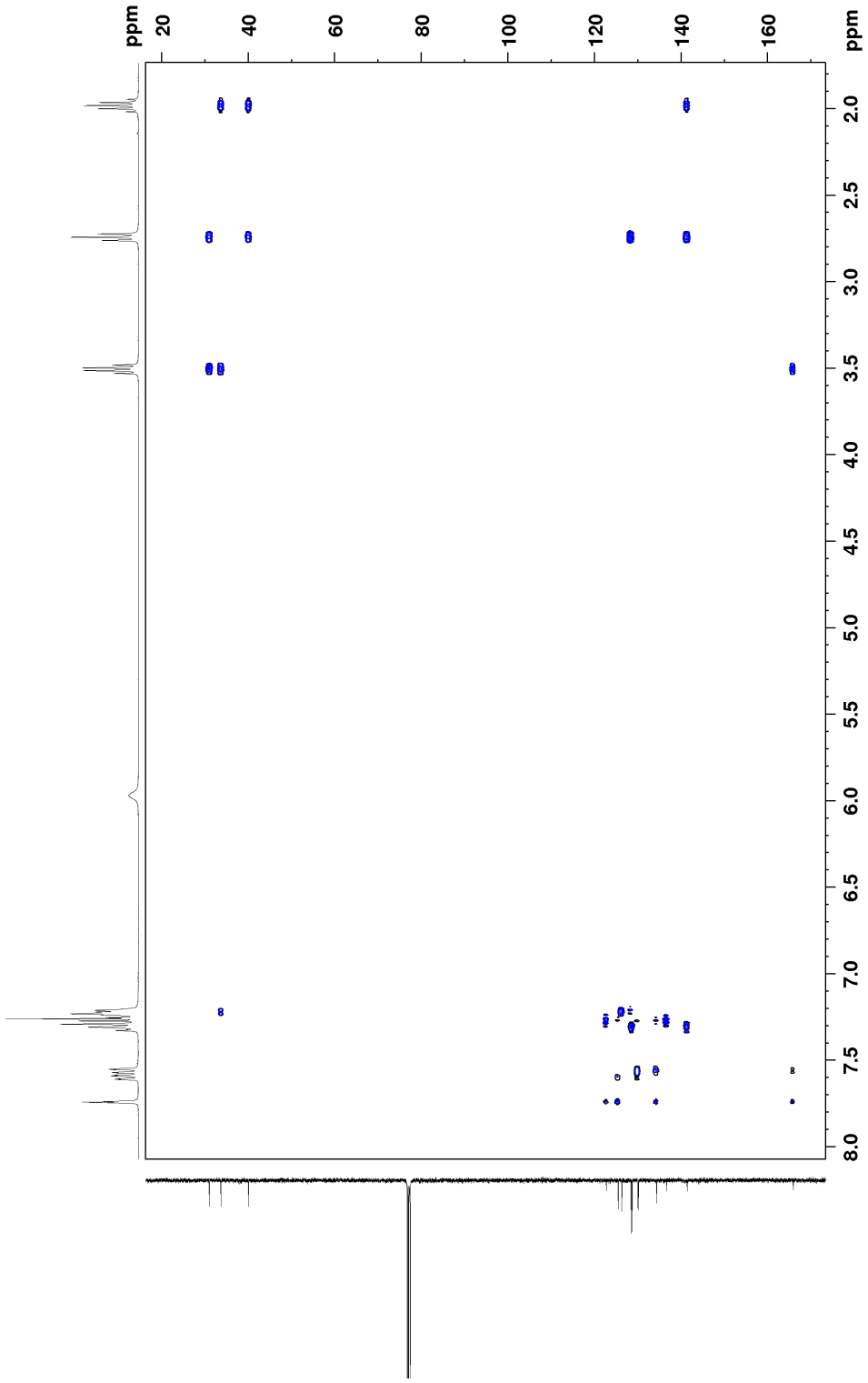

Figure G.6: HMBC spectrum of **5**.